DOCKET NO. **SA- 516**

EXHIBIT NO. **18B**

NATIONAL TRANSPORTATION SAFETY BOARD
WASHINGTON, D.C

METALLURGY / STRUCTURES SEQUENCING GROUP
CHAIRMAN'S
REPORT OF INVESTIGATION

Supporting Documentation for
OVERALL BREAKUP SEQUENCE
Materials Laboratory Report No. 97-38

Metallurgy / Structures Sequencing Group Report

Appendix B: Detailed Rationale

ZONE _____ **SEQUENCE ID NO.** US-1

COMPONENT UPPER SKIN **PART ID NO.** _____

DESCRIPTION OF POSSIBLE SEQUENCE	SUPPORTING OBSERVATIONS	NON-SUPPORTING OBSERVATIONS	Confidence Level
The loss of the front spar and spanwise beam #3 attachment to the upper skin panel would result in some loss of compression stability of the upper skin panel.			High
If the structure sustains thermal damage from fire, it will result in decreased structural capability.			High
Buckling of the upper skin is potentially initiated between the midspar and the rear spar and restraint would be provided by the BL 0 rib which is consistent with an inflection in the curvature at BL 0.	Upper skin panel has residual deflection of an upward bow to the left of BL 0 and slight upward curvature to the right of BL 0 with the inflection point at BL 0.		Medium
The initial fracture consistent with upper panel buckling is potentially along the attachment to spanwise beam #1. This fracture runs primarily through the single fastener row common to the upper chord of the spanwise beam.	1. Bending fracture in the skin panel at SWB #1 is through the fastener row and the fracture exhibits upward bending both fwd and aft of the fastener row. 2. Fore/aft fractures are not continuous forward or aft of the fracture running along SWB#1 suggesting that the fracture along SWB#1 existed prior to the fractures occurring at LBL 40, LBL 5, RBL 76, and RBL 100. (see figure B-1)		Medium

ZONE _____ SEQUENCE ID NO. US-2

COMPONENT UPPER SKIN PART ID NO. _____

DESCRIPTION OF POSSIBLE SEQUENCE	SUPPORTING OBSERVATIONS	NON-SUPPORTING OBSERVATIONS	Confidence Level
The upper panel fractures near LBL 11 at the rear spar and the fracture apparently propagates to spanwise beam #1 to connect with the fracture already existing at SWB #1. This fracture matches a fracture location on the rear spar.	1. Mating fracture between CW-135 and CW-103 is sooted on CW-103 and not sooted on CW-135. 2. The upper surface of CW-103 is heavily sooted and the upper surface of CW-135 is only slightly sooted. 3. Curvature/deflections of the upper skin panel shows bowing of skin to the left of BL 0.		Medium
The panel fractures between CW-115 and CW-102 are consistent with buckling of the upper skin in the bay between the midspar and spanwise beam #1. The buckling pattern takes a slightly different mode as compared with the shape of CW-135 as the outbd end of CW-115 also shows upward curvature.	1. Same general curvature of CW-115 and CW-135. 2. Sooted fracture on CW-102 and unsooted fracture on CW-135. 3. Upper surface of CW-102 is heavily sooted and less soot on the upper surface of CW-115.	CW-115 has curvature on the outbd end that CW-135 does not have.	Medium
The upper skin between SWB#2 and the midspar shows apparent spanwise buckling but the wave form changes as there is no BL0 rib fwd of the midspar to continue to force an inflection at BL 0. The fracture continues to follow the panel maximum curvature along approx. LBL 34.			Medium

ZONE _____ SEQUENCE ID NO. US-3

COMPONENT UPPER SKIN PART ID NO. _____

DESCRIPTION OF POSSIBLE SEQUENCE	SUPPORTING OBSERVATIONS	NON-SUPPORTING OBSERVATIONS	Confidence Level
During major wing breakup, a spanwise fracture occurs just fwd of spanwise beam #2 that extends from the left side of body to the right side of body.	The skin panel forward of the fracture shows a different deflected shape fwd of the spanwise fracture as compared with aft of the fracture. The skin panel fwd shows greater levels of curvature prior to failure as the absence of spanwise beam 3 and the front spar allows curvature both above and below a straight line passed between both side of body ribs.		Medium
Compression fractures of the upper skin panel potentially results in separation of CW-101 from CW-114 and CW-129.	Compression buckling fracture along approximately LBL34		Medium
There are numerous additional compression fractures that could occur as part of the final breakup of the wing. Most of these are to the left of approx. LBL 34 separation line.			Medium
The upper skin panel approximately to the right of LBL 34 remains attached to the right wing at major airplane breakup.	Heavy consistent soot patterns on internal and external surfaces to the right of approximately LBL 34.		Medium
Pieces close to the left side of body rib (to the left of LBL127) stayed with the left wing at major airplane breakup.	1. Compression fracture along LBL 127. 2. Consistent lack of sooting on the pieces to the left of LBL 127.		Medium
Pieces to the right of LBL 127 and left of LBL 34 could have separated independantly or stay with the right wing during a portion of the soot exposure.	1. Soot accumulations are not consistent with the pieces that remain with either the left or right wing. 2. Compression fractures on both inbd and outbd ends of pieces to the left of approximately LBL 34 and right of LBL 127.		Medium

ZONE _____ **SEQUENCE ID NO.** US-4

COMPONENT UPPER SKIN **PART ID NO.** _____

DESCRIPTION OF POSSIBLE SEQUENCE	SUPPORTING OBSERVATIONS	NON-SUPPORTING OBSERVATIONS	Confidence Level
CW-101 possibly separates independently from the right wing along a secondary fracture near the right side of body after major airplane breakup. This would possibly occur after some fire inside the center section prior to wing breakup with some fire in the center section after breakup.	1. Aft fracture of CW-101 unsooted with sooted fractures on CW-126, CW-125, CW-102, and CW-104. 2. CW-101 sooted on underside but not sooted on topside which is different than all other panels. 3. CW-104 is sooted on the inbd end from S-29 aft and lightly sooted fwd of S-29.		Medium

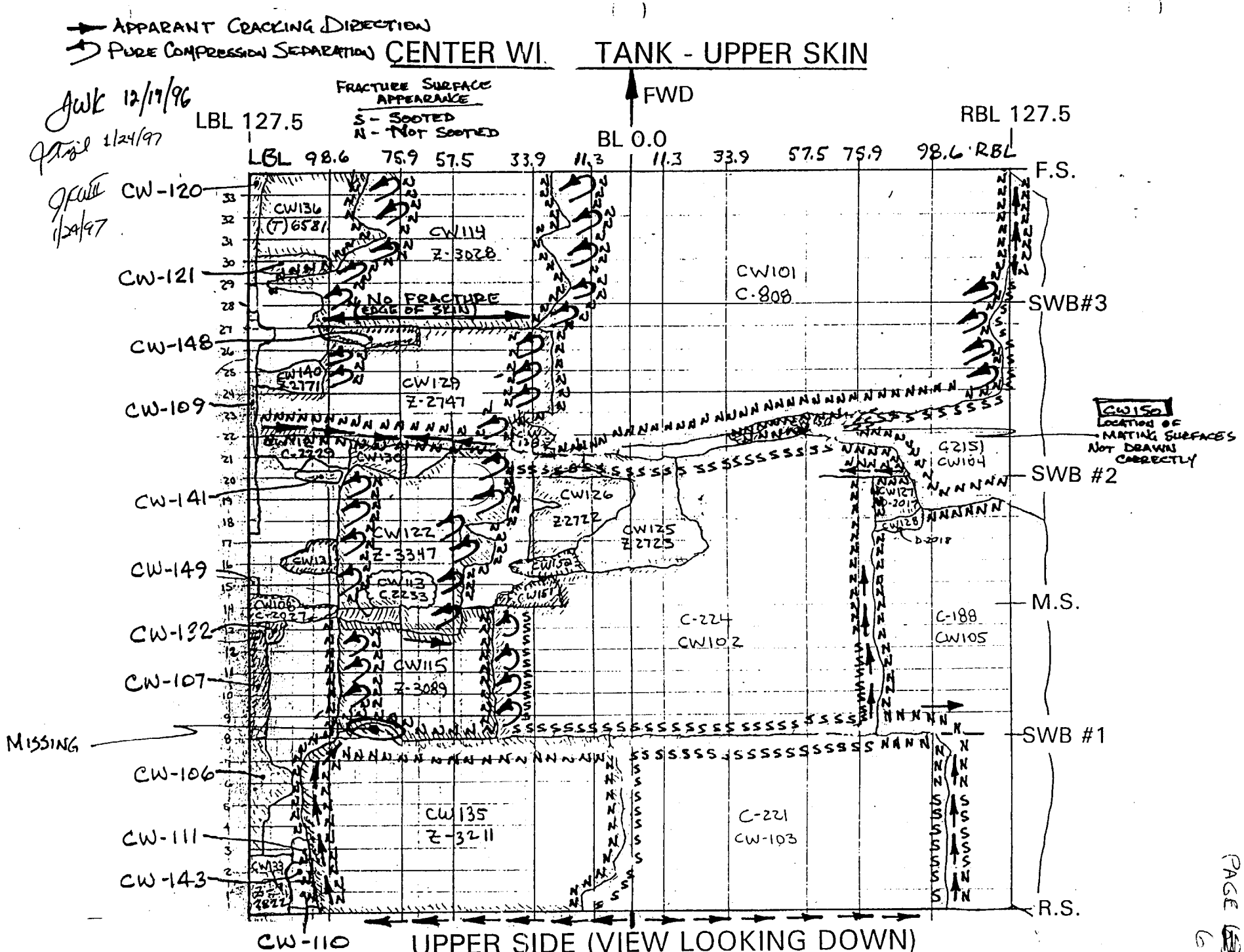
APPARANT CRACKING DIRECTION
PURE COMPRESSION SEPARATION
CENTER WI. TANK - UPPER SKIN
JWK 12/19/96
1/24/97
FRACTURE SURFACE APPEARANCE
S - SOOTED
N - NOT SOOTED
FWD
LBL 127.5
BL 0.0
RBL 127.5
LBL 98.6 75.9 57.5 33.9 11.3 11.3 33.9 57.5 75.9 98.6 RBL
F.S.
SWB#3
SWB #2
SWB #1
M.S.
R.S.
CW-120
CW-121
CW-148
CW-109
CW-141
CW-149
CW-132
CW-107
MISSING
CW-106
CW-111
CW-143
CW-110
CW136 (T) 6581
CW114 Z-3028
CW101 C-808
NO FRACTURE (EDGE OF SKIN)
CW140 Z-2771
CW129 Z-2747
CW130
C-2229
CW104 G215J
CW150 LOCATION OF MATING SURFACES NOT DRAWN CORRECTLY
CW126 Z-2722
CW125 Z-2725
CW127 D-2017
CW128 D-2018
CW122 Z-3347
CW113 C-2233
CW108 C-2027
CW115 Z-3089
C-224 CW102
C-188 CW105
CW135 Z-3211
C-221 CW-103
UPPER SIDE (VIEW LOOKING DOWN)

FIGURE B-1

ZONE _____ SEQUENCE ID NO. LS-1

COMPONENT LOWER SKIN PART ID NO. _____

DESCRIPTION OF POSSIBLE SEQUENCE	SUPPORTING OBSERVATIONS	NON-SUPPORTING OBSERVATIONS	Confidence Level
As a result of the wing breakup, the lower skin apparently separates into 2 major sections. 1. The aft left corner (LBL 100 to LBL 127 and R.S. to S-5) including CW-210, CW-222, CW-212, and CW-224 remain with the left wing. The section from LBL 90 to the S.O.B. from the midspar to S-15 including CW-206, CW-229, CW-219, AND CW-218 stays with the left wing. CW-221 also stays with the left wing. 2. A potential additional secondary failure occurs between CW-203 and CW-204 but CW-204 remains attached to the right wing portion through partial attachment to CW-202 and lower panel stringers 1,2, and 3. 3. The remainder of the lower panel remains with the right wing.	1. Sooted fracture faces on the panels that potentially remain attached to the right wing and unsooted fracture faces on thpse segments that potentially remain attached to the left wing. 2. Exterior surface of CW-210, CW-212, CW-224, and CW-222 are more heavily sooted in comparison to segments fwd and more inbd of them.	1. Exterior soot comparison between CW-221 fwd of stringer S-15 has much lower soot deposits than CW-218 and CW-219 aft of S-15 which could suggest that CW-221 did not remain with left wing. 2. Outbd wing lower skin at the side of body has sooted portions of the side of body interface that are not sooted on CW-221.	Medium
Additional mating clean fracture faces are consistent with water impact or are at least apparently subsequent to the primary wing breakup.		Some local indications of partially sooted fractures exist within areas of clean fracture faces.	Medium

CENTER WING TANK - LOWER SKIN

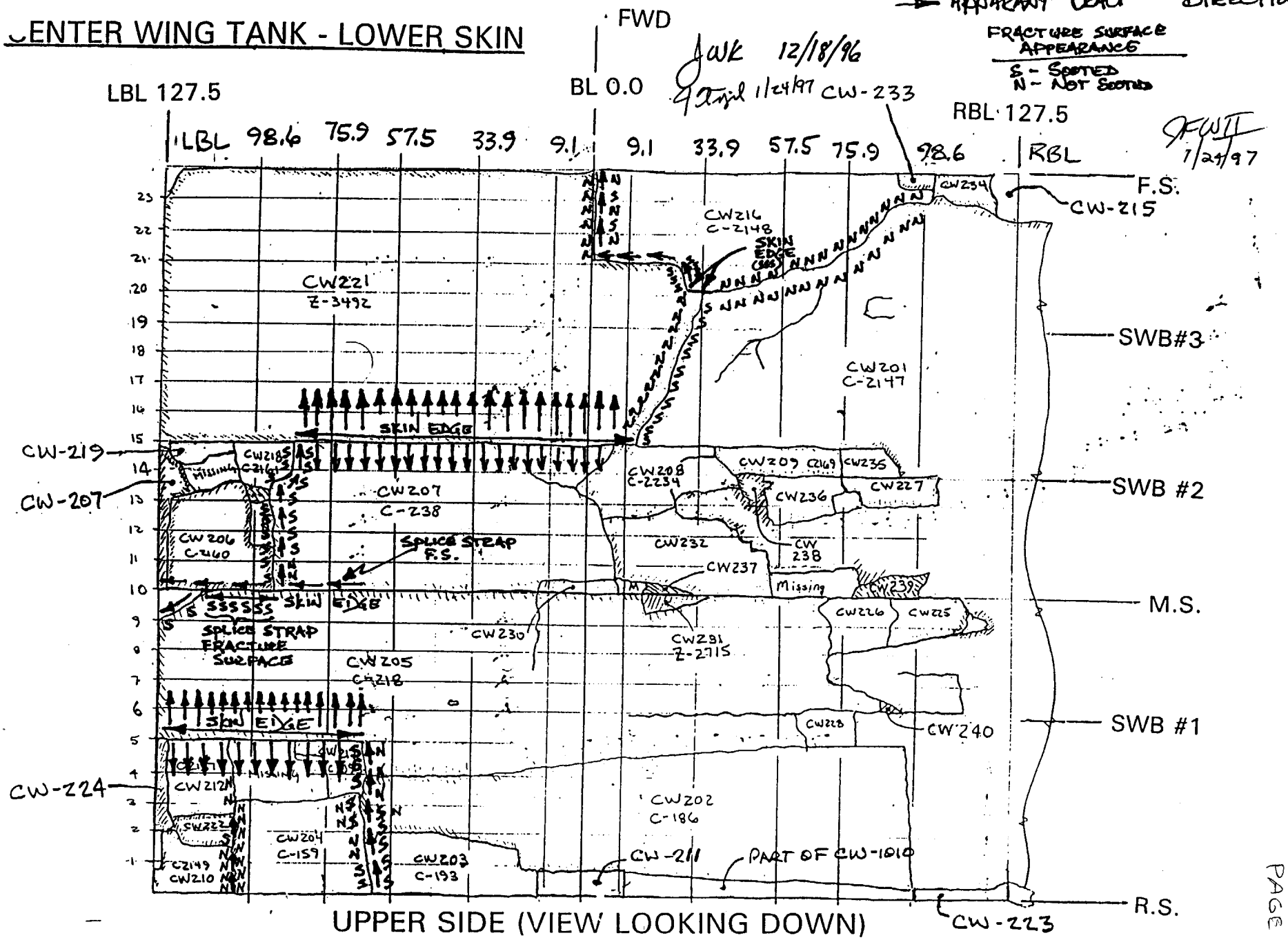

FIGURE B-2

ZONE _____ SEQUENCE ID NO. RS-1

COMPONENT Rear Spar PART ID NO. _____

DESCRIPTION OF POSSIBLE SEQUENCE	SUPPORTING OBSERVATIONS	NON-SUPPORTING OBSERVATIONS	Confidence Level
The upper spar chord web flange and the spar web fractures at LBL 11. The fracture apparently propagates down through the web to near the lower chord and progresses outbd to LBL 60. The lower chord fractures at LBL 60 and LBL 100 and the rear spar would possibly separate into two major sections.	1. The mating fracture between CW-1004 and CW-1006 is sooted on CW-1004 and not sooted on CW-1006. 2. The upper skin panel has a fwd running fracture originating at LBL 11 at the rear spar. This fracture is the major delineation of the upper skin panel for what remained with the right wing. 3. The lower skin panel has a fracture at LBL 100 which originates at the rear spar. This fracture is the major delineation of the lower skin panel between the left and right wing portions.		Medium

ZONE _____ SEQUENCE ID NO. RS-3

COMPONENT Rear Spar PART ID NO. _____

DESCRIPTION OF POSSIBLE SEQUENCE	SUPPORTING OBSERVATIONS	NON-SUPPORTING OBSERVATIONS	Confidence Level
The fractures through the segments to the left of LBL 100 and above CW-1005 and CW-1007 are consistent with water impact damage or at least possibly occurred subsequent to the wing breakup.	Unsooted fractures on mating surfaces of parts.		High

ZONE _____ SEQUENCE ID NO. RS-2

COMPONENT Rear Spar PART ID NO. _____

DESCRIPTION OF POSSIBLE SEQUENCE	SUPPORTING OBSERVATIONS	NON-SUPPORTING OBSERVATIONS	Confidence Level
The fracture patterns are consistent with the fracture in the upper chord propagating to the right to RBL 33 at which point the fracture extends vertically through the spar chord and web between CW-1002 and CW-1004. The fracture apparently continues to run horizontally between CW-1002 and CW-1003.			Medium
Segment CW-1002 separates from CW-1003 below it and the combined sections of CW-1003, CW-1011, and CW-1010 potentially buckle and bow aft which would allow a continuing fire to burn the sections nearest to RBL 33 and the portions that have bowed aft could be out of the direct fire resulting in decreased fire damage.	1. Residual curvature of the combined sections CW-1003, CW-1011, and CW-1010 result in CW-1003 being bent aft of the rear spar by almost 90°. 2. The regions nearest to RBL 33 show the greatest level of fire damage.	Heavy fire damage and distortions are extremely inconsistent across mating fractures and across both the internal and external surfaces.	Low

ZONE _____ **SEQUENCE ID NO.** SWB1-1

COMPONENT SWB #1 **PART ID NO.** _____

DESCRIPTION OF POSSIBLE SEQUENCE	SUPPORTING OBSERVATIONS	NON-SUPPORTING OBSERVATIONS	Confidence Level
Sooting is consistent with overpressure and fire occurring in the wing center section cavity prior to wing breakup with the major portion of the structure apparently remaining intact.	Deformation (with subsequent sooting) on aft side of access doors between nutplate attachments indicates intact pressure capability of not only the access doors but also the remainder of the local primary structure during an overpressure event and subsequent fire.		High
During wing breakup, the fractures in the spanwise beam occur between CW-902 and CW-901, between CW-901 and CW-906, and between CW-907 and the left side of body rib.	Electrical conductivity measurements between adjacent sections show similar conductivity readings indicative of similar thermal exposure.		Medium
Right to left wing separation may occur between left side of body rib and CW-907.	1. Soot inside upper splice fitting which is common to the left upper wing splice. 2. Electrical conductivity and sooting commonality on all adjacent spanwise beam segments.		Medium
Major damage to the access doors occurs after soot exposure.	No apparent soot on exposed honeycomb material on door.		Medium

ZONE _____ **SEQUENCE ID NO.** MS-1

COMPONENT Midspar **PART ID NO.** _____

DESCRIPTION OF POSSIBLE SEQUENCE	SUPPORTING OBSERVATIONS	NON-SUPPORTING OBSERVATIONS	Confidence Level
During the keel beam separation, the tension fasteners common to the keel beam fracture and the downward motion of the keel beam produces the residual bending of the keel beam tension bolts as shown in figure B-3.	1. Tension fasteners are bent aft 60 degrees as shown in figure B-1. 2. Drag mark exists on forward side of the tension fastener hole in the lower skin panel.		Medium

MIDSPAR

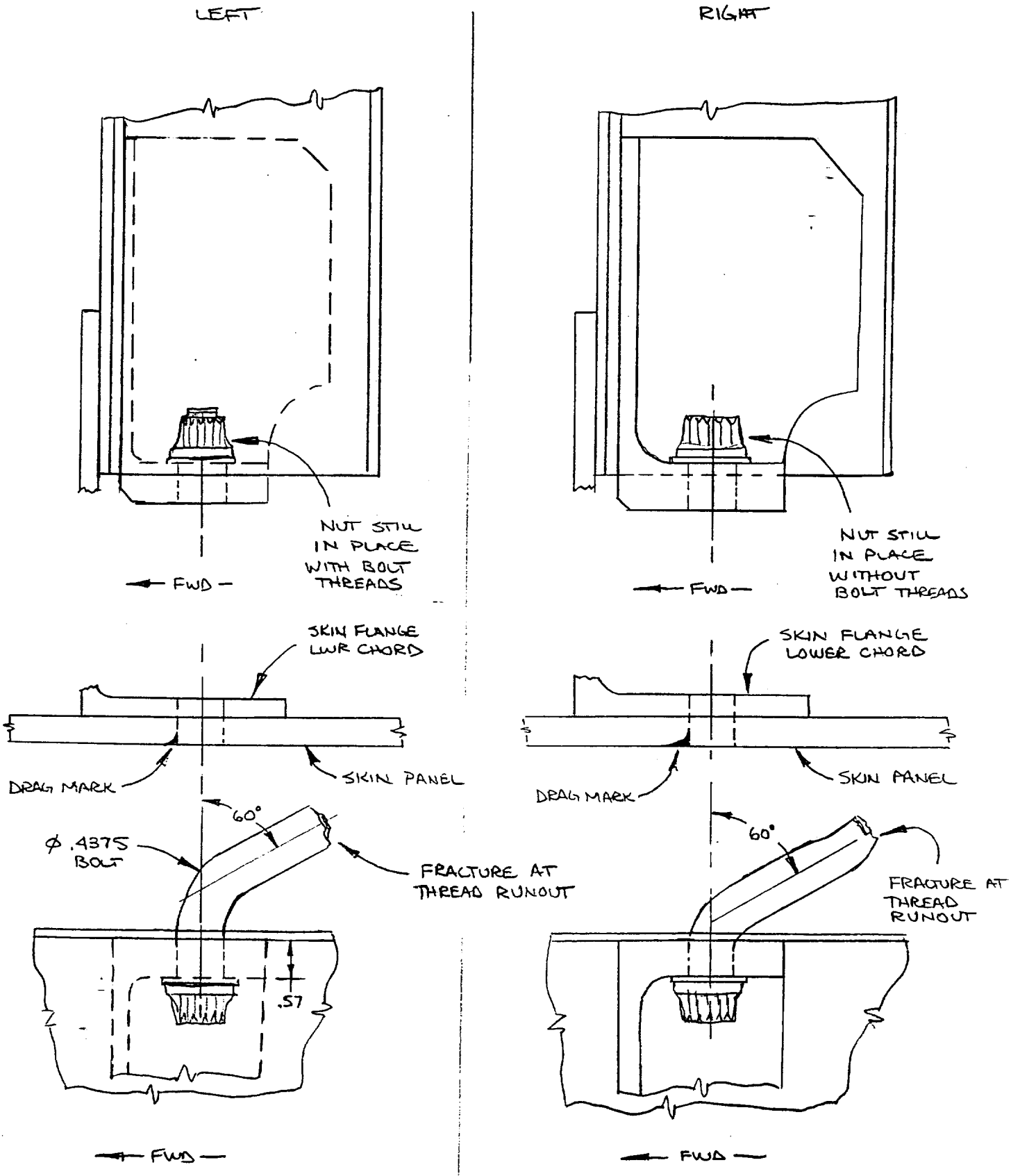

FIGURE B-3

ZONE _____ SEQUENCE ID NO. BL0-1

COMPONENT BL 0 Rib PART ID NO. _____

DESCRIPTION OF POSSIBLE SEQUENCE	SUPPORTING OBSERVATIONS	NON-SUPPORTING OBSERVATIONS	Confidence Level
An inflection point at BL 0 is forced during upper panel buckling and apparent subsequent compression fractures of the upper panel during wing breakup.	Buckling pattern of the upper wing skin shows inflection at BL 0.		Medium
BL 0 rib remained with the right wing after major airplane breakup.	Consistent level of fire damage and soot accumulation on the rib and adjacent structure that remained with the right wing after major airplane breakup.		Medium

ZONE _____ SEQUENCE ID NO. SWB2-1

COMPONENT SWB#2 PART ID NO. _____

DESCRIPTION OF POSSIBLE SEQUENCE	SUPPORTING OBSERVATIONS	NON-SUPPORTING OBSERVATIONS	Confidence Level
Spanwise beam is possibly intact prior to the keel beam tension bolt fracture. The condition of the related parts is shown in figure B-4.	Keel beam tension fasteners failed by stripping threads out of the nut indicating relatively pure tension loading with low bending forces.	Structure from left side of SWB#2 not recovered or identified	Medium
Resultant web shear from the keel beam loads induced while fracturing the keel beam tension bolts is consistent with initiating shear failure of the access door fasteners common to stiffeners and surround structure shown in zone A on figure B-5. This could also be as a result of overpressure in the WCS.	1. Shear failure of fasteners common to the stiffeners, surround structure, and the manufacturing access door. Examination of the sheared rivets in the stiffener shows the door attach structure moving down relative to the access door. 2. Indication of early shear tie failure at the upper panel attachment of stiffener at RBL 17.2 due to partially sooted fracture on skin flange of the upper chord.		Medium
Additional out of plane forces (pressure on aft surface of door) results in tension separation of the remainder of the fasteners holding the manufacturing access door to the adjacent web and stiffeners shown in zone B on figure B-3.	1. Zone B fastener failures are as a result of tension (prying). 2. Impact damage on lower inboard edge of door matches closely with two sets of witness marks on the underside of the upper skin panel and stringer.		Medium
Access door exits Wing Center Section after breakup of Spanwise Beam #3 and the Front Spar and exits fuselage (after breakup of fuselage red zone pieces). Access door exits prior to fire damage	1. Access door recovered from red debris field. 2. Access door has only apparent light sooting. 3. Front spar, spanwise beam #3, and fuselage must fail for door to exit. 4. Unsooted web fracture face on the web remaining attached to the access door with sooted fracture faces on the web remaining on CW-702.		High

ZONE _____ SEQUENCE ID NO. SWB2-2

COMPONENT SWB#2 PART ID NO. _____

DESCRIPTION OF POSSIBLE SEQUENCE	SUPPORTING OBSERVATIONS	NON-SUPPORTING OBSERVATIONS	Confidence Level
Impact forces subsequent to major fire damage result in separation of the web and lower chord on segment CW-702 with the lower chord moving up relative to the web.	1. Examination of sheared rivets in CW-702 show vertical directionality. 2. Impact marks in fillet radius of lower chord common to CW-702 with some evidence of damage to the web lower edge. 3. Impact marks on the lower skin panel consistent with rivet pattern on the lower chord skin flange and remaining portion of rivets in chord "pounded" upward out of the fastener hole.		Medium
Damage consistent with water impact or at least subsequent to major fire results in sections CW-701, CW-702, and CW-708 suffering impact related damage occurring at a location approx. 28 inches above the lower surface with an inboard directed impact originating near the right S.O.B. rib. The applied force could apparently fold up the sections to approx. RBL 66.	1. Deformations are subsequent to fire damage since the sections are equally sooted on all surfaces (inside or outside on folded material) 2. Section CW-702 lower web to chord attachment is unsooted on the web surface while the surrounding web is sooted. 3. Reconstruction activity shows extreme similarity in corrosion "halo" effect and soot accumulation levels on CW-701 and CW-702. 4. Side of Body rib web attached to CW-701 is sooted on the inbd surface but clean on the outbd surface.		Medium

SWB # 2

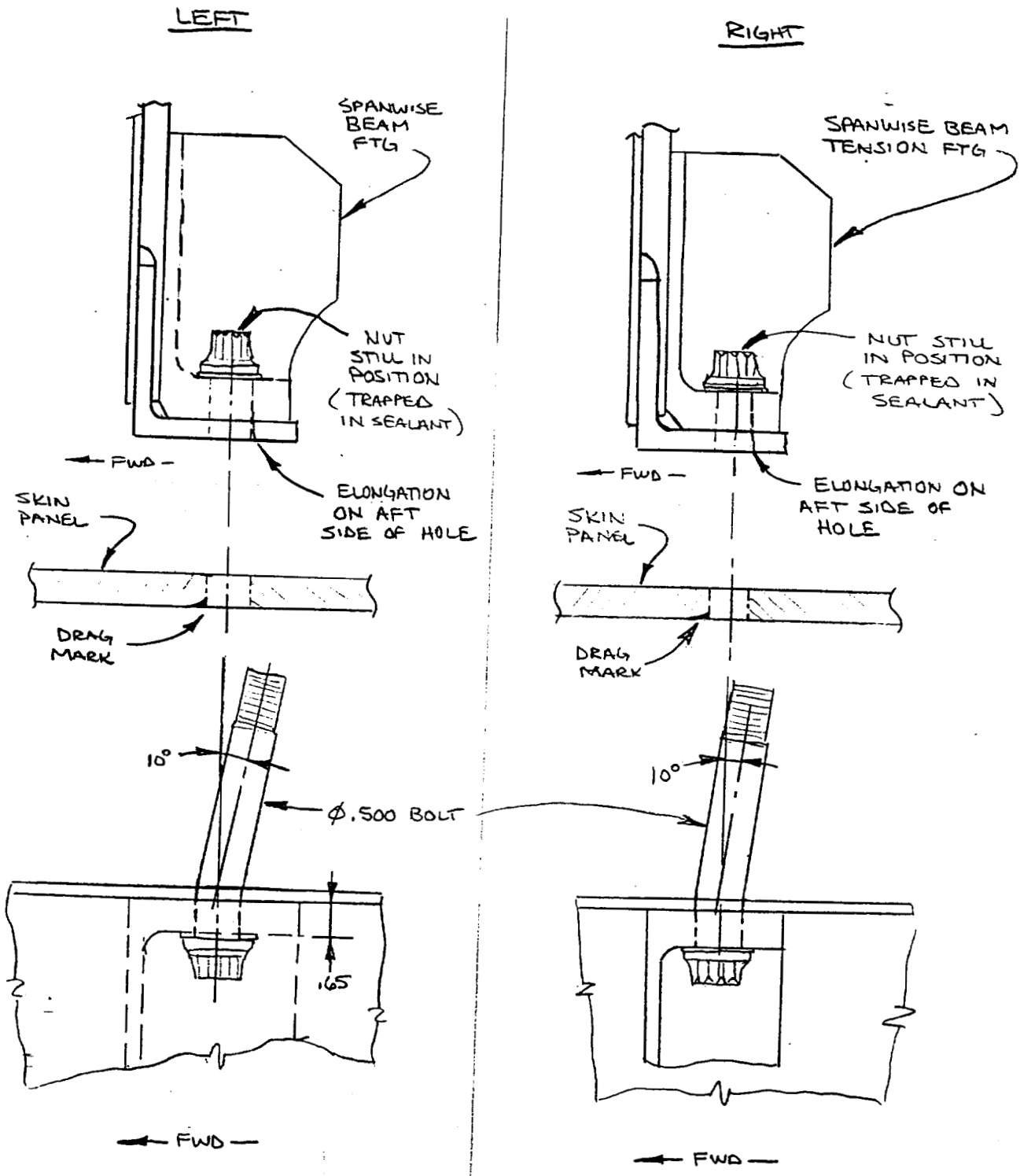

FIGURE B-4

SPANWISE BEAM # 2
MANUFACTURING ACCESS DOOR (CW703)

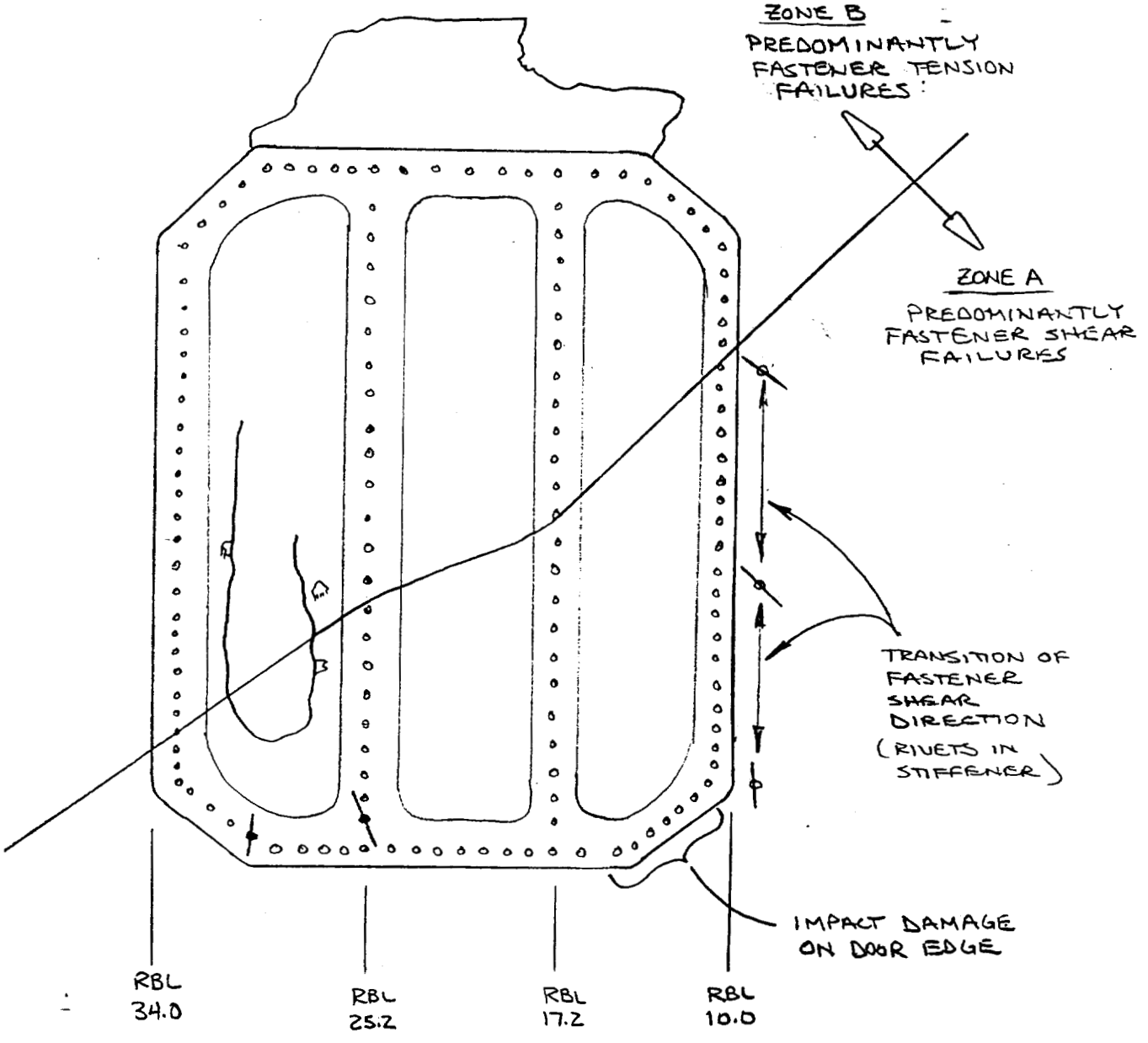

FRONT VIEW
UP
INBD

FIGURE B-5

ZONE _____ SEQUENCE ID NO. SWB3-1

COMPONENT SWB #3 PART ID NO. _____

DESCRIPTION OF POSSIBLE SEQUENCE	SUPPORTING OBSERVATIONS	NON-SUPPORTING OBSERVATIONS	Confidence Level
During an early event in the wing center section, the spanwise beam #3 apparently rotates fwd at the upper end of the beam and rotated aft at the lower end. The rotation of the beam was possibly centered around the top of the lower intercostals except for CW-603 (see SWB3-3). See figure B-8.	1. The lower shear ties have elongated holes and witness marks from the fasteners common to the lower skin showing an aft movement of the shear tie relative to the skin. 2. The three indicators of fwd movement of the upper chord are: (1) fastener tension failures common to the web flange of the SWB chord and the floor beam tension fittings, (2) fastener hole elongation in the skin panel at the shear tie attachments, and (3) witness marks on the remnant of the spar chord vertical flange where the fasteners common to the shear ties translated fwd.		High High
There was possible slight upward movement of the skin panel relative to the SWB upper shear ties while the SWB web was rotating fwd.	There is downward elongation of the holes in the floor beam tension fittings and witness marks on the forward side of the skin panel shear tie holes in the skin panel.		Medium

ZONE _____ SEQUENCE ID NO. SWB3-2

COMPONENT SWB #3 PART ID NO. _____

DESCRIPTION OF POSSIBLE SEQUENCE	SUPPORTING OBSERVATIONS	NON-SUPPORTING OBSERVATIONS	Confidence Level
The first fracture generated in the SWB web was possibly at the mating fracture of CW-610 (green zone) and CW-604 (red zone) at LBL 83. CW-610 could remain attached to CW-606 to its left and rotate fwd and to the left.	1. Shear fracture (tearing) between CW-610 and CW-604 indicates CW-610 shearing fwd of CW-604 (the burr is on the aft side of CW-610 and on the fwd side of CW-604). 2. The inbd edge of the web on CW-606 is bent fwd on a 90° angle indicating possible residual deformation.	Residual deformation may be secondary damage.	Medium Low
The remaining portions of SWB are apparently rotated fwd in progression starting with CW-604 (as noted above) and following with CW-603 and then CW-602.	1. Shear fractures between the successive SWB segments indicate the segment to the left of the fracture tearing fwd of the segment to the right. This fracture direction is consistent until the fracture progresses down to approx. 10" above the lower chord at which time the fracture angle and the burr generated from the tearing action switches from the aft side to the fwd side on the segment to the left of the fracture. 2. Recovery field location suggests CW-604 first SWB#3 segment in debris field followed by CW-603 and then CW-602. 3. Soot accumulation on the fwd side of the web generally increases from the left to the right.	There are minimal shear burrs produced on the mating fracture between CW-603 and CW-602 possibly indicating a different fracture type between those two segments and therefore the indicated progression may not be valid between those two segments based on fracture examination.	Medium

ZONE _____ SEQUENCE ID NO. SWB3-3

COMPONENT SWB #3 PART ID NO. _____

DESCRIPTION OF POSSIBLE SEQUENCE	SUPPORTING OBSERVATIONS	NON-SUPPORTING OBSERVATIONS	Confidence Level
As segment CW-603 rotates fwd, the lower tension fittings common to the keel beam may fracture through the pad of the tension fitting but not failing the tension bolts. Since there are no lower intercostals fwd of the spanwise beam in this section, this segment may rotate about the lower chord.	1. The tension bolt common to the left tension fitting has a portion that remains in the skin panel and a portion that remains in the keel beam. Based on the length of the remaining bolt segments, the tension fitting had to fracture prior to the tension bolt failure for the bolt to be able to remain in the hole and then be pulled down further into the hole as compared with it's original position when the SWB#3 tension fitting was intact. 2. The lower chord fracture (just above the chord fillet radius) originates near the left and right keel tension fittings and propagates outward from those locations. 3. The tension bolt common to the tension fitting at RBL 9.0 is fractured at the transition of the shank into the threads. 4. Fracture of tension fitting end pad is consistent with bending of tension fitting around the lower SWB chord. (See figures B-6 and B-7 to clarify supporting observations)		High
Tension fitting fracture results in loss of tension bolt clamp-up and .65 freeplay in the joint to the keel beam.	Review of structural features.		High

ZONE _____ SEQUENCE ID NO. SWB3-4

COMPONENT SWB #3 PART ID NO. _____

DESCRIPTION OF POSSIBLE SEQUENCE	SUPPORTING OBSERVATIONS	NON-SUPPORTING OBSERVATIONS	Confidence Level
The right portions of the spanwise beam which are heavily fire damaged may remain with the right wing. The sections of spanwise beam may not have remained attached to the upper panel during wing breakup but possibly remained in the cavity between the front spar and SWB#2.	1. The fire damage is consistent with the level of soot accumulation and fire damage to the upper skin panel interior. 2. Both the stiffener that attaches the spanwise beam web to the side of body rib and the spanwise beam web are sooted on the interface whereas the stiffener to side of body rib interface is unsooted on both the stiffener and the S.O.B. web.		Medium

SWB #3 - LEFT FTG.

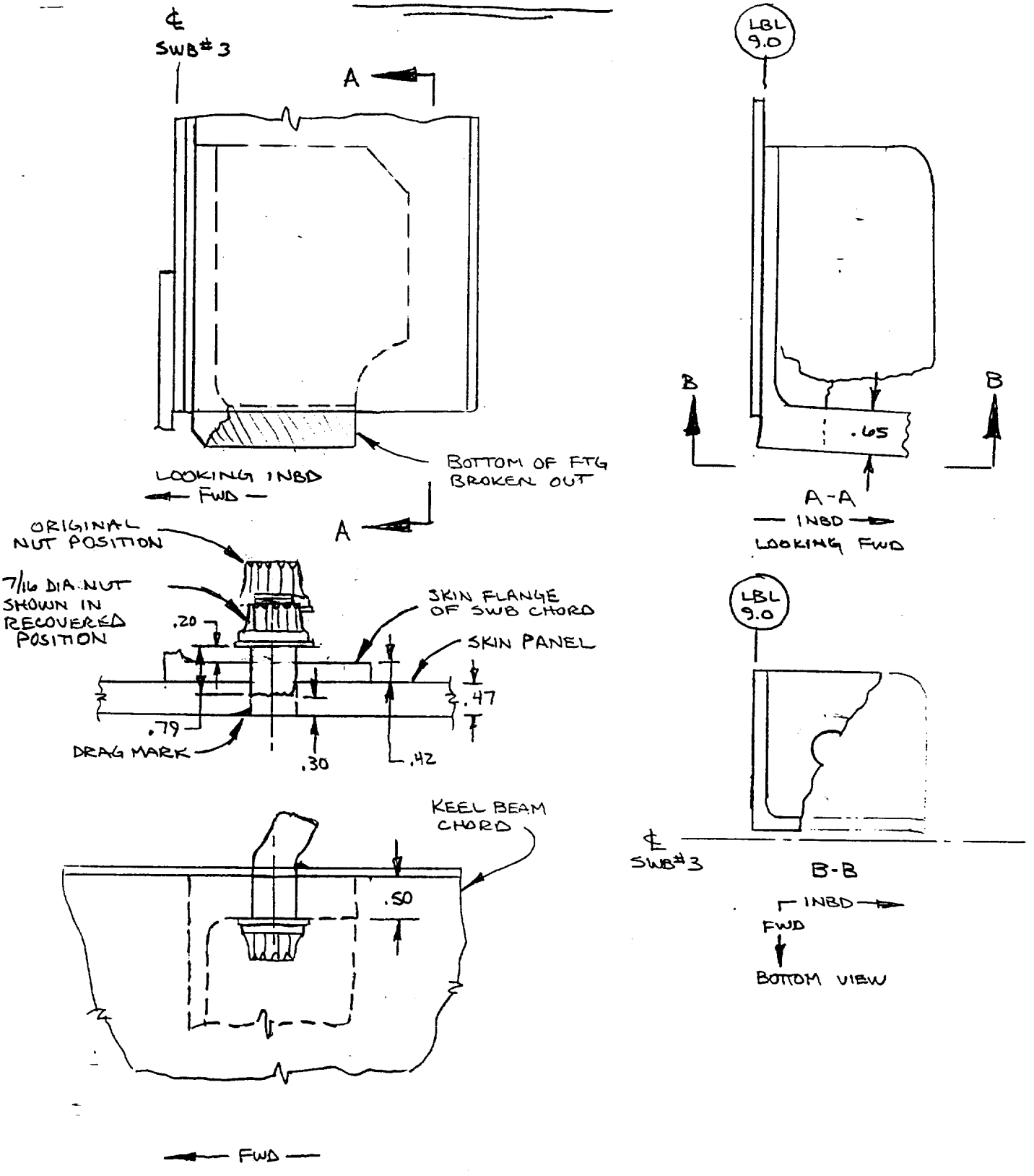

FIGURE B-6

SWB #3 - RIGHT FTG

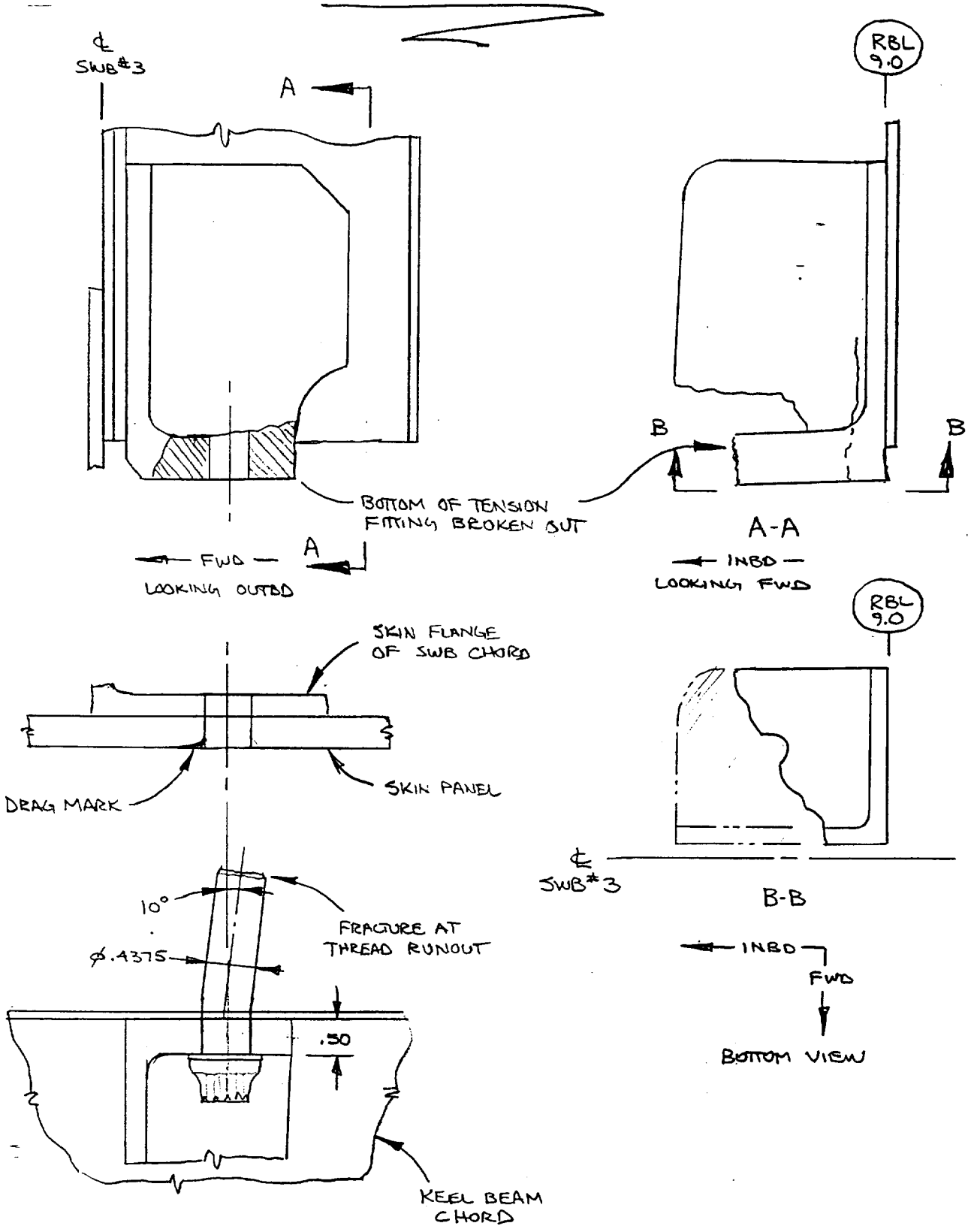

FIGURE B-7

ZONE _____ SEQUENCE ID NO. FS-1

COMPONENT FRONT SPAR AND LWR PRESSURE BULKHEAD

DESCRIPTION OF POSSIBLE SEQUENCE	SUPPORTING OBSERVATIONS	NON-SUPPORTING OBSERVATIONS	Confidence Level
As a result of spanwise beam #3 rotating fwd, the upper chord of the spanwise beam impacts the aft side of the front spar stiffeners. This results in crushing of the aft side of the stiffeners at a location shown in figure B-8.	Impact marks and damage on the aft side of the front spar stiffeners at a distance of approx. 12" below the upper stiffener shear ties. The damage on the aft side of some of the stiffeners shows two distinct impact marks with 3" vertical separation that equals the chord height of the spanwise beam upper chord.		High
The applied impact force on the aft side of the stiffeners and local buckling of the stiffeners at the impact zone results in bending of the upper spar chord between the vertical and horizontal flange. Overpressure loads may also contribute. This bending moment results in a fracture in the fillet radius of the upper spar chord.	Multiple initiation sites of the upper spar chord fracture coincident with the floor beam locations at RBL 75 and 57.5, and LBL 11, 33, 75, and 98. These fractures are a bending type fracture with the lower edge of the chord moving fwd relative to the skin flange of the chord. At all of these locations, the chord has a slight residual deformation indicative of an inbd/outbd bowing of the vertical flange of the chord. See figure B-13.		High
The one fracture in the upper spar chord fillet radius that originates at RBL 57.5 apparently progresses inbd from RBL 57.5 and propagates out of the fillet radius and down into the vertical flange near RBL 48.	Metallurgical review of fracture faces.		High
Once the upper chord of the front spar is separated from the upper skin, overpressure loads and the resulting downward loading of the forward end of the keel beam is reacted by shear loading of the front spar and lower pressure bulkhead.			High

ZONE _____ SEQUENCE ID NO. FS-2

COMPONENT FRONT SPAR AND LWR PRESSURE BULKHEAD

DESCRIPTION OF POSSIBLE SEQUENCE	SUPPORTING OBSERVATIONS	NON-SUPPORTING OBSERVATIONS	Confidence Level
The upper chord and web deflect fwd in a wave shape as depicted in figure B-13. The area around BL 0 is partially restrained by the mass of the water bottles and the keel beam attachment.	Residual curvature of the upper spar chord and web segments generally show maximum fwd curvature near LBL 66 and RBL 66 with reverse curvature near BL 0 as depicted by figure B-13.		High
Forward rotation of the front spar buckles the stiffeners splicing the lower pressure bulkhead to the front spar.	1. The lower pressure bulkhead stiffeners (except at LBL 18) are bent fwd and the forward free flange is buckled. 2. The stiffener at LBL 18 has minor fwd bending which is indicative of less fwd rotation near the center of the front spar above the keel beam.		High
The fractures through the fillet radius of the upper spar chord separate the front spar from the upper skin panel and the vertical flange of the upper spar chord and web is put into tension and results in tension fractures in the vertical flange of the spar chord and web at LBL 66.6 and RBL 48. There is also a tension type fracture of the upper spar chord near RBL 66.	Tension fracture of the vertical flange and adjacent upper edge of the spar web at LBL 66.6 and RBL 48. There is a tension fracture of the vertical flange of the spar chord at RBL 66 but the web exhibits bending prior to separation. It cannot be determined at this time if the vertical fracture at LBL66.6 or RBL 48 occurs first.		Medium
The tension loading of the spar web apparently continues and manifests itself as a tension failure of the spar web in vertical splits propagating downward occurring at LBL 66 and at both RBL 66 and 48. The vertical tearing of the web on the right side converges at RBL 66 near the lower spar chord.	The web of the front spar at LBL 66 in the region below CW-515 shows reversing slant fractures (indicative of a tension fracture) on both CW-504 and CW-502. The region just below the upper chord at RBL 48 also exhibits the same reversing slant fracture.	The remainder of the web fractures at LBL66 and both RBL 66 and 48, other than those noted in the previous paragraph indicate fractures other than tension.	Medium
The web fracture between CW-501 and CW-502 are secondary to the other primary fractures.	Bending indications at the mating fractures of the upper chord vertical flange and the web. Heavy bending and twisting fracture at the vertical flange fracture of the lower spar chord.		Medium

ZONE _____ SEQUENCE ID NO. FS-3

COMPONENT FRONT SPAR PART ID NO. _____

DESCRIPTION OF POSSIBLE SEQUENCE	SUPPORTING OBSERVATIONS	NON-SUPPORTING OBSERVATIONS	Confidence Level
With the front spar web separated at LBL 66 and RBL 66, the downward loads on the forward end of the keel beam result in a shear failure of the rivets connecting the lower pressure bulkhead web to the front spar web.	Web attachment fasteners common to the front spar web and lower pressure bulkhead web indicate a shear direction of approximately 45 degrees down and inward from LBL 33 to LBL 75 and from RBL 26 to RBL 75 (entire outboard portion of the web). See figure 4-10.		Medium
Continued downward loading on the forward portion of the keel beam results in vertical separation of the lower pressure bulkhead web at LBL 66 and RBL 66.	Downward progressing fractures through the lower pressure bulkhead web at LBL 66 and RBL 66 are at locations corresponding to early fractures in the front spar web. Fracture patterns are symmetric left to right. See figure 4-10.		Medium
Continued downward loading on the fwd portion of the keel beam is transmitted to the ring chord and fuselage skin just forward of the ring chord at LBL 66 and RBL 66.	Early fractures in the ring chord and fuselage at LBL 66 and RBL 66. See figure 4-11, 6-1, and 6-2.		Medium
Loss of cargo floor and fuselage structure forward of the front spar allows final liberation of the front spar red area pieces.	1. Minor damage to the front side of the potable water bottles mounted on the forward side of the front spar indicative of no impact between the bottles and cargo floor structure. 2. Bending/buckling fracture of the stiffeners between the front spar and lower pressure bulkhead. 3. Fracture of the front spar lower chord in the chord fillet radius, originating on each side near LBL 75 and RBL 75.		Medium

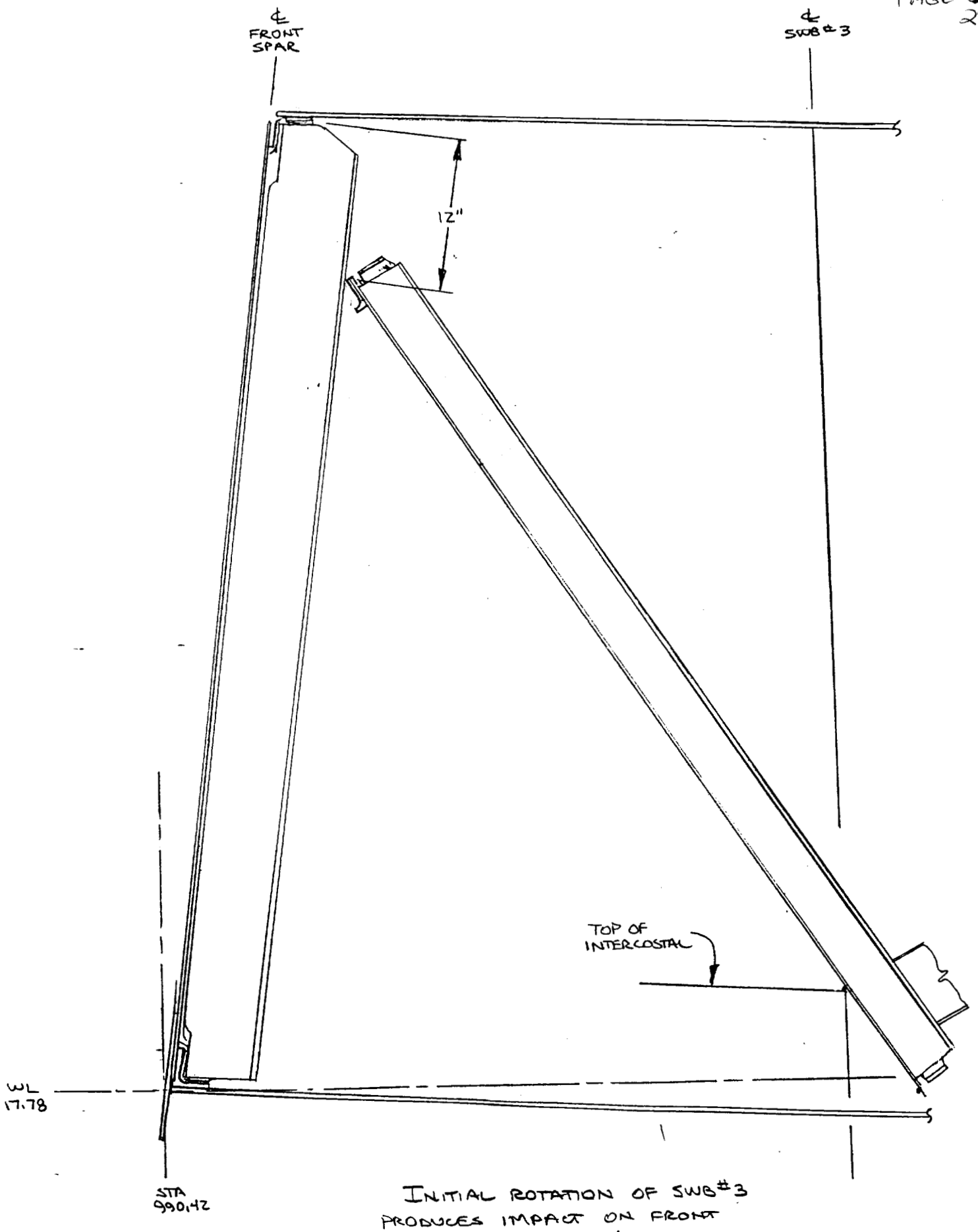

INITIAL ROTATION OF SWB #3 PRODUCES IMPACT ON FRONT SPAR IN A ZONE 12" BELOW THE UPPER SPAR CHORD.

FIGURE B-8

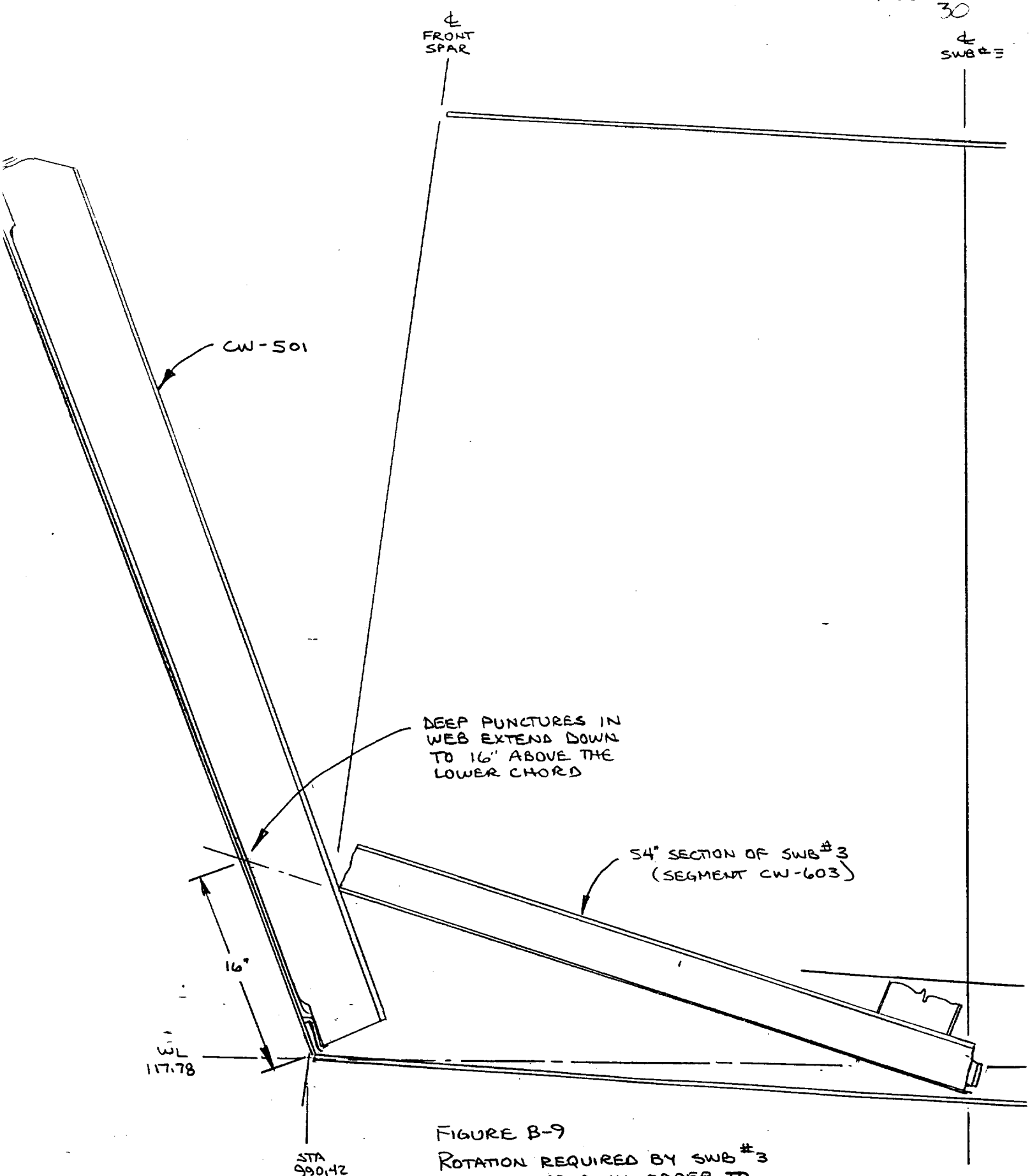

FIGURE B-9

ROTATION REQUIRED BY SWB #3 AND FRONT SPAR IN ORDER TO PRODUCE DEEP SPLITS IN THE FRONT SPAR WEB AT RBL AND LBL 6.0 (ASSUMING CW-603 ROTATES ABOUT LWR CHORD)

KEEL BEAM
BS. 1000

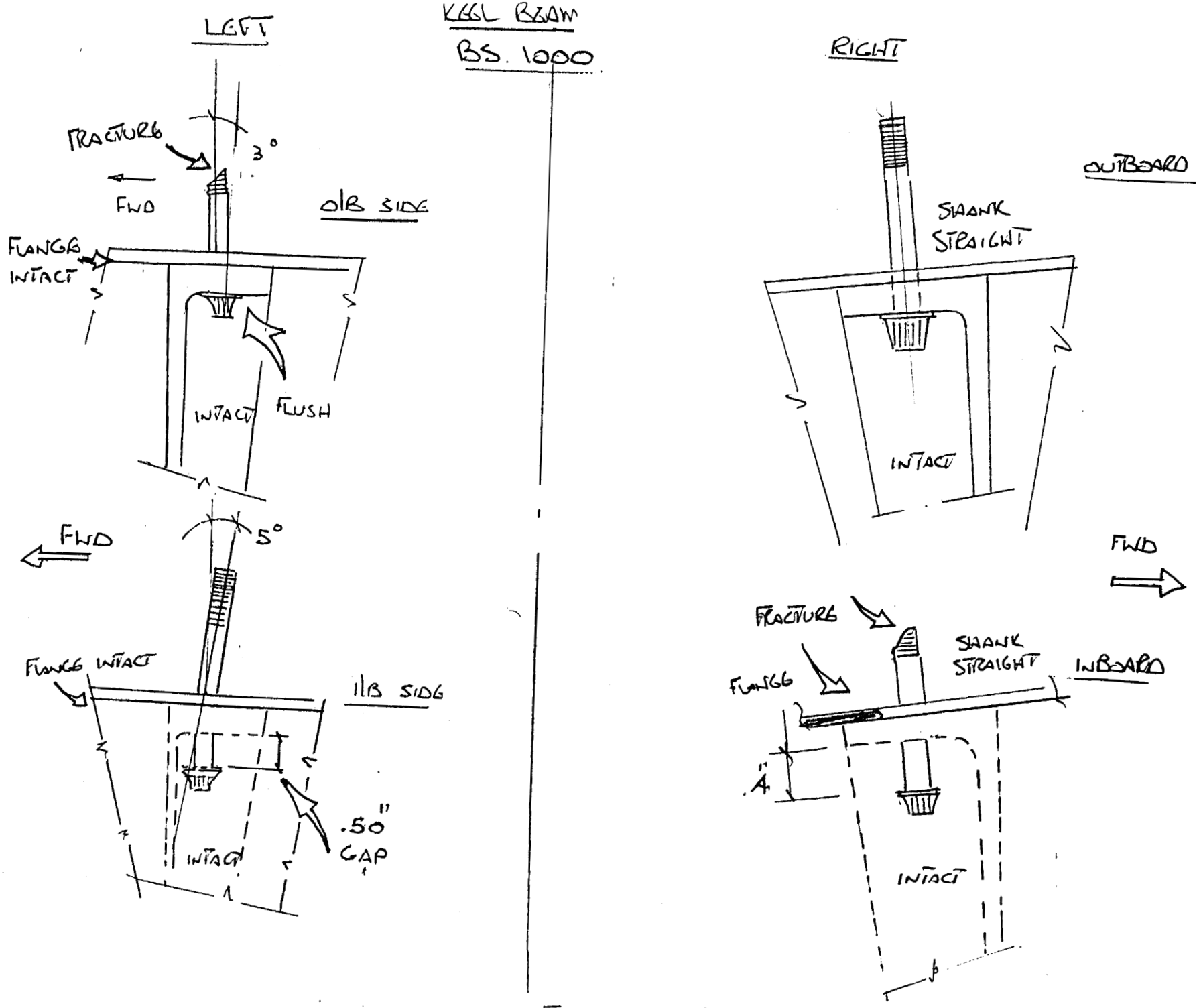

FIGURE B-10

FRONT SPAR AND KEEL BEAM INTERFACE

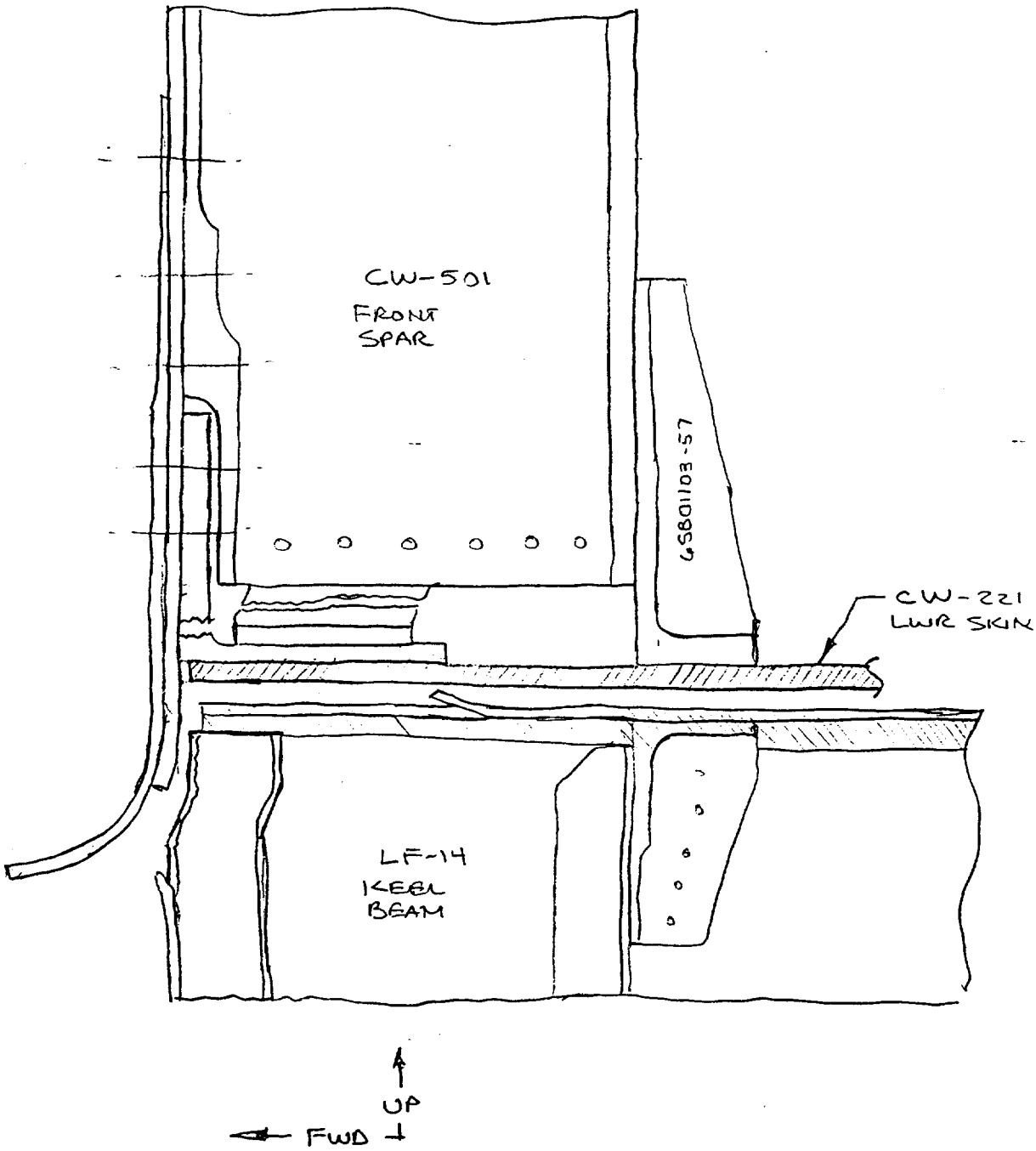

FIGURE B-11

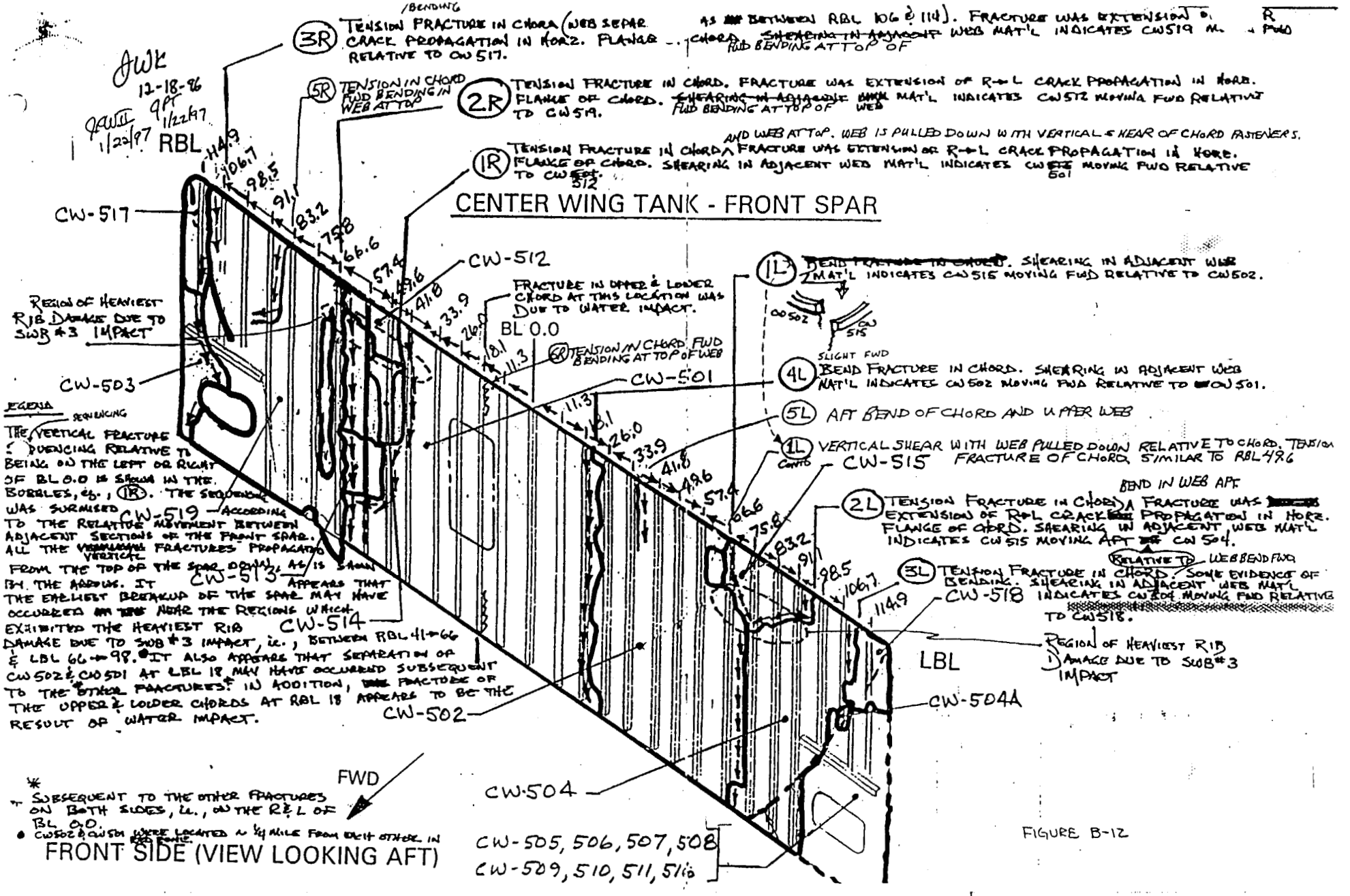

EGENCE SEQUENCING

THE VERTICAL FRACTURE SEQUENCING RELATIVE TO BEING ON THE LEFT OR RIGHT OF BL 0.0 IS SHOWN IN THE BUBBLES, e.g., (1R). THE SEQUENCE WAS SURMISED ACCORDING TO THE RELATIVE MOVEMENT BETWEEN ADJACENT SECTIONS OF THE FRONT SPAR. ALL THE VERTICAL FRACTURES PROPAGATED FROM THE TOP OF THE SPAR DOWN, AS IS SHOWN BY THE ARROWS. IT APPEARS THAT THE EARLIEST BREAKUP OF THE SPAR MAY HAVE OCCURRED AT OR NEAR THE REGIONS WHICH EXHIBITED THE HEAVIEST RIB DAMAGE DUE TO SUB #3 IMPACT, i.e., BETWEEN RBL 41 & 66 & LBL 66 & 98.* IT ALSO APPEARS THAT SEPARATION OF CW502 & CW501 AT LBL 18 MAY HAVE OCCURRED SUBSEQUENT TO THE OTHER FRACTURES* IN ADDITION, FRACTURE OF THE UPPER & LOWER CHORDS AT RBL 18 APPEARS TO BE THE RESULT OF WATER IMPACT.

* SUBSEQUENT TO THE OTHER FRACTURES ON BOTH SIDES, i.e., ON THE R & L OF BL 0.0.

• CW502 & CW501 WERE LOCATED ~ ½ MILE FROM EACH OTHER IN THE FWD FUSE.

FIGURE B-12

JWK 12-18-96
JWK 9PT 1/22/97
JWK 1/22/97

CENTER WING TANK - FRONT SPAR

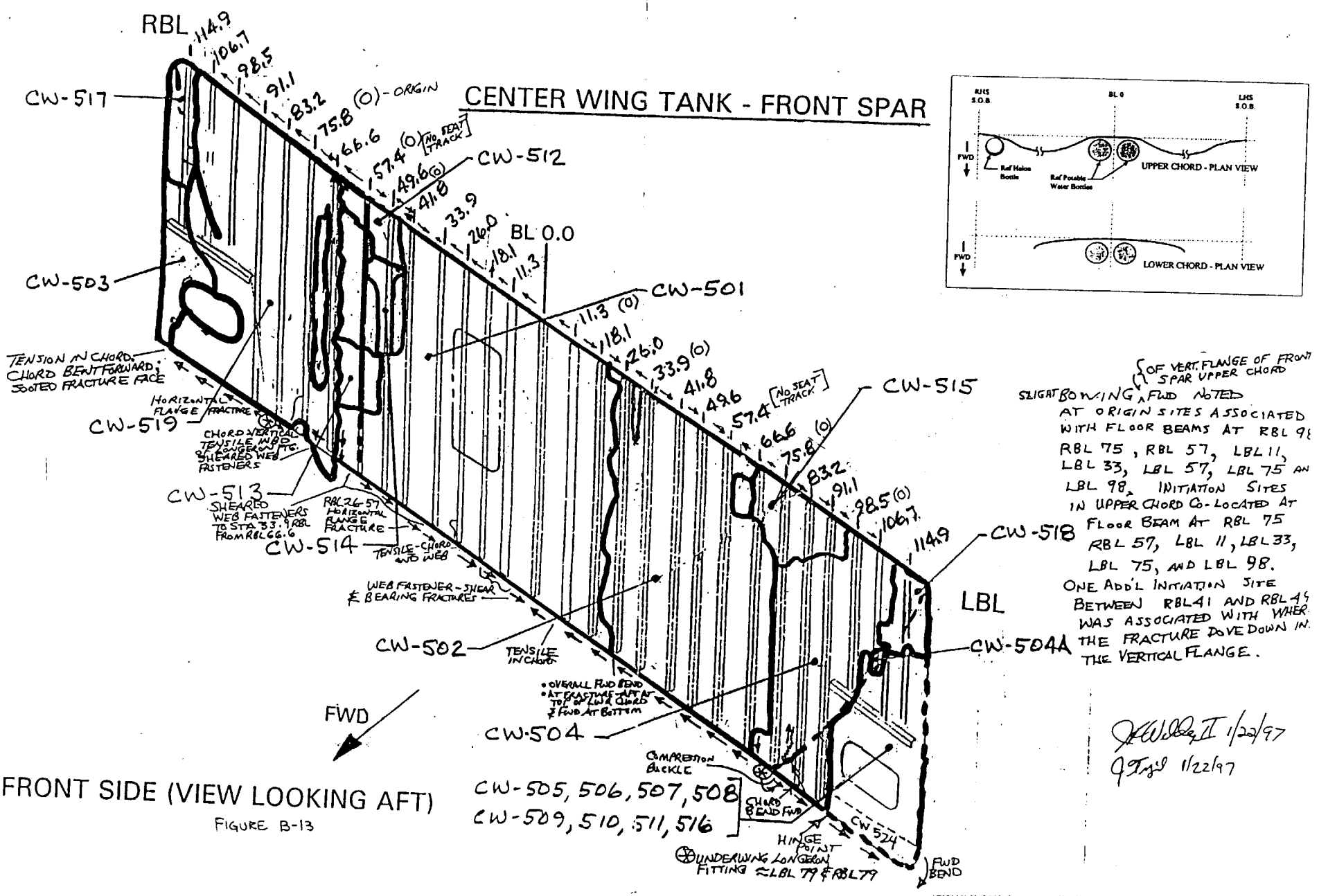

SLIGHT BOWING OF VERT. FLANGE OF FRONT SPAR UPPER CHORD FWD NOTED AT ORIGIN SITES ASSOCIATED WITH FLOOR BEAMS AT RBL 9[illegible] RBL 75, RBL 57, LBL 11, LBL 33, LBL 57, LBL 75 AND LBL 98. INITIATION SITES IN UPPER CHORD CO-LOCATED AT FLOOR BEAM AT RBL 75 RBL 57, LBL 11, LBL 33, LBL 75, AND LBL 98. ONE ADD'L INITIATION SITE BETWEEN RBL 41 AND RBL 49 WAS ASSOCIATED WITH WHERE THE FRACTURE DOVE DOWN IN THE VERTICAL FLANGE.

J K Wilday II 1/22/97

J Tigl 1/22/97

FIGURE B-13

ZONE _____ SEQUENCE ID NO. KBM-1

COMPONENT KEEL BEAM PART ID NO. _____

DESCRIPTION OF POSSIBLE SEQUENCE	SUPPORTING OBSERVATIONS	NON-SUPPORTING OBSERVATIONS	Confidence Level
The SWB#3 tension fittings common to the keel beam fracture through the end pad of the fitting resulting in loss of bolt clamp-up and .65 freeplay in the joint.	See sequence page SWB3-3 regarding tension fasteners common to the keel beam and the SWB#3 tension fittings.		
Front spar rotation results in separation of 5/16 diameter tension fasteners common to the keel beam.	The fastener common to the keel beam tension fittings have either fractured in the threads or have stripped the threads from the nuts. The shank of the fasteners that remain attached to the keel beam are relatively straight as shown in figure B-10.		High
With vertical loads being applied at the forward end of the keel beam common to the lower keel beam chord splice (to LF6A), fractures are initiated at the fwd end of the upper keel beam chord attachment common to the lower center section skin panel and the fasteners that attach the chord to the skin.	Separation of the keel beam upper chord from the lower center section skin panel was as a result of a combination of both rivet tension failure and upper chord horizontal flange tearing from the front spar to the midspar. The upper chord tearing failures have multiple initiation sites that predominantly initiate near the intersection of lower skin panel stringers. At the stringer locations, the keel chord is attached with titanium fasteners instead of rivets and would possibly provide additional restraint prior to separation of the keel chord and the skin. See figure B-14 for upper chord fracture directions common to forward keel beam.	There is a zone of fastener shear failures between S-11 and S-13 between zones of fastener tension failures.	Medium
Downward motion of the fwd end of the keel beam bottoms out the .65 freeplay in the tension fasteners common to SWB#3 and results in tension failure of the fasteners.	The fastener common to the left tension fitting indicates tension related failure and the remaining portion of the upper portion of the fastener has been pulled into the hole in the skin panel by an amount greater than the equivalent thickness of the end pad of the SWB#3 tension fitting. See figure B-6.		Medium
Continued downward motion of the forward end of the keel beam results in the tensile separation of the SWB#2 tension fasteners common to the keel beam.	See sequence page SWB2-1 regarding tension fasteners common to the keel beam.		

ZONE _____ SEQUENCE ID NO. KBM-2

COMPONENT KEEL BEAM PART ID NO. _____

DESCRIPTION OF POSSIBLE SEQUENCE	SUPPORTING OBSERVATIONS	NON-SUPPORTING OBSERVATIONS	Confidence Level
Continued downward motion of the forward end of the keel beam results in the tensile separation of the Midspar tension fasteners common to the keel beam.	See sequence page MS-1 regarding tension fasteners common to the keel beam.		
Continued downward deflection of the fwd end of the keel beam produces a bending moment in the keel beam that is sufficient to cause the fracture to propagate through the vertical flange of the upper keel beam chord, into the web resulting in a net area tension failure of the web and finally in a bending fracture of the keel beam lower chord at STA 1241. The fracture locations are symmetric about both sides of the keel beam box.	Review of the fracture types and directions associated with the fractures of the upper chord, web, and lower chord of the keel beam at the aft end of the keel beam segment LF14A.		High
During the rotation of the keel beam and the separation from the lower skin panel, the motion results in aftward bending of the portion of the keel beam tension fasteners that are protruding from the top surface of the keel beam upper chord and also produces the drag marks in the lower skin panel holes common to the tension bolts.	See figures B-3, B-4, B-6, B-7 and B-10.		High
Compression buckling of forward keel beam web and upper chord occurs after the upper chord separation from the lower web skin, possibly just after separation.	Compression buckling of web and remaining portion of upper chord of forward portion of keel beam.		Medium
Continued downward movement of LF6A relative to the forward keel beam results in a bending fracture of the keel beam lower chord splice and also initiates bending fracture of the lower pressure bulkhead ring chord at LBL 9.	1. Downward bending fracture of the keel beam lower chord splice. 2. Ring chord fracture initiates at LBL 9 and propagates left and right.		Medium

UPPER CHO[illegible]S OF KEEL BEAM

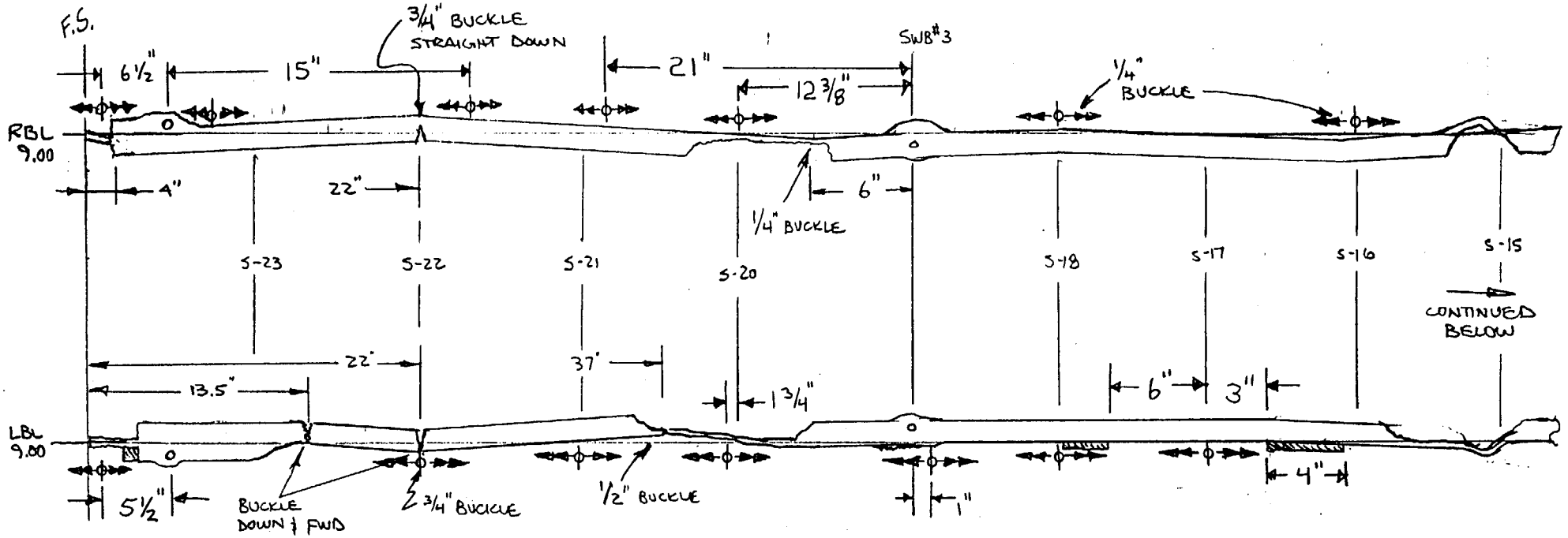

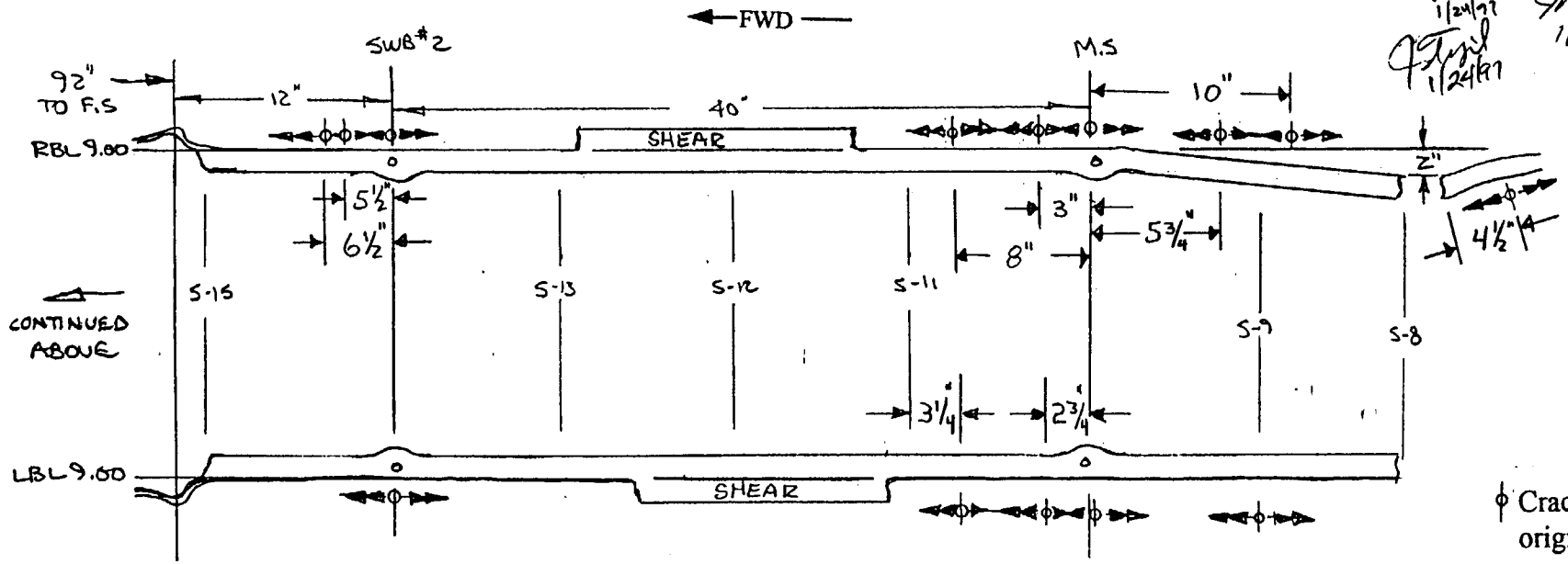

W. Stuart 1/24/97

JFWil 1/24/97

JFWil 1/24/97

VIEW LOOKING DOWN

FIGURE B-14

Crack origin

Crack direction

Floor Beam Characteristics of Segments Remaining Attached to Frames

Location / Tag Number	Indications of movement of floor beam relative to frame	Features and characteristics	Remarks
980 Left	Unknown		Floor beam attachment cut to fit into reconstruction
960 Left	Upward at body frame	Upper chord outboard of stanchion remnant shows upward bending on fracture and residual bending of rivet head.	No stanchion. Frame not attached to skin.
940 Left FBM 3C	Downward	24" length of separated and unsupported upper chord is bent down at LBL 75 and lower chord has local residual deformation downward at LBL 75	No frame at floor beam Frame not attached to skin.
920 Left FBM6D FBM6E	Upward	Upper chord fracture consistent with upward bending but no local residual deformation in chord. Upward residual bending of floor beam inbd of frame (FBM 6E)	Frame not attached to skin
900 Left FBM12C and FBM8A	Upward	Upper chord has local residual bending upward but lower chord has local residual bending down. Mating fracture on FBM12C shows loarge upward deformation of upper chord at frame.	Frame not attached to skin.
880 Left FBM31E	Upward	Upward deformation of small portion of floor beam at frame.	Frame not attached to skin
860 Left LF5	Upward at stanchion	Upper chord shows upward bending fracture (tension on lower edge of chord and fracture propagation direction. Lower chord has appearances of a tensile fracture	Frame and stanchion remain attached to skin
840 Left LF5	Upward at stanchion	Local bending of lower chord with upward residual deformation. Upper chord fracture propagation direction appears to be upward	Frame and stanchion remain attached to skin
820 Left LF5	Upward at stanchion	Tension fracture of lower flange of the lower chord. Upper chord fracture type and propagation direction appears to be consistent with upward fracture.	Same upper chord fracture type and shape as STA 840. Frame and stanchion remain attached to skin.
800 Left	Upward	Upper chord has free flanges torn in a manner that looks more like the floor beam deflected upward than it would if the floor beam had deflected downward. Lower chord tension? fracture of lower flange midway between stanchion and body frame.	Frame and stanchion remain attached to skin
780 Left	Unknown		No frame at floor beam.

Floor Beam Characteristics of Segments Remaining Attached to Frames

Location / Tag Number	Indications of movement of floor beam relative to frame	Features and characteristics	Remarks
980 Right	Unknown		No frame or stanchion
960 Right	Unknown		No frame or stanchion
940 Right	Unknown		No frame or stanchion
920 Right FBM6C FBM3A	Upward / Twist?	Upper chord fracture consistent with upward bending but no local residual deformation in chord. Local residual deformation in FBM3A near RBL 98	Frame not attached to skin
900 Right RF1 FBM8B	Downward at stanchion	Long portion of the upper flange of the upper chord has local downward bending at the inbd fracture and the entire chord is bent down near the stanchion. The lower chord also has local downward bending at the fracture.	Frame and stanchion remain attached to skin
880 Right RF1	Downward at stanchion	Long portion of the upper flange of the upper chord has local downward bending at the inbd fracture and the entire chord is bent down near the stanchion. The lower chord has a downward tearing fracture on the lower flange with little residual deformation.	Frame and stanchion remain attached to skin
860 Right RF1	Inconclusive	6" portion of the upper chord inboard of the stanchion is bent down but local residual deformation at the fracture is upward. The long portion of the lower chord is bent down and fwd at the stanchion but since it is unsupported over the remainder of it's length, it is inconclusive.	Frame and stanchion remain attached to skin
840 Right RF1	Downward at stanchion	Local residual deformation at the fracture of the upper chord at the stanchion is downward. The lower chord as a fracture (tension at the upper edge of the chord) consistent with down bending and has slight downward residual deformation. Web fracture direction is not apparent. Top half of aft fastener head broken off at lower chord stanchion shear tie.	Frame and stanchion remain attached to skin
820 Right RF1	Downward at stanchion	Upper chord has downward residual deformation at stanchion. Lower chord and web fractures are inconclusive. Indications are cracking and bending are from aft to forward	Frame and stanchion remain attached to skin
800 Right RF1	Downward?	Not 100% conclusive but the upper chord shows downward buckling near the stanchion. The lower chord and web are inconclusive.	Frame and stanchion remain attached to skin
780 Right RF1	Downward	16" length of upper chord is bent down at the stanchion. Inbd fracture has torn web flange from between free flange (producing a slot) which would be consistent with downward tearing but the inbd end has slight residual deformation upward. Lower chord inconclusive. Upper chord is bent aft and buckled aft outbd of stanchion	Frame and stanchion not attached to skin
760 Right FBM24C	Inconclusive	Some indication of bending down and aft for upper chord	Floor beam fractured outbd of stanchion

Metallurgy / Structures Sequencing Group Report

Appendix C: Summary of Pre-existing Fatigue

APPENDIX C

C.1 Front Spar Lower Horizontal Chord - Existing Fatigue Cracking

Fatigue cracks were found in the Front Spar lower horizontal chord in the fillet radius just outboard of the underwing longeron splice fittings at both RBL and LBL 80. The existing cracks were approximately 1.2 inch and 1.45 inch on the RHS and LHS, respectively. The cracks originated at the inside fillet radius and were part through cracks, progressing approximately one third through the chord thickness (approximately 0.10 inch deep and 0.125 inch deep on the RHS and LHS, respectively). A schematic illustration of the fatigue cracking is shown on the top of the following page.

The Front Spar lower horizontal chord in the vicinity of the fatigue cracking is subjected to inspection under the Supplemental Structural Inspection Document (SSID) program. A previous instance of cracking at this location was found on a different 747-100. Those cracks were larger than the ones identified on TWA800 but also did not extend through the thickness of the chord. Cracking between the horizontal and vertical legs of the chord is initiated by secondary deflections acting to open and close the angle between the lower chord legs as a function of body pressure and underwing longeron loads. The orientation and configuration of the cracking does not degrade the capability of the front spar lower chord in performing its primary function of reacting wing bending loads as part of the basic wing box structure. This region is affected by SB 747-53-2064 for adjacent ring chord cracking. The modification per SB 747-53-2064 had been installed on N93119 in 1982, incorporating two bathtub fittings on the Wing Center Section lower skin panel and a double bathtub fitting on the fuselage skin. These fittings are immediately adjacent to the underwing longeron splice fitting and serve to provide an alternate load path for the longeron forward/aft loads. It is apparent from the bathtub fitting arrangement that the post-modification configuration is very stiff and the deflection that would have initiated and propagated the fatigue cracking has been significantly limited. Without continued deflection, the fatigue growth cannot continue, indicating that the minor fatigue cracking existed prior to the installation of the bathtub fittings.

Examination of the area of fatigue cracking and adjacent material on the fracture face indicates an abrupt transition from slow crack growth to a sudden ductile fracture. This provides further confirmation that the cracking did not propagate to failure due to fatigue but rather was the result of a one time static overload associated with structural breakup. The NTSB Materials Laboratory has examined the larger of the two cracks and will issue a separate report. A more complete description of the fatigue cracking may also be found in the Metallurgical Field Notes.

Finally, the structural breakup pattern of the front spar has been discussed in Sections 4.11 and 4.12. The fracture of the lower chord through the fillet radius is consistent with the impact of SWB #3 on the front spar and the subsequent overpressure acting on the front spar rotating it forward about the lower chord. A similar fracture occurred in the fillet radius of the upper chords of the front spar and SWB #3 as well as through part of the lower chord of SWB #3. It should be noted that it is the propagation of the fracture at the fillet radius which has coincidentally exposed the two areas of localized, pre-existing fatigue cracking near RBL and LBL 80 in the lower chord.

C.1 Front Spar lower horizontal chord - existing fatigue cracking (continued)

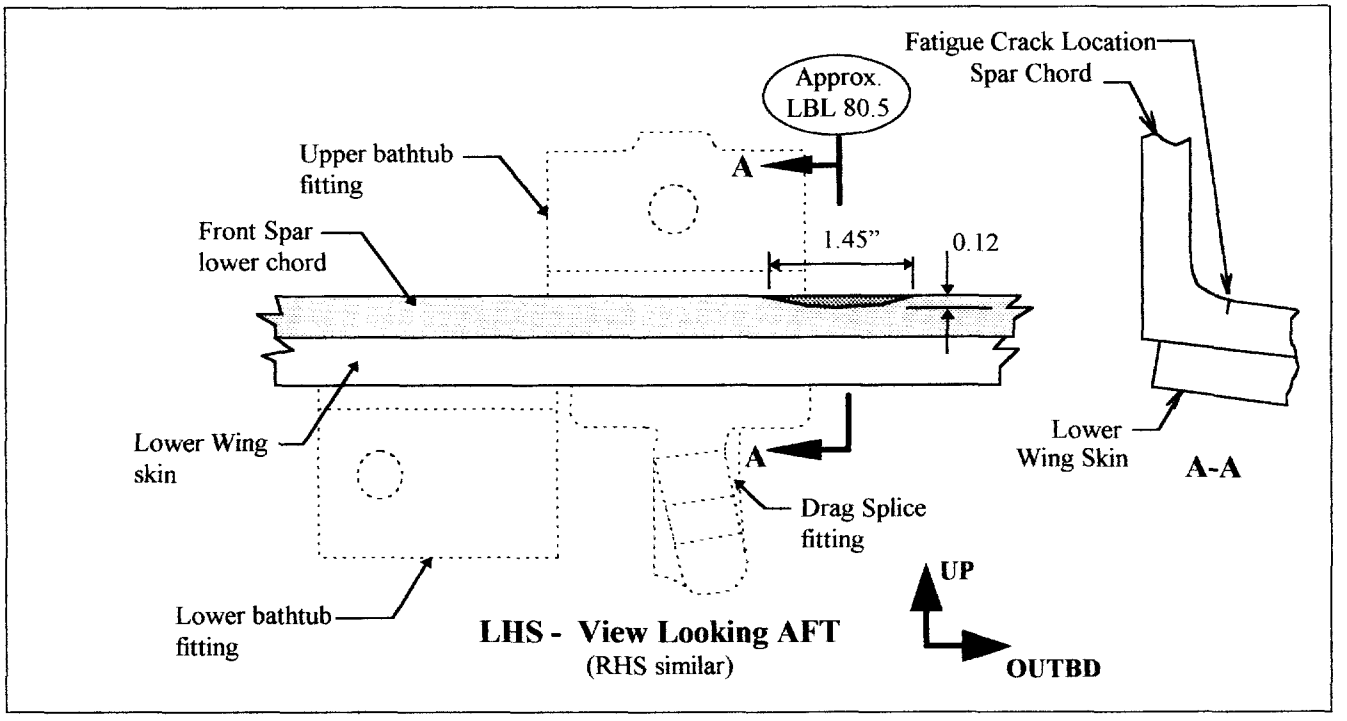

C.2 Front Spar vertical stiffener shear ties - existing fatigue cracking

Small existing fatigue cracks were found in the vertical stiffener shear ties at RBL 83.24 (lower), RBL 75.92 (upper and lower), LBL 75.92 (upper and lower), and LBL 83.24 (lower). The cracks were all in the shear tie radius near the base of the leg that attaches to the vertical stiffener at the aft edge. This cracking is the subject of SB 747-57-2249. The Service Bulletin was issued in 1989 after reports of in-service cracking. The maximum crack length on the subject airplane was 0.20 inch long. In service, operators have reported cracks ranging from 0.50 inch to 1.5 inch long without complete part fracture, demonstrating the capability of these shear ties to withstand cracking well in excess of the 0.20 inch detected cracking under normal operating conditions. Furthermore examination of the area of fatigue cracking and adjacent material on the fracture face indicates an abrupt transition from slow crack growth to a sudden ductile fracture. This provides further confirmation that the cracking did not propagate to failure due to fatigue but rather was the result of a one time static overload associated with structural breakup.

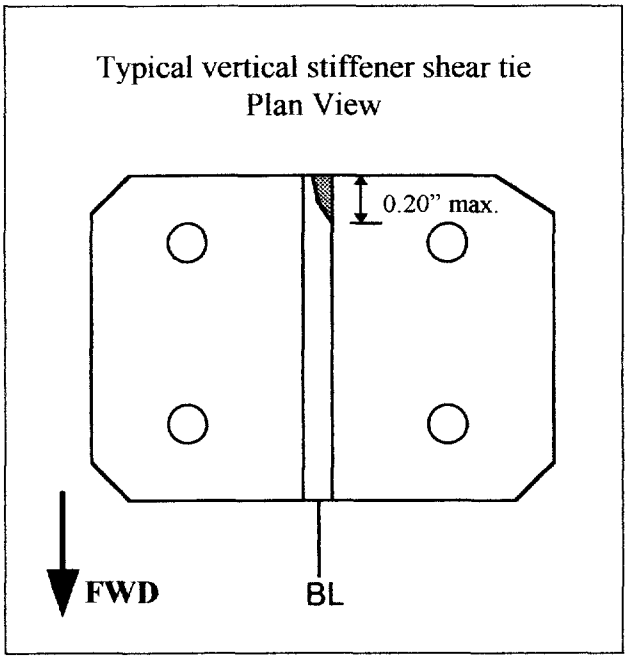

See the Metallurgical Field Notes for a complete cracking description.

C.3 Longitudinal Floorbeam at Front Spar - existing fatigue cracking

Small cracks were found in the shear tie of the LBL 75.92 and the LBL 33.99 longitudinal floorbeams at the intersection with the Front Spar upper chord at STA 1000. The LBL 75.92 shear tie has a 0.15 inch fatigue crack emanating from the aft side of the hole and a possible 0.125 inch fatigue crack emanating from the forward side of the hole as shown. The LBL 33.99 shear tie has a 0.25 inch fatigue crack emanating from the forward side of the hole. Examination of the area of fatigue cracking and adjacent material on the fracture face indicates an abrupt transition from slow crack growth to a sudden ductile fracture. This provides further confirmation that the cracking did not propagate to failure due to fatigue but rather was the result of a one time static overload associated with structural breakup.

The component is a secondary attachment for floor structure and does not contribute to carrying primary airframe loads.

See the Metallurgical Field Notes for a complete cracking description.

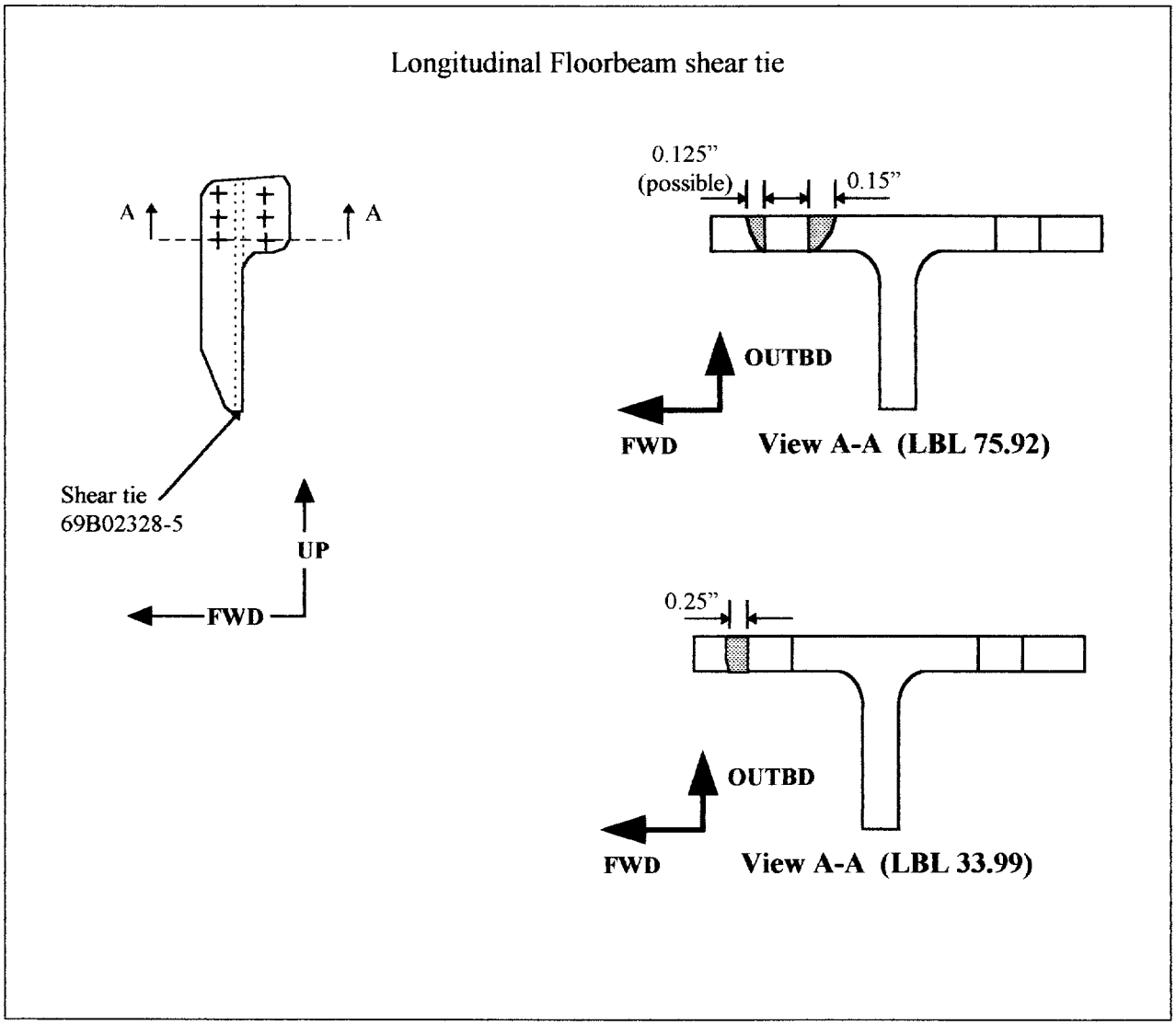

APPENDIX D

ANALYSIS FOR PREPARATION OF STRUCTURE SEQUENCING GROUP REPORT

NTSB EVALUATION OF TWA 800

CONTENTS:

* P.(8) – P.(9) RESERVED

1/23/97 (1)
1/30/97

DEVELOP WING LOADS & EVAL. STRENGTH @ WCS & WING OUTBD OF ENG.

- NOSE SECT. STA 100 → STA 1000 DEPARTS A/C.
- AIRFLOW DISRUPTION @ INBD. WING DUE TO BLUNT/OPEN END.
- M.S. = 0 @ 3.75G & 734K G.W. @ OUTBD. ENG. & @ WCS.
- EVALUATE A/C WTS. & LOADS @ OUTBD. ENG. & @ WCS.

WT. EVAL.: REF. NTSB & BOEING INFO @ GALVESTON MTGS.**

** MAX. DES. G.W = 734K

@ JULY 17, 1996; TWA 800 @ T.O. WAS AT THESE WTS.

**T.O.G.W = 590K

**WING FUEL = 180K

ASSUME PASS + BAGS = 60K (230 @ 260 LB.)

ASSUME CARGO = 50K

∴ STRUCT. = 300K

ΣW = 590K

STRUCT = 300K
FUEL = 277K
PASS. (450 @ 260 LB) = 117K
CARGO = 40K
734K

ASSUME AS FOLLOWS:
FUS. + TAIL + L.G. = 150K
WING + ENG. + L.G. = 150K

APPROX.
WCS FUEL (FUS.) = $5' \times 24' \times 16' \left(7.48 \frac{GAL}{FT^3}\right)\left(6.5 \frac{LB}{GAL}\right)$ = 93K

WING FUEL = 184K (MAX)

184K
ΣW = 277K

BAL. A/C @ 1.0G ~ ASSUME TAIL LOAD = 10% G.W ACTING DOWN.

(A) MAX.:
STRUCT = 300
FUEL = 277
PASS = 117
CARGO = 40
734 → GW = 734

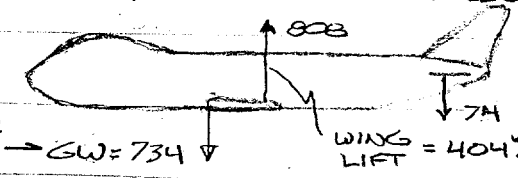

(B) EVENT:
STRUCT = 300
FUEL = 164
PASS = 60
CARGO = 50
574 → GW = 574

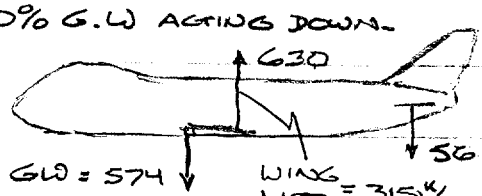

AFTER EVENT: [WITHOUT AIRFLOW DISRUPTION]
STRUCT = 250
FUEL = 164
PASS = 142
CARGO = 30
486 → GW = 486

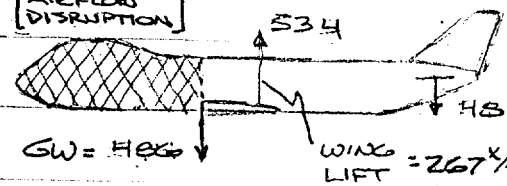

(C) AFTER EVENT:
STRUCT = 250
FUEL = 164
PASS = 142
CARGO = 30
486 → GW = 486

NO TAIL LOAD

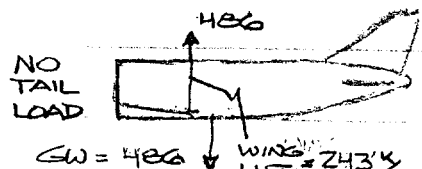

1/23/97
1/30/97 (2)

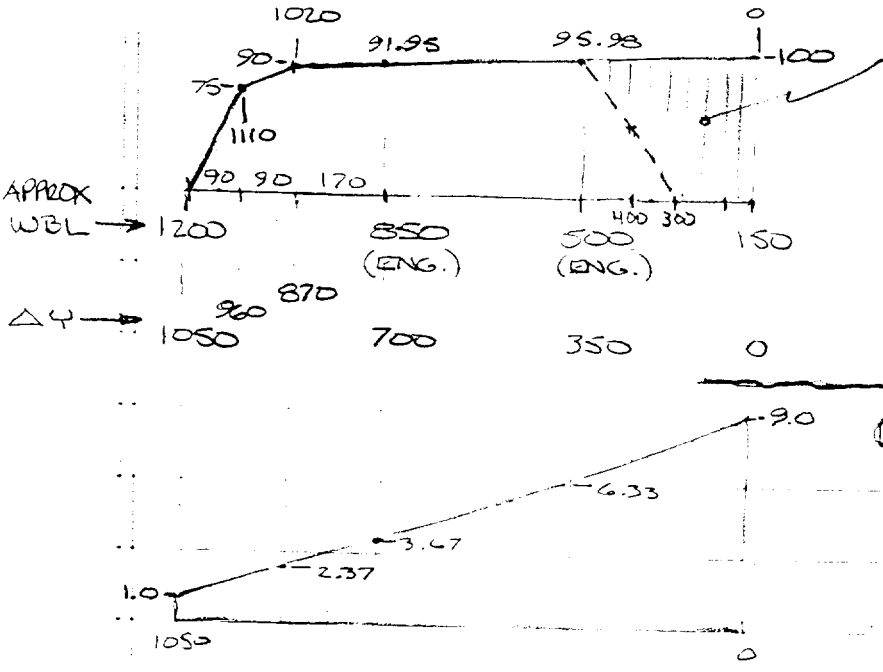

DISTURBED AIRFLOW BY OPEN BLUNT END *Δ

WING SPANWISE LIFT DISTR. (APPROX.)

SEE P. (5) FOR BAL. A/C:

ΣL_{1G} = 404 K/SIDE [NORMAL DISTR @ 734K G.W (A)

= 315 K/SIDE [NORMAL DISTR. @ 574 K GW (B)

= 179 K/SIDE AFTER EVENT @ 486K GW (C)

WING SPANWISE WT. DISTR. (APPROX.)

BOTH CHORD & RIB HEIGHT INCR. BY FACTOR ≠ 3 FROM TIP TO ROOT.

ΣW_{1G} = 167 K/SIDE @ MAX GW

= 157 K/SIDE @ EVENT

= 157 AFTER EVENT

EMPTY WT.:

FUS. + TAIL + LG = 150 K

WING + ENG. + LG = 150 K = 75 K/SIDE

WING FUEL = 184 K = 92 K/SIDE } 167 K/SIDE

@ TIME OF EVENT:

WING FUEL (20K FUEL USED) = 164 K = 82 K/SIDE

(A) MAX:

		W	ΣW	
STRUCT.	FUS.	150	150	
	WING	150	300	
PASS. 450 @ 260.		117.	417	
CARGO		40	457	
FUEL	FUS	93.	550	
	WING	184	734	= MAX GW

*Δ - DISTURBED AIRFLOW: DESTROYS LIFT @ INBD WING SECT. FOR APPROX. 1 FUS. DIA. (LIFT IS ½ RESTORED @ 250 IN. OUTBD FROM ROOT)

(B) EVENT:

		W	ΣW	
STRUCT.	FUS	150	150	
	WING	150	300	
PASS 230 @ 260		60	360	
CARGO		50	410	
FUEL	FUS	0	410	
	WING	164	574	= EVENT G.W

(C) AFTER EVENT:

		W	ΣW	
STRUCT.	FUS	100*	100	
	WING	150	250	
PASS 162 @ 230		42	292	← NTSB DATA 162 PASS IN "GREEN" SECT.
CARGO 60% REMAINING		30	322	
FUEL	FUS.	0	322	
	WING	164	486	

* FUS. STRUCT. SEPARATED END OF STA 1000; W = 50K (STA 100 → 1000)
REMAINING STRUCT. FROM STA 1000 - 2600; W = 100K

1/23/97
1/30/97
2/22/97

(3)

LIFT DISTR. (APPROX.)

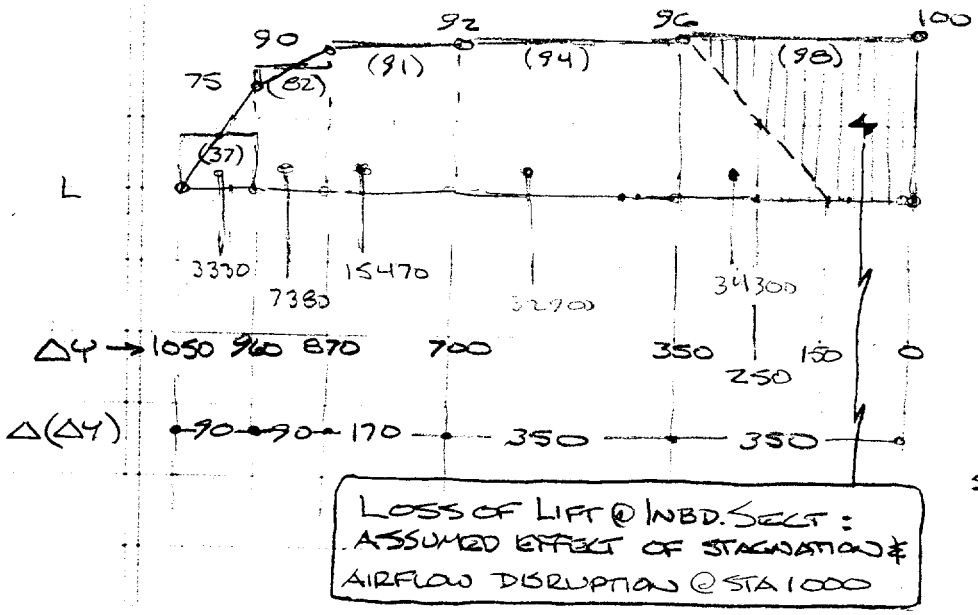

LOSS OF LIFT @ INBD. SECT: ASSUMED EFFECT OF STAGNATION & AIRFLOW DISRUPTION @ STA 1000

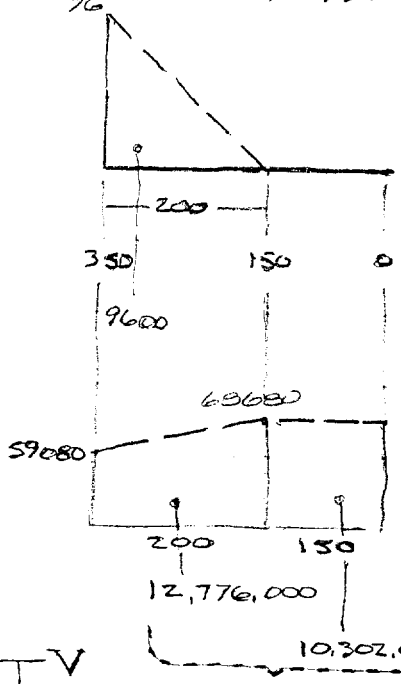

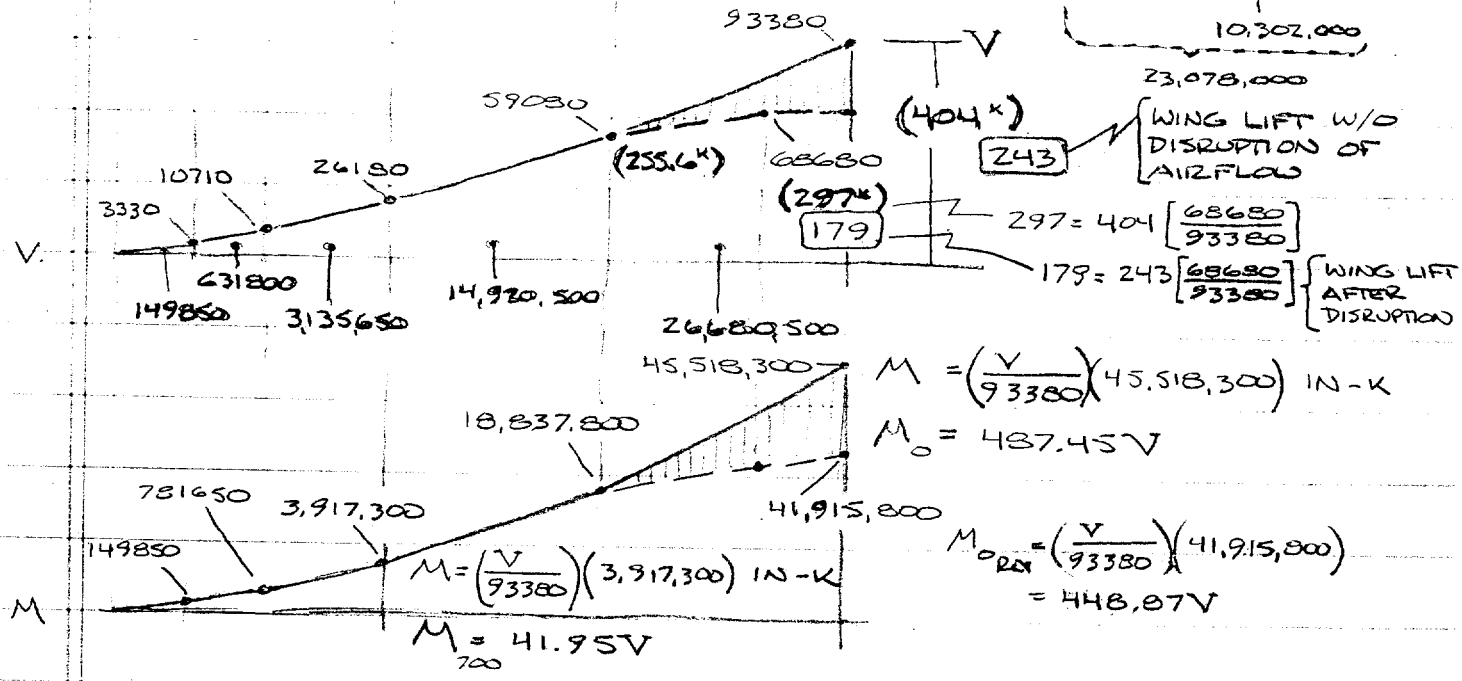

AIRLOAD + INERTIA LOAD @ WING ROOT:

	L	DISTR	$M_{o(L)}$	W	$M_{o(W)}$	ΣM_o @ IG	
				167			
(A)	404	N	$196.93(10^6)$	157	$-58.56(10^6)$	138.37×10^6	× 3.75 = 518.89
(B)	315	N	153.55	157	-55.43	98.12	
	267	N	130.15	157	-55.43	74.72	
(C)	179	REV	80.35		-55.43	24.92	

WCS STRENGTH

SEE ABOVE: $M_o = 487.45V$ OR $448.87V$

SEE P.(4): $M_{o(W)} = 396.62V$ (STRUCT) $= 313.17V$ (FUEL)

WT. DISTR. (APPROX.)

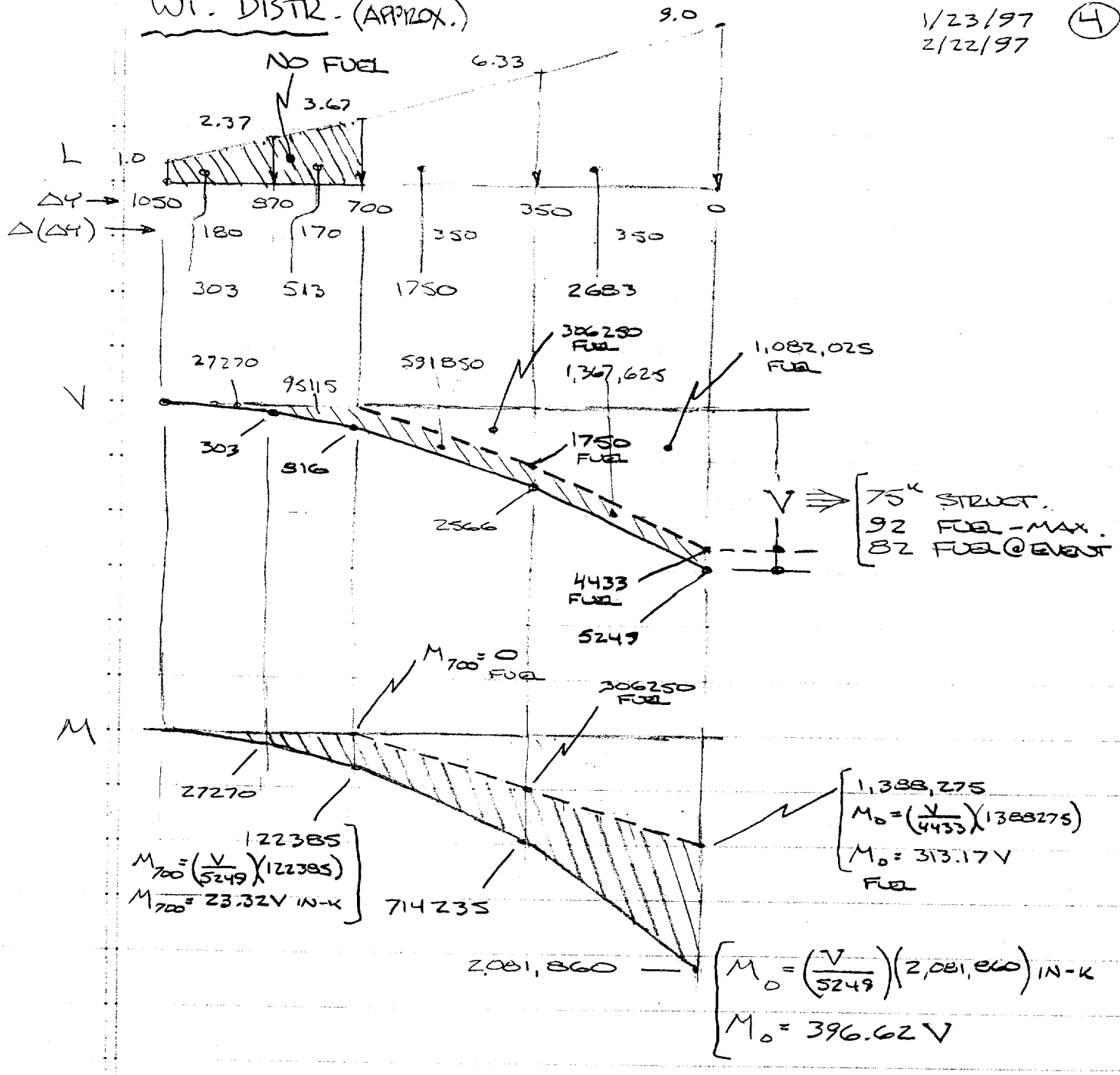

AIRLOAD + INERTIA LOAD @ WBL 850 (Δy = 700): SEE P. (6)

INERTIA LOAD / STRUCT. & FUEL:

STRUCT. $M_{700} = 23.32V = 23.32(75) = 1749$ IN-K
(V=75K) $M_o = 396.62V = 396.62(75) = 29746$ IN-K

FUEL: $M_{700} = 0$ ——— = 0

{V = 92K (MAX.) / V = 82K @EVENT} $M_o = 313.17V = 313.17(92) = 28812$ IN-K
$= 313.17(82) = 25680$ IN-K

TOTAL: $\Sigma M_o = 29.75 + 28.81 = 58.56 \times 10^6$ @ V = 167K (92K FUEL)
$\Sigma M_o = 29.75 + 25.68 = 55.43 \times 10^6$ @ V = 157K (82K FUEL)
ΣM_{700} = STRUCT. ONLY = 1.75×10^6

1/23/97 (5)
1/30/97
2/22/97

M.S. = 0 @ 3.75 G @ 734^K G.W. @ OUTBD. ENG. (ΔY=700)
$ @ WCS (ΔY=0)

∴ BEND. MOM. @ THESE LOC. FOR COND. (A) REPRESENT THE STRENGTH @ EACH LOC. FOR INTACT STRUCTURE.

COND (A): NORMAL LIFT DISTR. @ 734 K G.W.

L = 404 K/SIDE
W = 167 K/SIDE [75 K STRUCT.; 92 K FUEL]

$M_{700} = 41.95L - 23.32W_{STRUCT} - 0W_{FUEL}$
$= 41.95(404) - 23.32(75) = 15198$ IN-K @ IG

FAILURE LOAD @ CRIT. SECT. $= 3.75(15198) = 56995$ IN-K @ FAIL

$M_0 = 487.45L - 396.62W_{STRUCT} - 313.17W_{FUEL}$
$= 487.45(404) - 396.62(75) - 313.17(92) = 138370$ IN-K @ IG

$3.75M_0 = 518890$ IN-K = WCS STRENGTH

COND (B): NORMAL LIFT DISTR. @ 574 K G.W.

L = 315 K/SIDE
W = 157 K/SIDE [75 K STRUCT.; 82 K FUEL]

$M_{700} = 41.95(315) - 23.32(75) = 11465$ IN-K @ IG

$M_0 = 487.45(315) - 396.62(75) - 313.17(82) = 98120$ IN-K @ IG

COND (C): EFFECT OF DISTURBED AIRFLOW @ 486K G.W.

L = 243^K/SIDE W/ADJ. FOR AIRFLOW DISRUPTION – SEE P. (3) & (6)
W = 157 ^{K}/SIDE

ASSUME THAT WING LIFT IS DESTROYED @ INBD WING SECT. DUE TO DISTURBED AIRFLOW AROUND BLUNT/OPEN FUS. @ STA 1000 W/NEAR ZERO VELOCITY IN VICINITY OF STAGNATION POINT & THAT LIFT IS AFFECTED FOR APPROX. 1 FUS. DIAM. @ EACH SIDE SUCH THAT LIFT IS RESTORED TO 1/2 ITS FULL VALUE @ THE 1 DIAM. (ΔY=250) LOCATION. – SEE P. (3) DISTR.

THERE ARE QUITE A FEW PLACES WHERE THE WORDS "ASSUME" & "APPROX." APPEAR IN THIS ANALYSIS (I COUNT 6 OF EACH), BUT THE PURPOSE WAS TO EVALUATE THE POSSIBILITY OF FAILURE AT THE WING OUTER SECT. (@ OUTBD. ENG.) WHEN THE WCS HAD SUFFERED ((SOME)) LOSS OF STRENGTH.

1/23/97 (6)
1/31/97
2/22/97

AIRLOAD + INERTIA LOAD @ WBL 850 ($\Delta y = 700$):

	$L_{(DISTR)}$	$M_{700(L)}$	W	$M_{700(W)}$	$\Sigma M_{700(@16)}$	
(A)	$404_{(N)}$	16.95×10^6	167	-1.75×10^6	15.20×10^6	$\times 3.75 = 57.0$
(B)	$315_{(N)}$	13.21 "	157	-1.75 "	11.46 "	FAIL. LOAD @ BL 850
	$267_{(N)}$	11.20 "	157	-1.75 "	9.45 "	
(E)	$179_{(REV)}$	7.51 "	157	-1.75 "	5.76 "	

$M_{700} = 41.95V$ ← SEE P.③

$M_{700_W} = 23.32V$ [75K STRUCT. ONLY] ← SEE P.④

← SEE P.③

$$M_o = \frac{24.92}{5.76}(57.0) = 246.6$$ ← ∴ LOAD APPLIED TO WCS AT SAME TIME AS FAILURE @ BL 850 IS;

WCS STRENGTH = 518.89 (REF. P.⑤)

$$\%\text{WCS FAILURE LOAD} = \frac{246.6}{518.89} = .475 \ (47.5\%)$$

CONCLUSION:

THE WING WILL FAIL @ SECT. OUTBD OF ENG. (BL 850); AT THE SAME TIME, THE WCS IS LOADED TO ONLY 47.5% OF ITS FULL STRENGTH. ∴ A COMPROMISED WCS COULD INDEED STILL FORCE THE WING FAILURE @ BL 850.

STOWAGE BIN BASE PLATES:

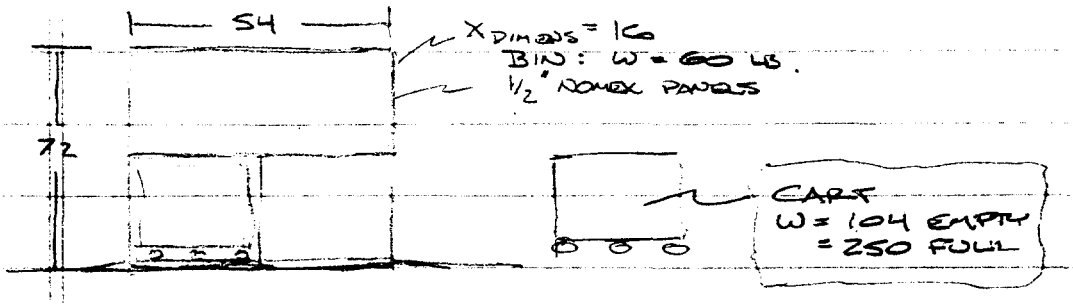

FOOTPRINT AREA OF CART:

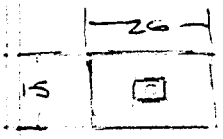

$\Sigma W = 60 + 250 = 310$ LB

ASSUME: BIN W/ 1 CART IN PLACE HITS WATER AT TERMINAL VELOCITY & DESCENDS 7 FT. BELOW SURFACE BEFORE STOPPING (TERM. VEL ≈ 110 MPH ≈ 160 FT/SEC FOR FREE-FALLING BODY OF THIS SIZE & SHAPE — REF. NTSB BALLISTIC PROFILE CHARACTERISTICS).

CALCULATE: DECELERATION AFTER CONTACT @ WATER SURFACE
MAX. PRESSURE EXERTED ON BOTTOM OF BASE PLATES.

DETERMINE: IF THE CALCULATED CHARACTERISTICS APPROXIMATE THE OBSERVED CONDITIONS.

NOTE: CALCULATIONS BY THE A/C MFGR. INDICATE THAT 30 PSI IS REQD. TO CREATE THE "PILLOWED" DEFORMATIONS OF THE BASE PLATES.

DECELATION IS A FUNCTION OF VELOCITY AFTER IMPACT W/WATER; ASSUME THAT DECEL. IS CONSTANTLY DECREASING VS. TIME AS SHOWN BELOW:

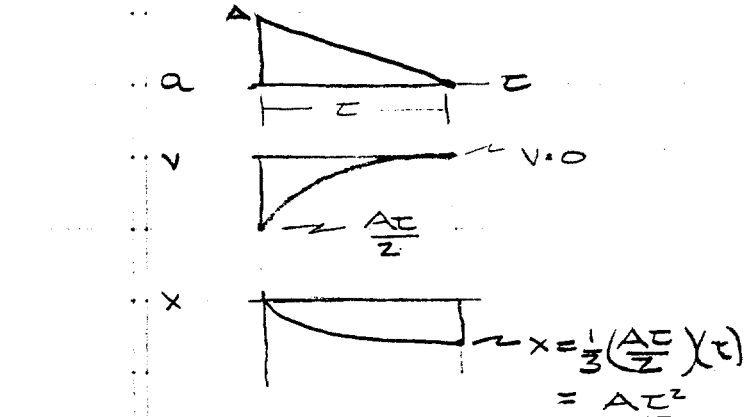

$X = \frac{At^2}{6} = 7.0$ $\qquad V = 160 = \frac{At}{2}$

$At^2 = 42$ $\qquad At = 320$

$\frac{At^2}{At} = t = \frac{42}{320} = .131$ SEC

$At = 320$

$A = \frac{320}{t} = \frac{320}{.131} = 2438 \text{ FT/SEC}^2$

$F = MA = \frac{310}{32.2}(2438) = 23470$ LB

$F = p(\text{AREA}) = p(15)(26)(2) = 23470$

$p = 30.1$ PSI [MAX. PRESSURE ACTING UPWARD ON BOTTOM OF BASE.

THIS AGREES EXACTLY WITH THE MFGR. DATA FOR PRES. REQD. TO CREATE THE DEFORMATION OBSERVED IN THE BASE PLATES, AND CAN BE CONSIDERED AS VALID IF THE ASSUMED DESCENT OF 7 FT BELOW THE WATER SURFACE IS VALID. ON THE BASIS OF OTHER OBSERVED WATER ENTRY BEHAVIORS, THIS ASSUMPTION IS JUDGED TO BE APPROXIMATELY CORRECT, AND IT DOES RESULT IN THE EXPECTED RESULT FOR THE BASE PLATE.

FUS. SKIN FRACTURE @ STA 990:

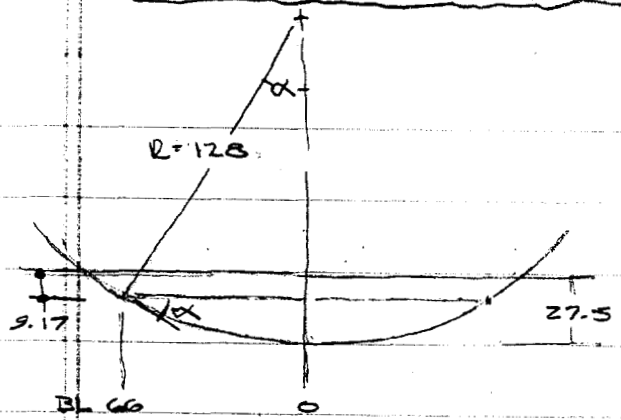

$128 \sin\alpha = 66$

$128(1-\cos\alpha) = UNK.$

$\sin\alpha = \frac{66}{128}$

$\alpha = 31.0°$

$\cos\alpha = .8568$

$1-\cos\alpha = .1432$

$128(1-\cos\alpha) = 18.33$

VIEW LKG DOWN WCS LOWER SKIN

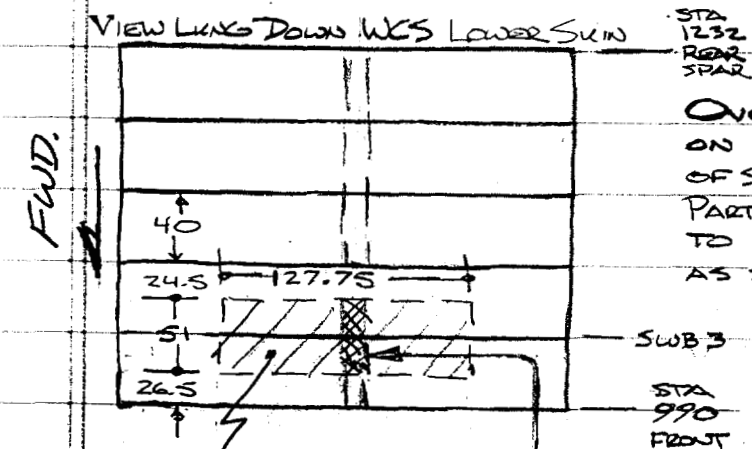

OVERPRESSURE IN WCS TANK PUSHES DOWN ON LOWER SKIN & CAUSES TENS. SEPARATION OF SWB 3 LOWER CHORD FROM SKIN (SEE P. (12)) PART OF THE UNSUPPORTED BAY LOAD IS DISTR. TO KEEL BEAM & IS DISTR. TO PRES. BLKD. AS SHOWN ON P. (11) [$V_{PRES.\ BLKD.} = 63.6^K$]

THE RESULT IS A TENS. LOAD IN THE PRES. BLKD. LOWER CHORD / FUS. SKIN @ BL 66 OF 61.7^K. THE TENS. STRESS DUE TO THE KEEL LOAD IS COMBINED WITH HOOP STRESS DUE TO CABIN (DIFFERENTIAL) PRES. OF 4.0 PSI WHICH IS ADDED TO BY THE OVERPRES. IN THE TANK AS THE EXPANDING GASES SPILL INTO THE FWD. CARGO COMPARTMENT.

$\Sigma A = \frac{13030}{2} = 6515\ in^2$

$V_{KEEL} = 6515(20) = 130.3^K$

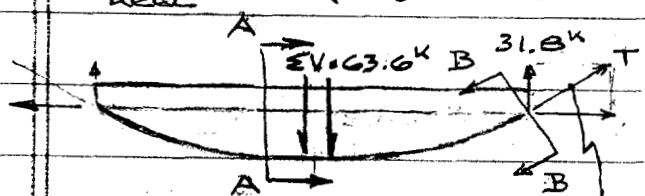

SECT B-B:

$T = \frac{31.8}{\sin 31} = 61.7^K$

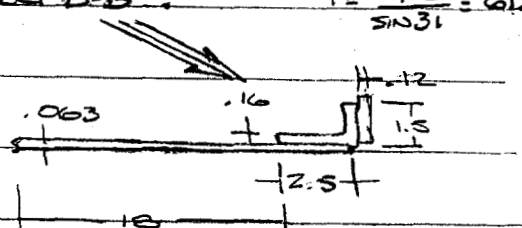

$A = 1.5(.12) + 4.0(.16) + 20.5(.063) = 2.11\ in^2$

$f_t = \frac{61.7}{2.11} = 29.2\ KSI$ [KEEL LOAD]

$f_T = \frac{4.0(128)}{.063} = 8.1\ KSI$ [CABIN PRES.]

$f_T = \frac{2.3(128)}{.063} = 4.7\ KSI$ [TANK OVERPRES.]

$\Sigma f_T = 42.0\ KSI$

F_{TU} (ALLOW) = 42 KSI – 2024 T3 EXTR @ 12% ε
= 55 KSI – 2024 T3 CLAD @ 12% ε
SEE P. (22)
[ASSUME EQUAL STRAIN IN SHT. & EXTR.]

*WITH THE ASSUMPTIONS USED HERE, AN ADDITIONAL PRES. FROM EXPLOSION OF ONLY 2.3 PSI IS REQD. TO CAUSE FAILURE @ BL 66;

*A CHANGE IN THE ASSUMPTIONS WILL ALTER THE AMOUNT OF OVERPRES. REQD TO CAUSE FAILURE (RESULTING FAILURE IS THE SAME).

SECT A-A:

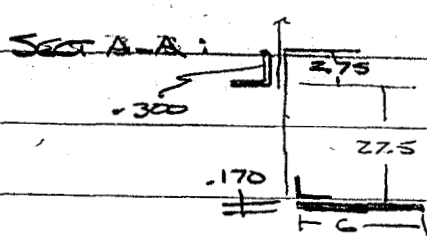

$M = 49.5(66) = 3267$

$M/H = \frac{3267}{27.5} = \pm 118.8^K$

$H = 82.4\left(\frac{18.3}{27.5}\right) = 54.8$

$\frac{27.6}{82.4}$

UPPER = −118.8 + 54.8 = −64.0 K

LOWER = 118.8 + 27.6 = 146.4 K

PRES. BLKD.

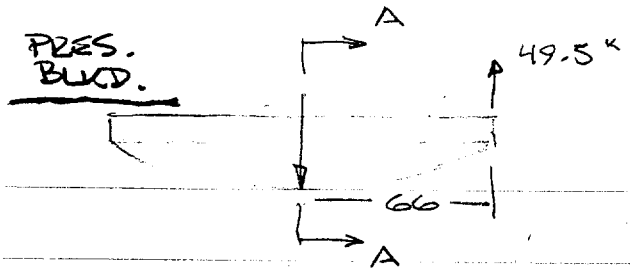

SECT A-A:

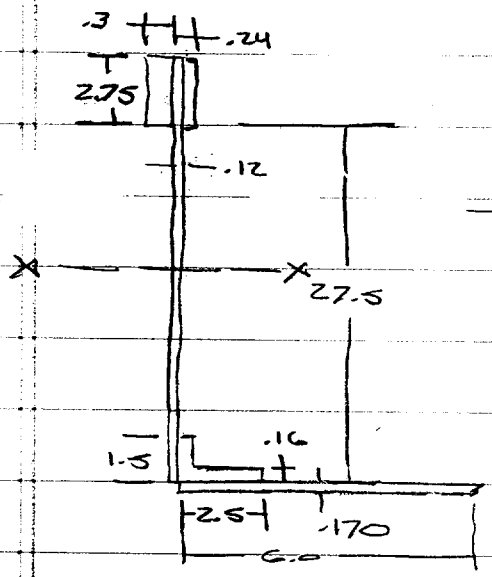

A	$\bar{y}$	$A\bar{y}$	$A\bar{y}^2$	I_o
1.48	28.88	42.9	1238	.94
3.30	13.75	45.4	624	209.9
1.66	—	—	—	.04
6.44	42.63	88.3	1862	208.9

$\bar{y} = \frac{88.3}{6.44} = 13.7$ $\quad \bar{c} = 16.55$

$I_x = \Sigma I_o + \Sigma A\bar{y}^2 - \Sigma A\bar{y}(\bar{y}) =$

$I_x = 208.9 + 1862 - 88.3(13.7) = 861$

$\delta = 3.43 \times 10^{-6} V$

$K = \frac{10^6}{3.43} = 290^{K/IN}$

SEE P. (11.1)

KEEL BEAM:

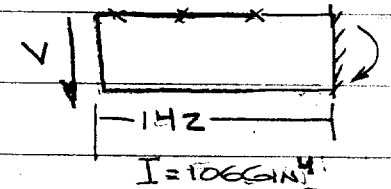

$I = 1066 IN^4$

SEE P. (14)

$K_{BEND.} = \frac{V}{\delta} = \frac{3EI}{\ell^3} = \frac{3(10^7)(1066)}{(142)^3} = 11.3^{K/IN}$

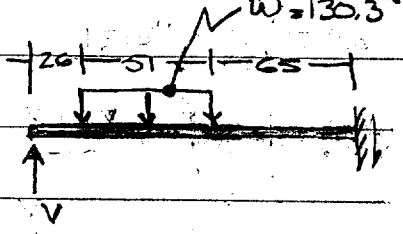

PRES. BLKD.

$K = 290^{K/IN}$

$\delta_3 = \frac{V}{K} = 3.43 \times 10^{-6} V$ SEE P. (11.1)

$\delta_2 = \frac{V}{K} = 88.7 \times 10^{-6} V$

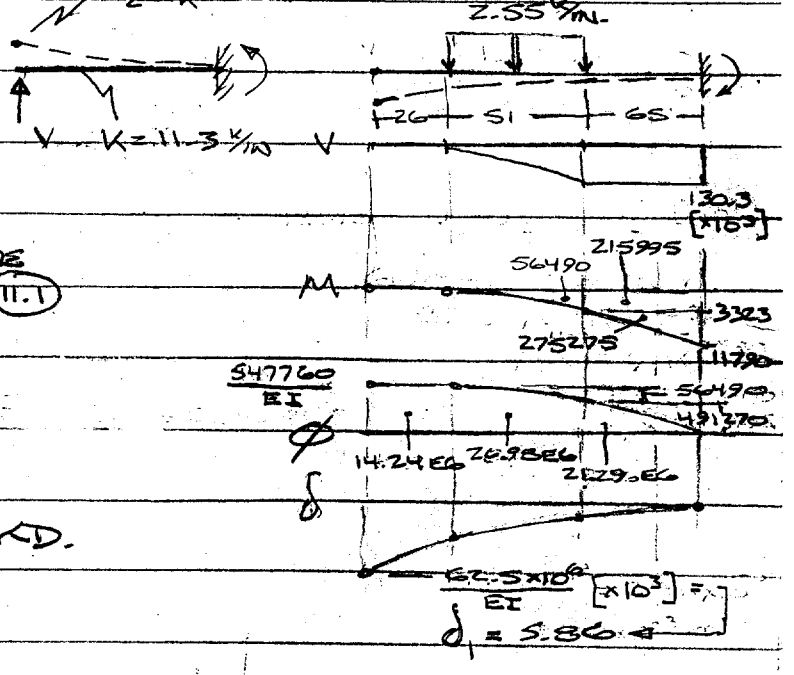

$\delta_1 - \delta_2 = \delta_3$

$5.86 - 88.7 \times 10^{-6} V = 3.43 \times 10^{-6} V$

$5.86 \times 10^{-6} = 92.13 V$

$V = 63.6^K$ @ PRES. BLKD.

~~$130.3 - 63.6 = 66.7^K$~~

PRES. BLKD.

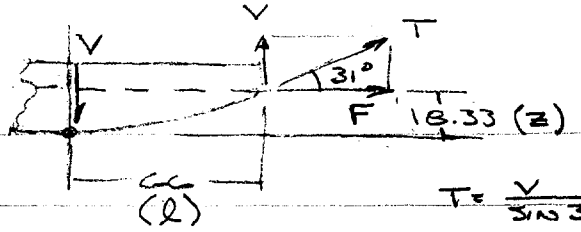

$T = \frac{V}{\sin 31} = 1.94\,V$

$F = T\cos 31 = 1.66\,V$

$$U = \int \frac{M^2\,dx}{2EI}$$

$$dU = \int \frac{M}{EI}\,\partial M\,dx$$

$$\delta_v = \frac{dU}{\partial V} = \int_0^{\ell} \frac{M}{EI}\frac{dM}{dV}\,dx$$

$$M = Vx - Fz$$

$$\frac{\partial M}{\partial V} = x$$

$$EI\delta = \int_0^{\ell}(Vx - Fz)[x]\,dx = \int_0^{\ell}(Vx^2 - Fzx)\,dx = \left[\frac{Vx^3}{3} - \frac{Fzx^2}{2}\right]_0^{\ell}$$

$$EI\delta = \frac{V\ell^3}{3} - \frac{1.66\,V\,z\,\ell^2}{2} \qquad \ell = 66 \quad z = 18.33$$

$$EI\delta = \frac{V(66)^3}{3} - \frac{1.66V(18.33)(66)^2}{2} = 29560\,V$$

$$\delta = \frac{29560\,V}{10^7(EGI)} = 3.43\times10^{-6}\,V$$

$$K = \frac{V}{\delta} = \frac{10^6}{3.43} = 290^{K/IN}$$

KEEL BEAM: SEE P. (11)

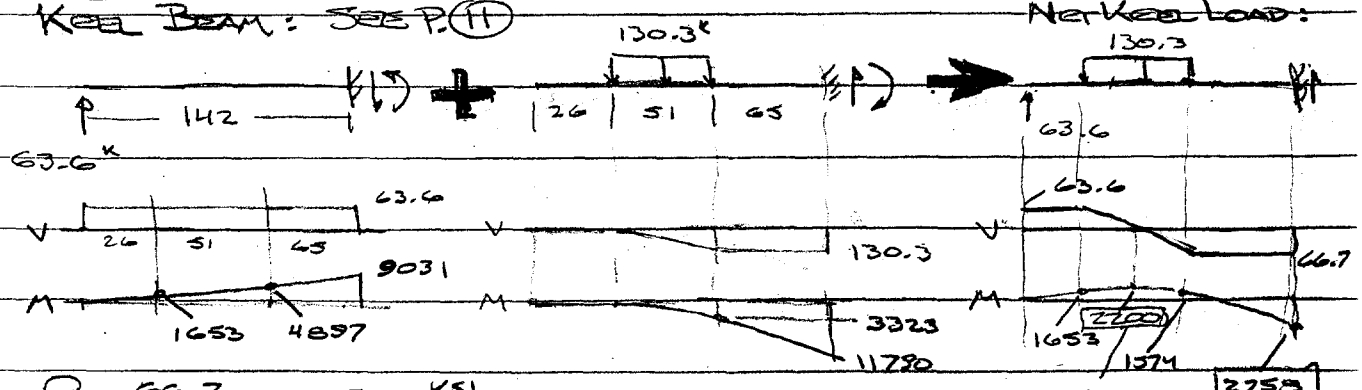

SEE P. (22)

$f_s = \frac{66.7}{26(2)(.063)} = 20.0^{KSI}$

$(-)\,M_{MAX} = 3138 \longrightarrow MS = \frac{3138}{2758} - 1 = +.14$

$(+)\,M_{MAX} = 2353 \longrightarrow MS = \frac{2353}{2200} - 1 = +.07$

SWB 2 LOWER CHORD SEPARATION:

VIEW LOOKING DOWN - WCS LOWER SKIN:

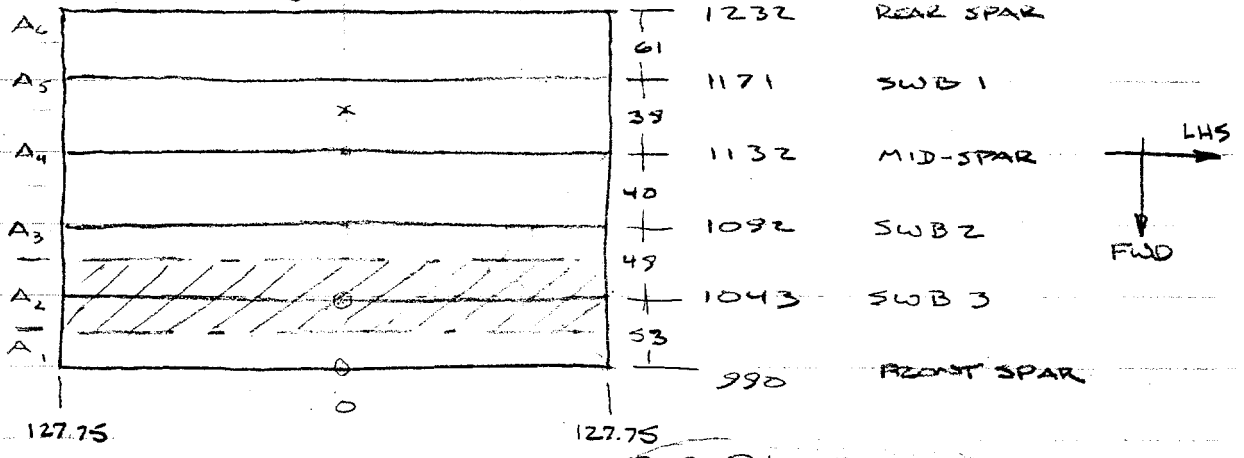

	Y	X	A	V @ 25 PSI
A_1	255.5	26.5	6770 IN²	169.2 K
A_2		51	13030	325.7
A_3		44.5	11370	284.2
A_4		39.5	10090	252.3
A_5		50	12780	319.5
A_6		30.5	7790	194.8

$\Sigma V = 1545.7^K$

DEFL. @ LOWER SKIN:

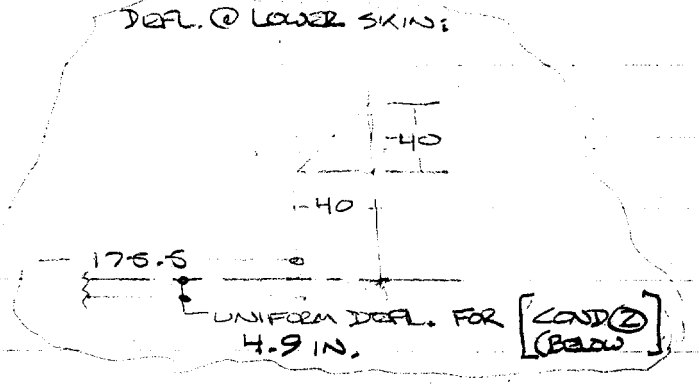

LOWER CHORD @ SWB 2:

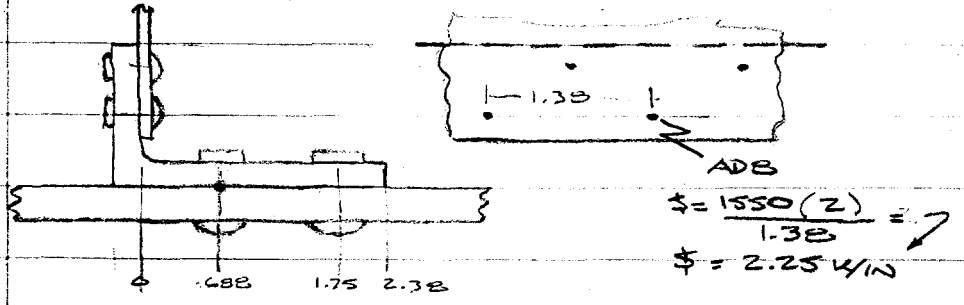

$f = \frac{1550(2)}{1.38} = 2.25\ K/IN$

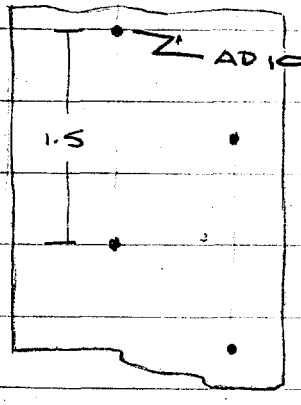

$T = 2460\left(\frac{50}{30}\right) = 4100$

$T = \frac{4100}{1.5} = 2.73\ K/IN$

MIN. STRENGTH IS TENS. RIVETS

$V_{ERIVN\ TO\ FAIL\ TENS.\ RIVETS} = \frac{2.73}{1.52} = 1.796\ K/IN$

$\Sigma V = 255.5(V_{EQ}) = 458.9^K$

UNIFORM LOADING ONLY

W/CONSIDERATION OF PANEL DEFL.:

UNIFORM STRAIN ON ALL RIVETS OVER 162.5 IN WIDTH ∴

$V_{ERIVN.} = 175.5(1.796) = 315.2^K$ @ 25 PSI

$= 284.2^K$ @ 22.54 PSI

$\rightarrow M.S. = \frac{284.2}{284.2} - 1 = 0$

LOWER SKIN DEFL. REF. GRUMMAN DESIGN DATA P.5.3.3 MEMBRANE LOAD ON PLATES

ASSUME FAILED SWB 3 LOWER CHORD:

$\frac{wb^4}{ET^4} = \frac{25(102)^4}{10^7(.38)^4} = 13000 \rightarrow \delta = 8.2(.38) = 3.1\ IN$

SEE P. (13.1)

ASSUME FAILED SWB 3 & SWB 2 LOWER CHORDS: [COND 2]

$\frac{wb^4}{ET^4} = \frac{25(142)^4}{10^7(.38)^4} = 48500 \rightarrow \delta = 13(.38) = 4.9\ IN$

$WB 2 LOWER CHORD:

UNZIPPING OF TENS. RIVETS AFTER DEPARTURE OF KEEL BEAM:

- SHEAR DEFL. OF JT.

$$K_{JT} = 2(84)(.25)\left(1 - \frac{.25}{10(.38)}\right) = 39.2\ K/IN \left(\frac{2}{1.38}\right) = 56.8\ K/IN$$

- TENS. DEFL. OF JT.

$$K = \frac{AE}{\ell} = \frac{.075(10^7)}{.65} = 1161\ K/IN \left(\frac{2}{1.3}\right) = 1550\ K/IN$$

$$A = \frac{\pi}{4}(.31)^2 = .075$$

- BEND. DEFL. OF FLANGE

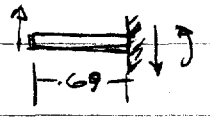

$$K = \frac{P}{\delta} = \frac{3EI}{\ell^3} = \frac{3(10^7)(.00225)}{(.69)^3} = 205\ K/IN$$

$$I = \frac{1(.3)^3}{12} = .00225\ IN^4/IN$$

- $K_{EQ} = \frac{1}{f_{EQ}}$ ← $f_{EQ} = f_1 + f_2 + \cdots$

$$\therefore K_{EQ} = \frac{1}{.02313} = 43.2\ K/IN$$

$$f_1 = \frac{1}{56.8} = .01761$$

$$f_2 = \frac{1}{1550} = .00064$$

$$f_3 = \frac{1}{205} = .00488$$

$$f_{EQ} = .02313$$

- COND. (2). DEFL.

UNIFORM VERT. DEFL. OVER 175.5 IN., DECR. TO 0 @ BL 127.75
RIVETS WILL DEVEL. FULL TENS. STRENGTH OVER THAT WIDTH

$V_{EQUIV} = 1.796\ K/IN\ (175.5\ IN) = 315.2\ K$ @ 25 PSI

KEEL BEAM BOLT PULL-THRU @ WCS LOWER SKIN:

$$\frac{P}{D^2(F_{TU})} = 1.4 \longrightarrow P_{\text{PULL THRU}} = 1.4(.5)^2(62 \times 1.1) = 23.9^K$$

$D/t = \frac{.5}{.38} = 1.33$ — [SKIN ONLY]

$D/t = \frac{.5}{.7} = .7$ $P_{\text{PULL THRU}} = .5^2(68)(2.0) = 34.0^K$ ← BOLTS WILL FAIL IN TENS. PRIOR TO SKIN FAILURE; $P_{MAX} = 32.6^K$ FOR 1/2" BOLTS

[SKIN + BEAM FLANGE]

REF. GRUMMAN DESIGN DATA: TENS. LOAD ON BOLTS / PLATES

(13.1)

SEE DEFL. ANAL. @ P. (12)

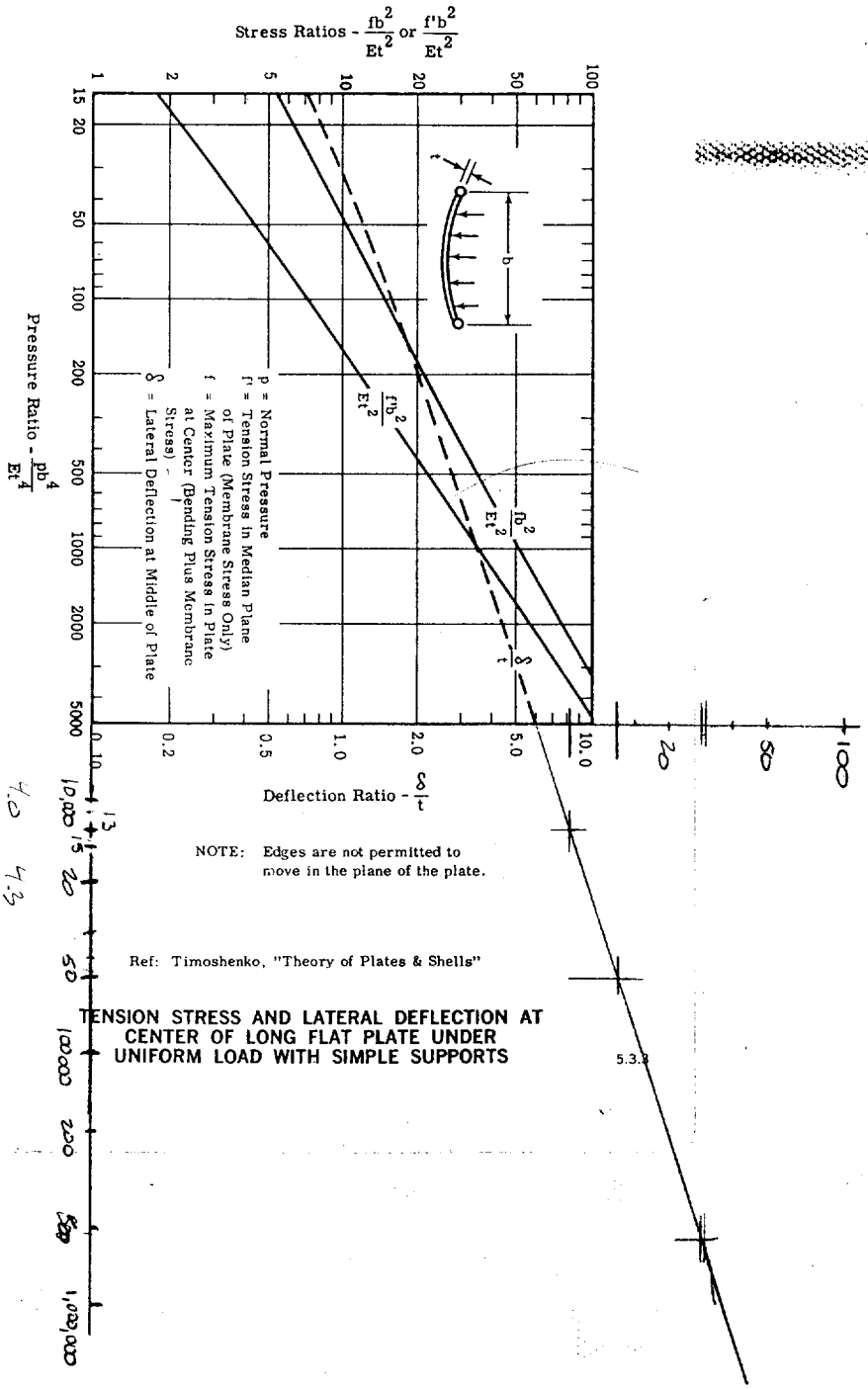

NOTE: Edges are not permitted to move in the plane of the plate.

Ref: Timoshenko, "Theory of Plates & Shells"

TENSION STRESS AND LATERAL DEFLECTION AT CENTER OF LONG FLAT PLATE UNDER UNIFORM LOAD WITH SIMPLE SUPPORTS

5.3.3

KEEL BEAM DEFL.:

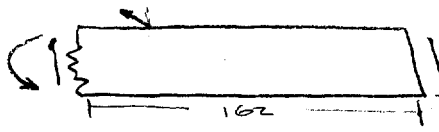

$V_{FAIL} = 24.4^K$ SEE P.(23)

LFGA IS ± 13'x12' = 156 FT² = 22460 IN²

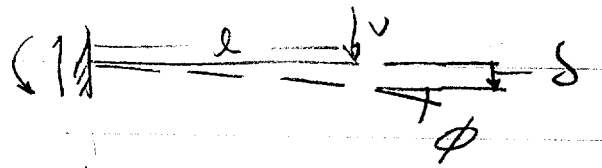

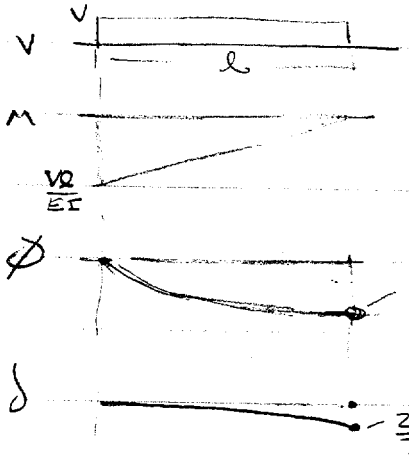

$E = 10^7$

$I = 1066\ IN^4$

$\delta = \frac{24.4(162)^3}{3(10^7)(1066)} = 3.24$ IN.

$\phi = \frac{24.4(162)^2}{2(10^7)(1066)} = .030$ RAD (1.7°)

KEEL STIFFNESS: (MOM. OF INERTIA)

$I = I_o + \Sigma(A\varphi^2) - \Sigma A\varphi(\bar{\varphi})$

$I = 94.57 + 597.7 - \frac{33.67(4.73)}{159.22} = [533.0\ IN^4/SIDE] \times 2 = 1066\ IN^4$

SEE P.(22)

A	φ	Aφ	Aφ²	I_o
5.00	0	0	0	5.45
1.62	12.85	20.82	267.5	89.12
.50	25.7	12.85	330.2	—
7.12		33.67	597.7	94.57

$\bar{\varphi} = \frac{\Sigma(A\varphi)}{\Sigma A} = \frac{33.67}{7.12} = 4.73$

$\Sigma = 20.97$

LFGA LOADS:

ASSUME LFGA RETAINS "SCOOP" SHAPE & WILL NOT EXHIBIT BEND. DEFL.

$\delta_{\substack{FWD \\ EDGE \\ LFGA}} = 3.24 + .030(156) = 3.24 + 4.68 = 7.92$ IN.

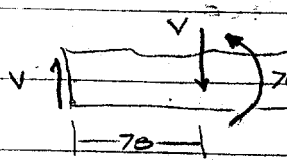

STRINGERS (11)

$V = \frac{1}{4}(.1)156 = 16.2^K$

$W = 16.2(.1) = 16.2$ LB.

$I = \frac{Ml^2}{3} = \frac{16.2(156)^2}{386(3)}(11) = 1433\ IN\text{-}LB\text{-}SEC^2$

SKIN: (156x160)

$V = 160(.1)(156) = 2500$

$W = 2500(.1) = 250$

$I = \frac{Ml^2}{3} = \frac{250(156)^2}{386(3)} = 5250\ IN\text{-}LB\text{-}SEC^2$

(15)

FRAMES (7)

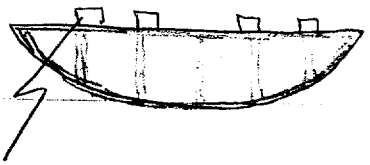

CARGO RAILS (4)

ITEM	W	ΣW
STRINGERS	68	68
SKIN	250	318
FRAMES	140	458
RAILS	40	498 ← LFCA

FRAMES (7)

$A = 2570$

$W = 20$

$\Sigma W = 140$

$I = \frac{140(156)^2}{386(3)} = 2940$

$W_{EST} = 10$

$\Sigma W = 40$

$I = \frac{40(156)^2}{386(3)} = 840$

$\Sigma I = 1433 + 5250 + 2940 + 840 = 10463 \quad IN-LB-SEC^2$

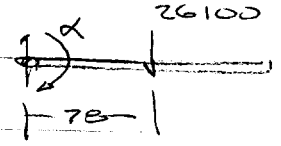

$M = 78(26100) = 2.03 \times 10^6$

$I = 10463$

$M = I\alpha$

$\alpha = \frac{M}{I} = \frac{2.03\,E6}{10463} = 194 \; RAD/SEC^2$

$X = V_0 t + \frac{1}{2} A t^2$

$V^2 = V_0^2 + 2AX$

$V = V_0 + At$

$\phi_{.012} = \frac{1}{2} A t^2 = \frac{194}{2}(.012)^2 = .014 \; RAD \; (0.8°)$

$\phi_{.025} = \frac{194}{2}(.025)^2 = .061 \; RAD \; (3.47°)$

$\phi_{.050} = \frac{194}{2}(.05)^2 = .242 \; RAD \; (13.9°)$

ALL OF THESE ANGULAR DISPLACEMENT VALUES (FOR 12 MILLISEC, 25, & 50 MILLISEC.) ARE WITHIN A REASONABLY EXPECTED RANGE WHICH CORRESPONDS TO THE ANGULAR DEFLECTION OF THE KEEL BEAM FORWARD END (SEE P.(14); $\phi_{BEAM} = 1.7°$).

(16)

12/13/96

VIEW LKNG AFT ~ LOWER BLKD FS 990

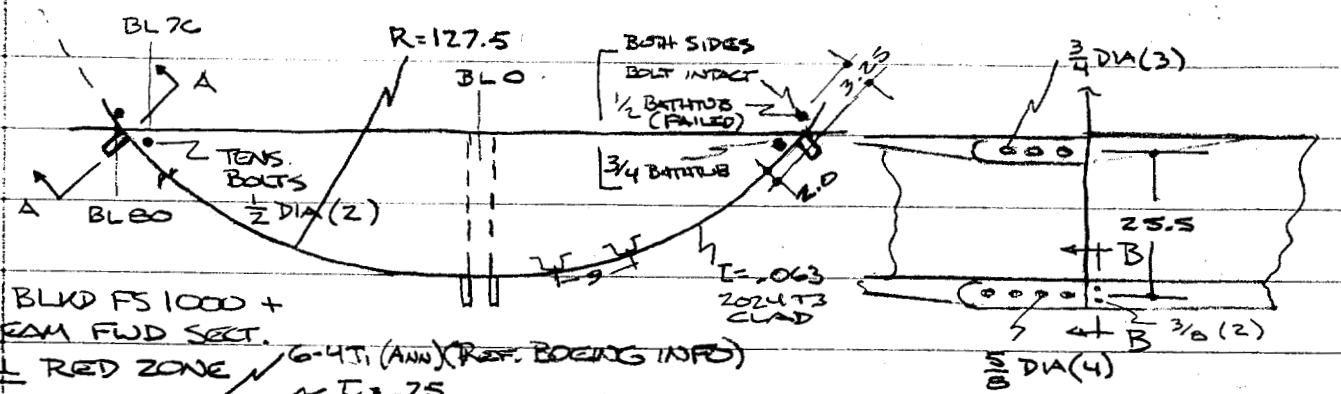

NOTE: LFGA, BLKD FS 1000 + KEEL BEAM FWD SECT. ARE ALL RED ZONE

A-A:

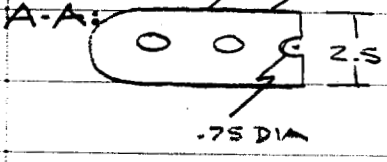

$A = .75(2.5 - .75)$

$A = 1.312$

$P = 130(1.312) = 170.6^K$

$I_x = \frac{.75(2.5)^3}{12} - \frac{.75(.75)^3}{12} = .95$

$P_{BOLT} = 32.6^K/BOLT$

$M_x = \frac{1.4(130)(.95)}{1.25} = 138.3$

$M = 2\left[\frac{1.75}{2}(.75)(130)\right][.81] = 138.5$ ✓

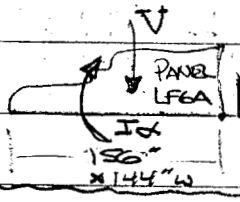

M_{BOLT} 32.6(3.25) = 106.0

$f_{BATHTUB} = 2.73W = 78^{KSI}$

$W_{BATHTUB} = 28.5^K$ ✓ BOLT WILL SURVIVE

PANEL RF9S & LFS1:

PANEL @ A-A IS 60L x 54W

$A = 60(54) = 3240 IN^2 = 22.5 FT^2$

$D = 270(22.5) = 6075$

$D = \frac{1}{2}\rho AV^2 C_D = \frac{1}{2}(.00238 \frac{LBS\ SEC^2}{FT^4})(348500 \frac{FT^2}{SEC^2})(1.0)(A_{FT^2})(.65) = 270A$ → $\frac{270}{144} = 1.87\ PSI$

$V = 350^{KT} = 402^{MPH}(\frac{44}{30}) = 590\ FT/SEC$; $V^2 =$ DENSITY RATIO @ 14000' → $\therefore M = 6.07(30) = 182 IN\text{-}K$

$M_{FAIL} = 2(28.5)(3.25) = 185\ IN\text{-}K$

∴ AIRFLOW STAGNATION PRES (+ CABIN PRES.) WILL FAIL THIS PANEL & FTGS IN DOWNWARD DIRECTION.

FAILURE WILL OCCUR @ 2X THE LOW VALUE OF BOLT / BATHTUB STRENGTH (BOTH ARE LOADING EQUALLY UNTIL WEAKEST JOINT FAILS - THEN Ti FTG. WILL FAIL IMMED. BECAUSE IT'S BOOD. STRENGTH IS LESS THAN 2X THE LOW JOINT FAIL. LOAD).

B-B:

SECT. @ FAILURE

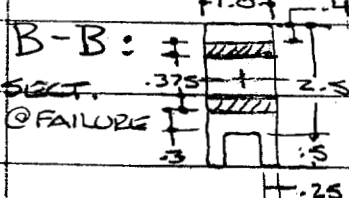

$A = (2.5 - .75)(1.0)$

$A = 1.75$

$P = 78(1.75) =$

$I = \frac{1(2.5)^3}{12} - 1(.38)[.71]^2(2) = 1.68$

$M = \frac{1.4(78)(1.68)}{1.25} = 147.2 IN\text{-}K$

$M = 78V$

$V_{MAX} = \frac{147.2}{78} = 1.9^K$

12/10/96

	ΣA	$K \frac{LB}{IN}$	$\Omega = \frac{1}{K}$
.250 (4)	.196	5.89×10^6	$.17 \times 10^{-6}$
.437 (2)	.300	9.00×10^6	.111
.500 (2)	.39 T_1	6.24×10^6	.16
.375 (2)	.22	6.60×10^6	.152
RIVETS	.096/IN	$.96 \times 10^6$	1.042
	WEB	$.29 \times 10^6$	3.448

RIVETS .077(2)/1.6 = .096/IN

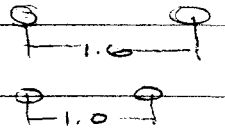

KEEL BEAM/BOLT REL. STIFFNESS:

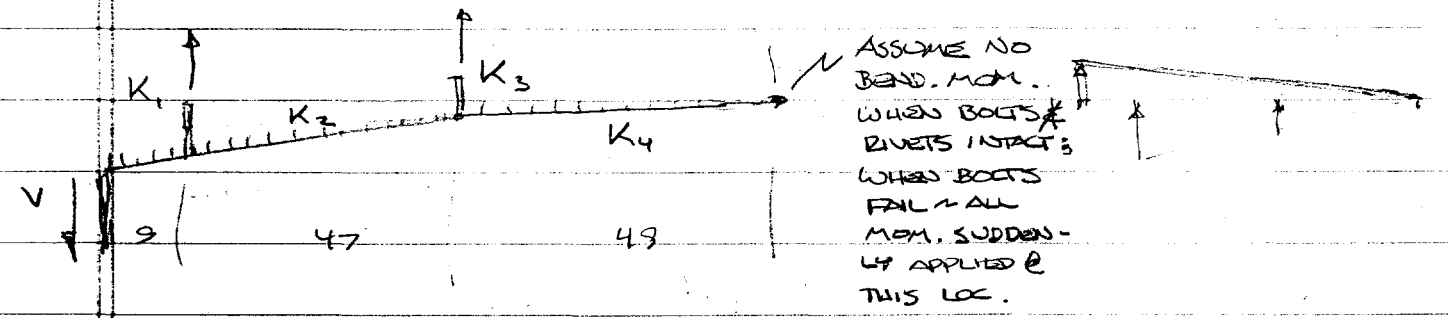

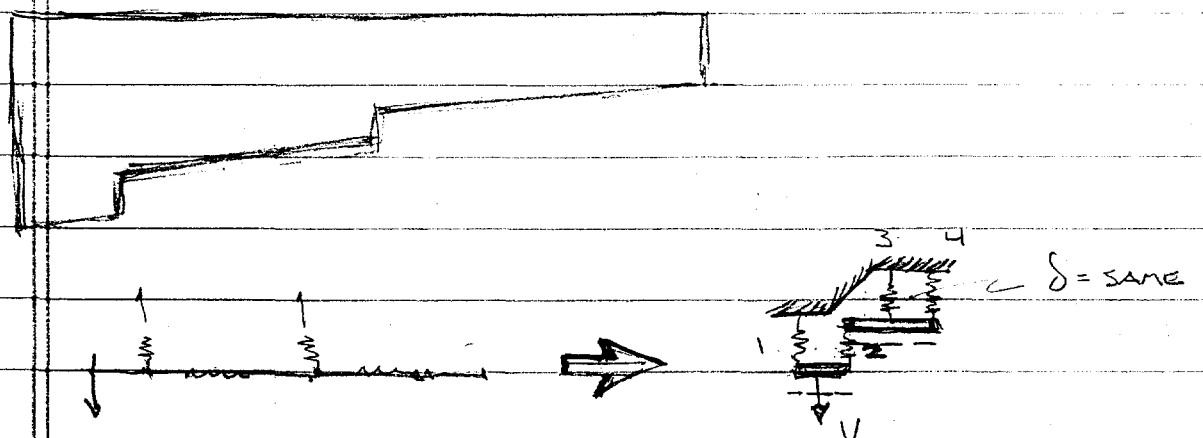

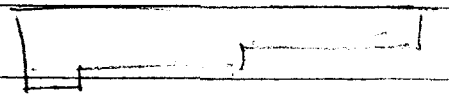

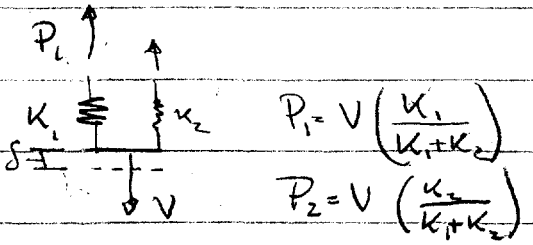

$$P_1 = V\left(\frac{K_1}{K_1+K_2}\right)$$

$$P_2 = V\left(\frac{K_2}{K_1+K_2}\right)$$

$$P_1 = K_1\delta$$

$$P_2 = K_2\delta$$

$$V = P_1 + P_2 = K_e\delta = K_1\delta + K_2\delta$$

$$K_e = K_1 + K_2$$

12/11/96

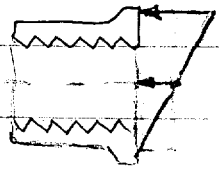

SEVERAL SOURCES HAVE STATED THAT THIS LOADING DISTR. ON NUT CAN STRIP THE INTERNAL THREADS. LET'S LOOK AT IT & SEE IF WE AGREE.

THIS ANAL. WILL BE COMPLETED AT A LATER DATE.

VELOCITY OF CRACK TIP PROPAGATION:

$38\% V_{SOUND} = .38(16750 FT/SEC)$

FRACTURE @ 6360 FT/SEC

$R = \frac{127.5}{12} = 10.62$ FT

$\Sigma l_{FRACT} = (13 + 2\pi R) = 79.7$ FT

$\Delta T = .012$ SEC = 12 MILLISEC.

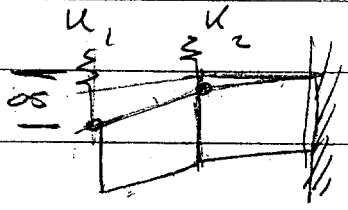

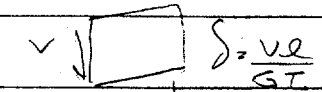

$\delta = \frac{Pl}{AE}$

$K = \frac{P}{\delta} = \frac{P}{\frac{Pl}{AE}}$

$K = \frac{AE}{l}$

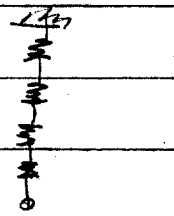

$-\frac{3}{3}$

BOLT GRIP LENGTH $\cong$ 1.0

$K_{BOLT} = \frac{A(30\,10^6)}{1.0} =$

RIVET GRIP LENGTH $\cong$ 1.0

$K = \frac{A(10\,10^6)}{1.0} = \frac{.077\,10^7}{1.0 \times 1.6} \times 2 = .77 \times 10^6$

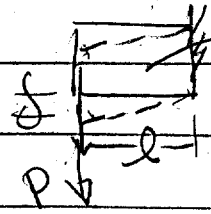

$\delta = \frac{P\,l}{htG}$

$K_{RIVET} = \frac{htG}{l} = \frac{26(.063)(2)(4\times10^6)}{l} = \frac{13\times10^6}{l}$

$K = \frac{P}{\delta} = \frac{htG}{l}$

$$\delta_1 = \frac{P_1}{K_1} \qquad \delta_2 = \delta_1 - \delta_3 = \frac{P_2}{K_2} \qquad \delta_2 = \frac{P_1}{K_1} - \frac{P_3}{K_3} = \frac{P_2}{K_2}$$

$$\delta_3 = \frac{P_3}{K_3} = \frac{P_4}{K_4} = \delta_4$$

$$V = P_1 + P_2 \qquad P_2 = P_3 + P_4$$

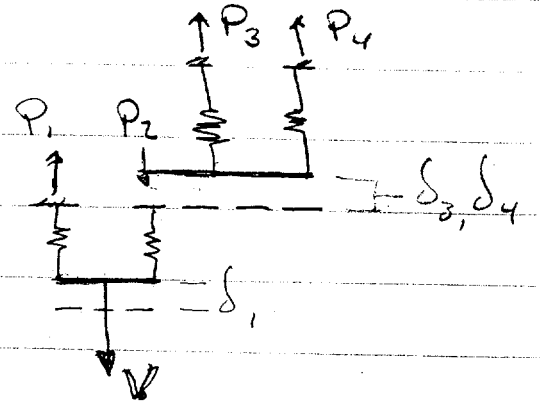

$$P_1 = V - P_2 = V - (P_3 + P_4)$$

$$\delta_1 = \frac{V - P_3 - P_4}{K_1} \qquad \delta_2 = \frac{P_1}{K_1} - \frac{P_3}{K_3} = \frac{V - P_3 - P_4}{K_1} - \frac{P_3}{K_3} = \frac{P_2}{K_2}$$

$$P_3 = \left(\frac{K_3}{K_3 + K_4}\right) P_2 \qquad P_4 = \left(\frac{K_4}{K_3 + K_4}\right) P_2$$

$$\delta_3 = \frac{P_2}{K_3 + K_4} = \frac{P_2}{K_{e_{34}}}$$

$$\delta_2 = \delta_1 - \frac{P_2}{(K_3 + K_4)} = \frac{P_2}{K_2}$$

$$= \left[\frac{P_1}{K_1} - \frac{P_2}{(K_3 + K_4)}\right] = \frac{P_2}{K_2}$$

$$\frac{P_1}{K_1} = \frac{P_2}{K_2} + \frac{P_2}{K_3 + K_4} = P_2\left\{\frac{1}{K_2} + \frac{1}{K_3 + K_4}\right\}$$

$$P_1 = P_2\left[\frac{K_1}{K_2} + \frac{K_1}{K_3 + K_4}\right] = V - P_2$$

$$V = P_2 + P_2\left[\frac{K_1}{K_2} + \frac{K_1}{K_3 + K_4}\right] = P_2\left[1 + \frac{K_1}{K_2} + \frac{K_1}{K_3 + K_4}\right]$$

$$P_2 = \frac{V}{\left[1 + \frac{K_1}{K_2} + \frac{K_1}{K_3 + K_4}\right]}$$

12/11/96

(A) K_1/K_2	(B) $K_1/(K_3+K_4)$	(C) $1+(A)+(B)$	$P_2 = V/(C)$	P_1	$\left(\frac{K_3}{K_3+K_4}\right)\left(\frac{K_4}{K_3+K_4}\right) P_3$	P_4
$\frac{5.88}{.29}$	$\frac{5.88}{9.00+.29}$				$\frac{9.0}{9.29}$ $\frac{.29}{9.29}$	
20.28	.633	21.91	.046V	.954V	.969 .031	.044V .002V

THE WEB HAS VIRTUALLY NO STIFFNESS COMPARED TO THE BOLTS;
∴ NO LOAD IS TRANSFERRED AFT TO 2ND GROUP OF BOLTS;
∴ DO NOT PURSUE THIS ANAL. FURTHER ~ ORIG. ANAL. FOR SEQUENTIAL FAILURE IS SUFFICIENT ALTHOUGH WE SHOULD ATTEMPT TO ACCOUNT FOR THE 5/16 RIVETS.

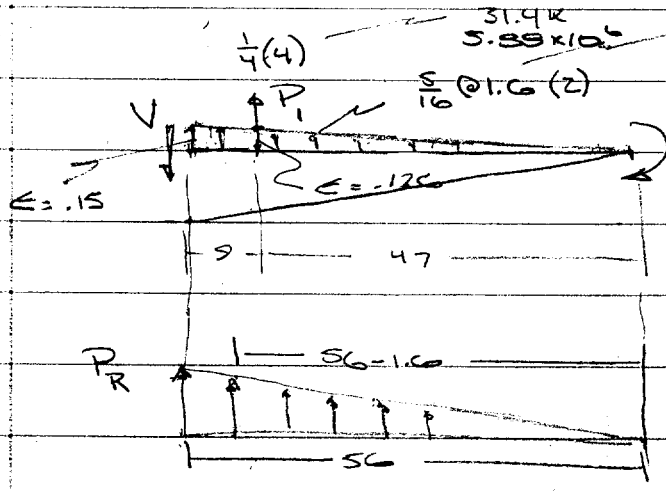

$M = P_R[1008] + 4P_1[47]$

$M = 1008P_R + 188P_1 = 56V$

$\delta_R = \frac{P_R}{K_R} = \frac{P_R}{1.54\times10^6}$ (2 RIVETS)

$\delta_1 = \frac{P_1}{K_1} = \frac{P_1}{5.88\times10^6}$ (4 BOLTS)

$\delta_1 = \frac{47}{56}\delta_R$

$\frac{P_1}{5.88\times10^6} = \frac{47}{56}\left(\frac{P_R}{1.54\times10^6}\right)$

$P_1 = \frac{47}{56}\left(\frac{5.88}{1.54}\right)P_R = 3.2P_R$

$\Delta M_0 = 2P_R\frac{56}{56}[56]$

$\Delta M_1 = 2P_R\left(\frac{56-1.6}{56}\right)[56-1.6]$

$\Delta M_2 = 2P_R\left(\frac{56-2(1.6)}{56}\right)[56-2(1.6)]$

$\Delta M_{34} = 2P_R\left(\frac{56-34(1.6)}{56}\right)[56-34(1.6)]$

$\Sigma M = 2P_R(\approx.5)[1008]$

$56V = 1008P_R + 188(3.2P_R)$

$V = \frac{1609P_R}{56} = 28.74P_R$

$P_R = \frac{V}{28.74} = .0348V$ (2 RIVETS)

$P_1 = 3.2P_R = .1113V$ (4 BOLTS)

BASED ON FAILURE OF RIVETS: $V_{max} = \frac{4.1(2)}{.0348} = 235^K$

BASED ON FAIL. OF BOLTS: $V_{max} = \frac{31.4}{.1113} = 282^K$

IF BOLTS ONLY: $P_1 = \frac{56}{47}V = 1.19V$ → $V_{max} = \frac{31.4}{1.19} = 26.4^K$

THIS APPARENT INCR. IN STRENGTH DUE TO ADDITIONAL SUPPORT PROVIDED BY RIVETS IS BASED ON THE ASSUMED FLAT PLATE OF THE WCS LOWER SKIN, BUT THAT SKIN IS UNSUPPORTED 3/8" PLATE & WILL ADOPT A CURVATURE, ALLOWING RIVETS TO PULL AWAY 1 ROW AT A TIME ∴ THERE IS NO WAY THAT THE ALUM. RIVETS WOULD INCR. THE STRENGTH AS SHOWN ABOVE TO APPROX. 10 TIMES THAT OF THE BOLTS ALONE! (IF THE RESULT HAD BEEN 10 - 20%, I MAY HAVE BELIEVED IT!)

LET'S LOOK AT WCS LOWER SKIN CURVATURE:

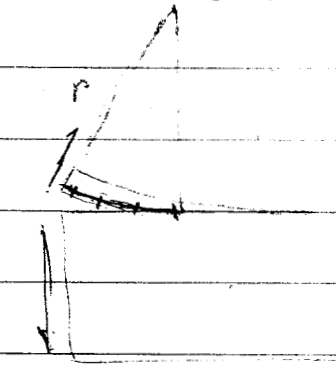

$$\frac{1}{r} = \frac{M}{EI} = \frac{Vl}{EI}$$

$$r = \frac{10^7(36)(.38)^3}{12\,Vl} = \frac{1.65\times10^6}{Vl}$$

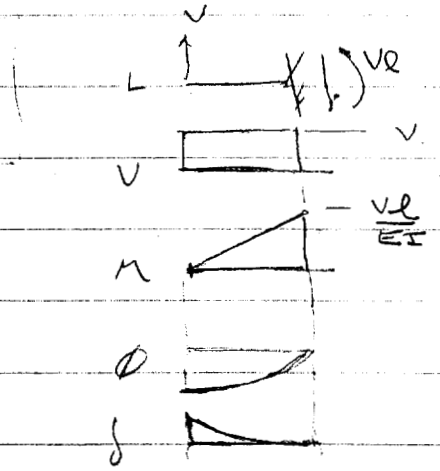

$$r = \frac{1.65\times10^6}{26400(l)} = \frac{62.5}{l}\ \text{IN.}$$

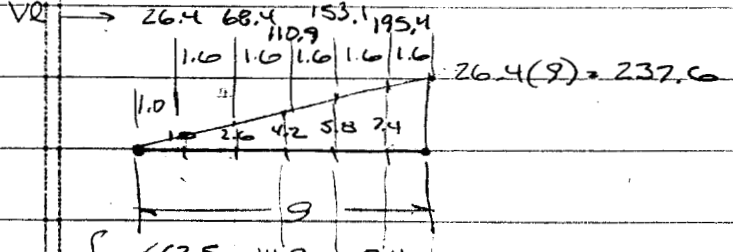

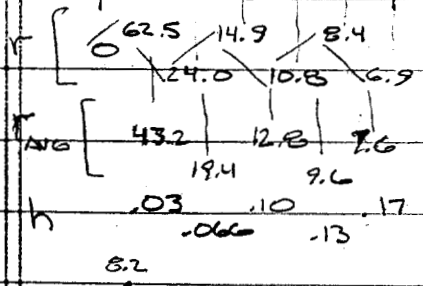

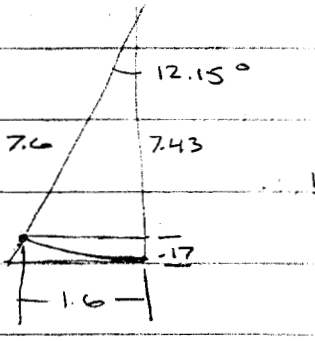

$$\frac{1.6}{r} = \sin\alpha$$

$$h = r - r\cos\alpha$$
$$= r(1-\cos\alpha)$$

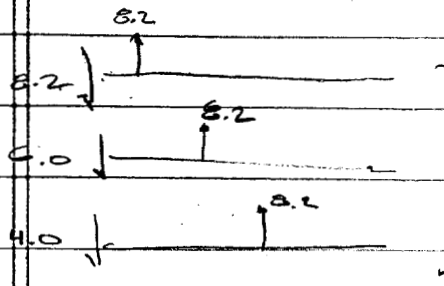

THE RIVETS WILL UNZIP AT A LOAD SIGNIF. LESS THAN REQD TO FAIL BOLTS ∴ THE RIVETS DO NOT CONTRIB. TO KEEL PEEL-AWAY STRENGTH!

ANAL. OF KEEL BEAM FAILURE SEQUENCE :

GEOM. :

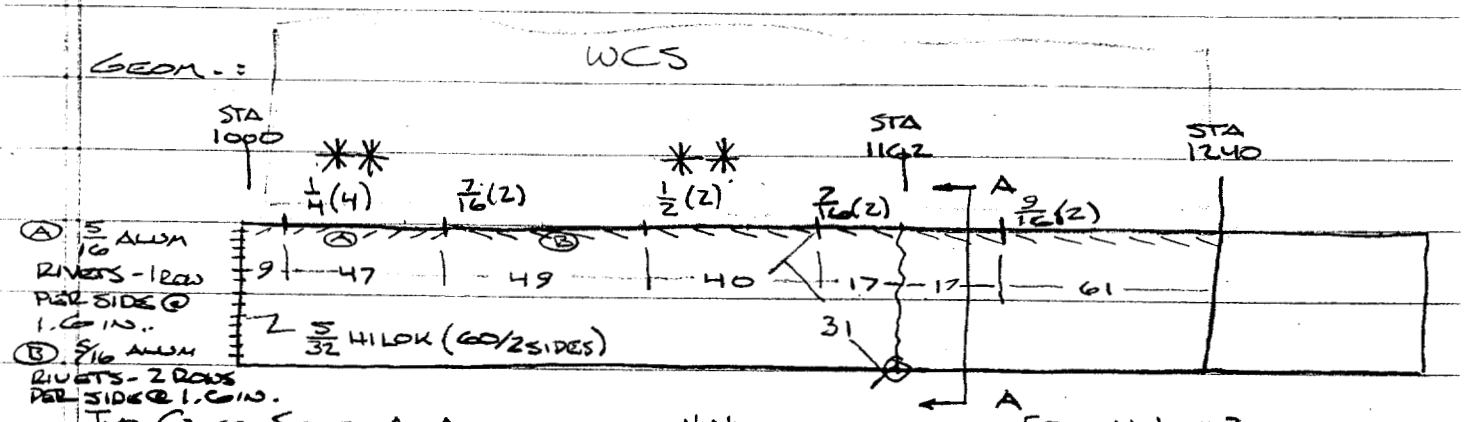

TYP. CROSS-SECT. A-A :

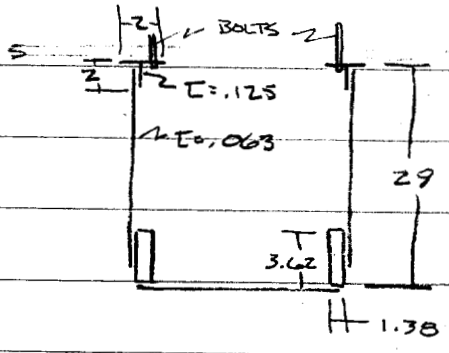

** NUTS STRIPPED [2 OF 4 ¼" / 2 OF 2 ½"]

	D	A	F_{TU}	T	$	ΣT	Σ$
2 SIDES	.156	.019	220		1.80	—	108
	.25		(132)	7.18	4.65	28.7	—
	.437			24.0	14.25	480	—
	.50			32.6	14.7	65.3	—
	.562				23.56	79.4	—
	.312	.077	50	4.1	@ 2 RIV. 1.6 IN	5.12 K/IN 10.25 K/IN	

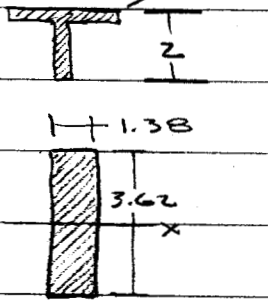

A = .50

I = NEGL.

$P_{MAX} = 42(.5) = 21^{K}$/SIDE

A = 5.0

I = 5.45

$M_{MAX} = \frac{F_{TU} I}{c} = \frac{60(5.45)}{1.81} = 181$ IN-K/SIDE

$M_{PLASTIC} = 1.4(181) = 253$ IN-K/SIDE

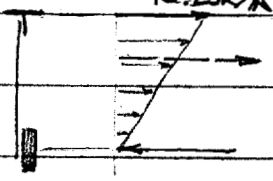

2024 T351 EXTR.

$F_{TU(B)} = 47$ KSI

$F_{ALLOW} = .82(47)(1.1) = 42$ @ ε = 12%

2024 T3 CLAD SHT.

$F_{TU(B)} = 62$ KSI

$F_{ALLOW} = .82(62)(1.1) = 56$ @ ε = 15%

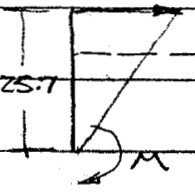

$\frac{3M}{b t^2} = F_{ALLOW}$

$M = \frac{56}{3}(.06)(25.7)^2$

$M = 776.7$ IN-K/SIDE

$\frac{2}{3}(25.7)P = M$

$P = 45.3^{K}$

$\Sigma M_{FAIL} = 21(25.7) + 776.7 + 181 = 1497$ IN-K/SIDE (MIN.)

$= 2994$ IN-K TOTAL 2 SIDES (MIN.)

$= 2994 + 2(253 - 181) = 3138$ (MAX.)

PROGRESSIVE FAILURE OF TENS. BOLTS IN KEEL BEAM:

HINGE MOVES TO NEXT BOLT ROW AFTER FAILURE OF FIRST ROW ~ DOES KEEL BEAM SURVIVE?

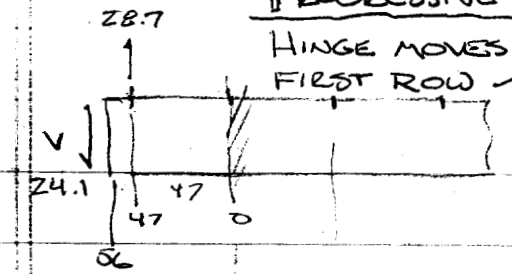

$V = 28.7\left(\frac{47}{56}\right) = 24.1^{K}$

$M_{O_{\text{AFTER BOLT FAILURE}}} = 24.1(56) = 1349 \text{ IN-K}$

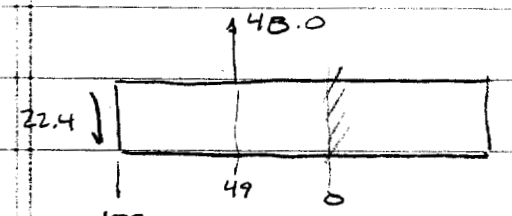

$V = 48\left(\frac{49}{105}\right) = 22.4$

$M_O = 22.4(105) = 2352$

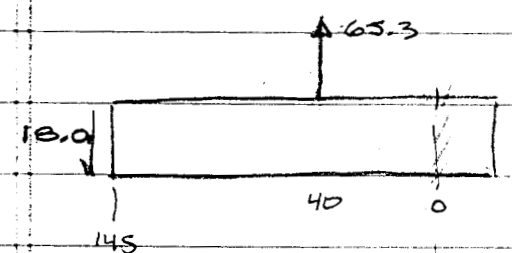

$V = 65.3\left(\frac{40}{145}\right) = 18.0$

$M_O = 18.0(145) = 2612$

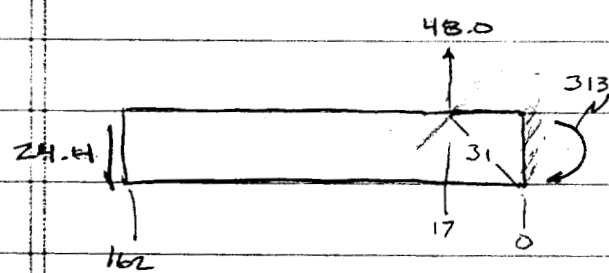

$\Delta V = 48.0\left(\frac{17}{162}\right) = 5.0$

$M_O = 1816$

$M_{O_{FAIL}} = 3138$ } $\Sigma M_O = 3954$

$V_{MAX} = \frac{3954}{162} = 24.4^{K}$ (@ $M_{FAIL} = 3138$)

OVERLOAD FAILURE OF KEEL

$M_{FAIL} = 2984 - 3138$ IN-K

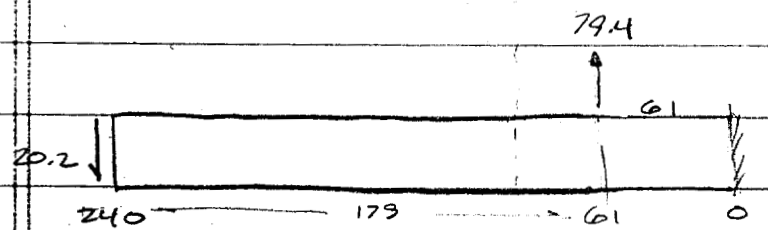

$V = 79.4\left(\frac{61}{240}\right) = 20.2$

$M_{61} = 20.2(179) = 3612$

KEEL WILL FAIL BEFORE THIS BOLT GROUP FAILS!

THE FAILURE SEQUENCE BEGINS WITH LOAD BUILD-UP AT FRONT OF KEEL FROM "SMILEY-FACE" BLKD. TO A LEVEL WHICH WILL INITIATE FAILURE OF 1ST ROW OF BOLTS (@ 24.1K). SUBSEQUENTLY, THE BOLTS WILL "UNZIP" ONE AFTER ANOTHER (BECAUSE THE SUBSEQUENT FAILURE LOADS ARE LESS (THAN 26.4K) & YET THE KEEL BENDING STRENGTH IS NOT EXCEEDED AT ANY POINT UNTIL THE 4TH SET OF BOLTS (THE 7/16" BOLTS WHICH ARE SEVERELY BENT AFT). WHEN THE 1ST THREE BOLT GROUPS HAVE FAILED & THE 4TH SET IS NEXT IN LINE, THE 3/8 BOLTS BEGIN TO ELONGATE & ALL ADDITIONAL LOAD IS TRANS. TO KEEL WEB WHICH THEN FAILS AT FS 1162 ALONG WITH THE BOLTS (THIS ENTIRE SEQUENCE TAKES PLACE IN MILLISECONDS).

THE SEQUENCE DESCRIBED IS BASED ON CONCEPT OF INPUT LOAD RESPONDING TO RESISTANCE OF FAILURE PATH

∴ V BEGINS AT ZERO, BUILDS TO 26 THEN DROPS TO 20 AS FAILURE PROGRESSES

MAX. DEFLECTION OF FRONT SPAR UPPER CHORD VERT. FLANGE:

CHORD ANGE IS 7075 T6511 EXTRUSION
F_{TU} = 85 KSI
e = 7%

ASSUME: UNIFORM PRES. @ AFT SIDE
PIN END @ WCS CLOSURE RIB (Y = 120)

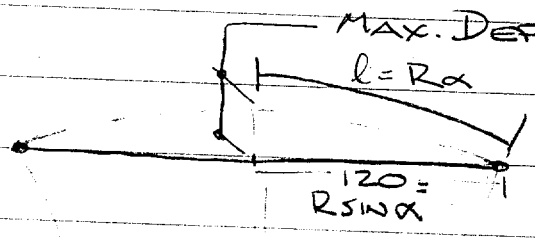

$$\delta = R(1-\cos\alpha)$$

$R\cos\alpha$ — R

$$e = \frac{\Delta\ell}{\ell} = \frac{R\alpha - R\sin\alpha}{R\sin\alpha} = .07$$

$$\frac{R\alpha}{R\sin\alpha} - 1 = .07$$

α

$$\frac{R\alpha}{R\sin\alpha} = 1.07 = \frac{\alpha}{\sin\alpha}$$

2 UNKNOWNS W/ 1 EQ.:
∴ TRIAL & ERROR SOLUTION REQ'D

α	SIN α	COS α	$\frac{\alpha}{\sin\alpha} = 1.07$	$\ell = 120(1.07)$	$R = \frac{\ell}{\alpha}$	$\delta = R(1-\cos\alpha)$
.635	.593	.805	1.07054	128.4	202.2	39.4 IN.

OTHER TRIAL & ERROR NOT SHOWN - FOR BREVITY

EVIDENCE OF DEFORMATION AT THIS TANK FWD SPAR WEB UPPER CAP IS APPARENT FROM EXAMINATION OF FS 980 & 960 FLOOR BEAMS.

FOR THE EFFECT OF HOLES IN THIN SHEET, A NOTCH REDUCTION FACTOR IS APPLIED TO THE "TYPICAL" TENS. ULT. STRENGTH AS FOLLOWS

F_{TU} = 62 FOR 2024 T3 CLAD .063

TYP. TENS. ULT. = 1.10 × F_{TU} = 1.1(62) = 68.2 KSI

NOTCH REDUCT. FACTOR = .82 × TYP. TENS. ULT. = .82(68.2) = 55.9 KSI

THE UPPER CHORD, HOWEVER, IS .300 IN. THK. & ∴ THE ABOVE REDUCTIONS DO NOT APPLY! ∴ ANAL. AS SHOWN IS VALID FOR MAX. STRAIN UP TO F_{TU} @ 7% ELONG.

TWA 800

RHS LOWER SKIN/STRINGER DEFORMATION : 12/11/96

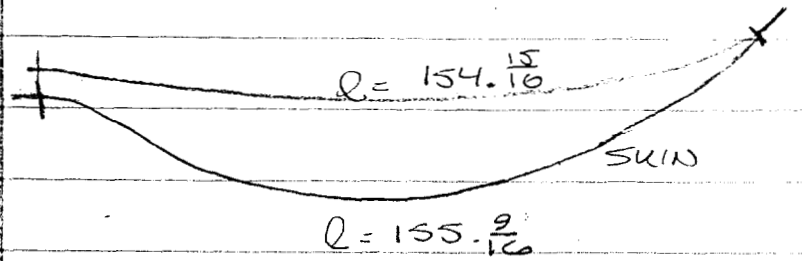

155.562 SKIN
154.937 STR
.625

$\epsilon = \frac{.625}{155} \approx .004$

$f = 002(10^7)$

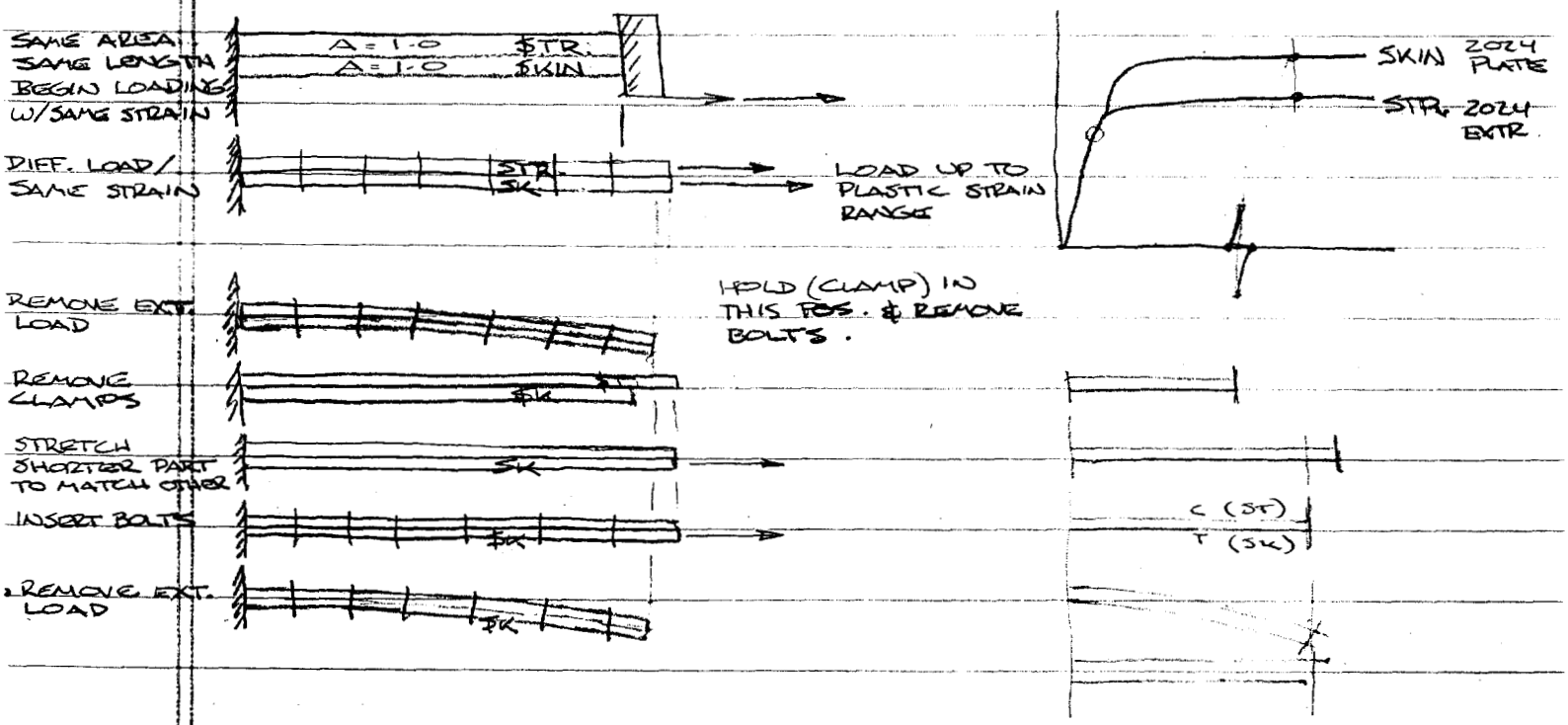

THE ABOVE OBSERVATIONS DESCRIBE THE EXPECTED CONDITION OF A BOLTED COMBINATION OF 2024 PLATE (SKIN) & 2024 EXTRUSION (STRINGER) AFTER EXPOSURE TO UNIFORM TENSION STRESS INTO THE PLASTIC RANGE WHILE RESTRAINED TO FORCE EQUAL STRAINS IN BOTH PARTS.

THE CONDITION FOUND @ THE RHS LOWER SKIN (WS 382 ⊕ FRONT) WAS AS SHOWN ABOVE WITH THE STRINGER SEPARATED OVER A LENGTH OF 155 IN. THE SKIN ELEMENT WAS LONGER THAN THE STRINGER, INDICATING THAT THESE PARTS DID NOT ARRIVE AT THE OBSERVED STATE AS A RESULT OF UNIFORM TENSION INTO THE PLASTIC RANGE WHILE ACTING AS PART OF THE INTACT WING WITH APPLIED WING BENDING LOADS. [FOR THIS LOCATION]. OTHER LOCATIONS EXHIBIT DIFFERENT CONDITIONS OF THE SKIN/STRINGERS WHICH COULD SUPPORT THE BOEING VIEW THAT THE WING WAS YIELDED BY BENDING INTO THE PLASTIC RANGE.

MIL-5G DATA:

		2024 T351 EXTR t = < .25		2024 T3 CLAD SHT t = .063	
		A	B	A	B
F_{TU}	L	42	47	62	63
	LT	37	41	61	62
F_{TY}	L	42	47	45	47
	LT	37	41	40	42
F_{CY}	L	34	38	37	38
	LT	41	45	43	45
F_{SU}		29	31	38	39
e_{MIN}		12%		15%	
F_{BRU}		84	94		
E		10.8×10^6		10.5×10^6	

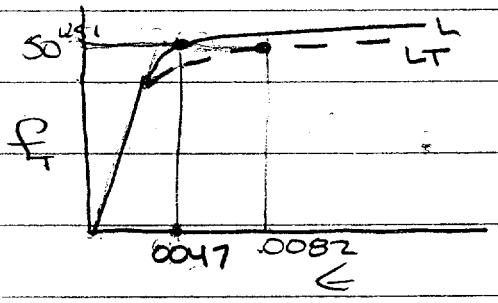

TYP @ R.T. t = .25

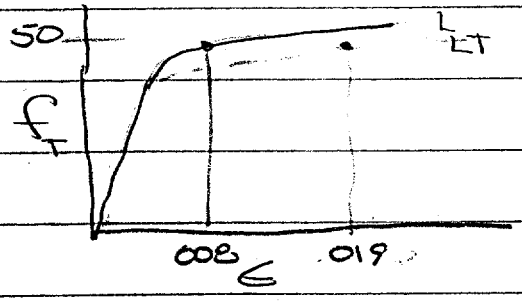

TYP @ R.T. t = .064

7075 T651 QQ-A-200/11
t = .300

SUMMARY OF OBSERVATIONS:

CONDITION OF TWA 800 STRUCTURE:

- PRIOR TO ARRIVAL AT THE CALVERTON NAVAL WEAPONS CENTER, SEVERAL AREAS OF TRANSPORT AIRPLANE STRUCTURES WHICH ARE CHARACTERISTICALLY SENSITIVE TO FATIGUE CRACKING HAD BEEN CONSIDERED AS SUSPECT AREAS TO BE EXAMINED FIRST.
- THESE AREAS WERE;
  (1) FUSELAGE SKIN LONGITUDINAL LAP SPLICE JOINTS
  (2) WING REAR SPAR LOWER CAP AT THE WING ROOT, SPLICE JOINT
  (3) FLAP SUPPORT STRUCT - ATTACHMENTS AT WING REAR SPAR
  (4) AND OTHER HIGHLY LOADED POINTS WITH LOAD TRANSFER THRU SPLICE JOINTS (HIGH LOADED FASTENERS)
- THE ABOVE AREAS WERE EXAMINED WITH RESULTS AS FOLLOWS:
  (1) FUSELAGE LONGITUDINAL LAP SPLICES WHERE FUS. SKIN HAD SEPARATED ("RED AREA" SKINS) → NO EVIDENCE OF PRE-EXISTING CRACKS WAS OBSERVED. (NEPCO)
  (2) WING REAR SPAR LOWER CAP @ WING ROOT SPLICE JOINT; LHS & RHS → (NEPCO)
  (3) WING LOWER SKIN FORE/AFT SPLICE JOINT, LHS & RHS → (NEPCO)
  (4) WING LOWER SKIN, OUTBD OF ROOT SPLICE JOINTS, LHS & RHS → (NEPCO)
  (5) WING LOWER SKIN, OUTBD OF OUTBD ENG. (#1 @ LHS & #4 ENG @ RHS) → (NEPCO)
- THE FOLLOWING ADDITIONAL AREAS WERE EXAMINED WITH RESULTS AS NOTED:
  (1) WING CENTER SECT (TANK) FRONT SPAR LOWER CAP ANGLE WITH CRACKS FOUND BY PREVIOUS INSP. TEAM, 2 PLACES AT INTERSECTION W/ RING CHORD. → THESE CRACKS NOT CONSIDERED AS CONTRIBUTING TO ANY SUBSEQUENT EVENTS (NCCTSE).
  (2) FUS. LONGERON @ WCS UPPER SKIN FWD SPAR → NCCTSE
  (3) WING CENTER SECT. FRONT SPAR UPPER SKIN "T" SECT. FITTINGS FOR ATTACHMENT OF SPAR WEB STIFFENERS, 4 PLACES → (NCCTSE)

JON HJELM
FAA-NYACO

APPENDIX E

BOEING SUPPORTING DATA

Appendix E: Boeing Supporting Data

E.1 Introduction

Both concurrent with and subsequent to the determinations of the Sequence Group, Boeing conducted separate analyses in the Seattle area to address various steps of the documented breakup sequence. This exercise was done with the intent of providing added assurance that the sequence as determined from the wreckage evaluation on site would in fact be rational from the perspective of a much more rigorous analytical assessment of airplane loads, stresses, and predicted structural behavior.

The primary analysis tool used was an ANSYS finite element model comprised of the fuselage from FS 520 to FS 1480 and the majority of the wing box. Due to the very large size of the model (approximately 120,000 degrees of freedom) and the need to run thousands of iterations to address the nonlinear, dynamic effects of the structural behavior, a number of weeks of run time were required on the Cray T94 computer.

Only selected aspects have been presented in this appendix added as part of the April, 1997 reconvening of the Sequence Group. The analysis work is still ongoing and further tasks may possibly be defined as a result of the latest efforts by the Group. This data is presented with the intent of supplementing, not replacing, the stress analysis done on site within the Group and summarized in Appendix D.

E.2 Failure Initiation in the Red Area Fuselage

The computer model was adapted to simulate the failure of SWB #3 and the front spar as described in Sections 4.10 and 4.11. For the purpose of these analyses a sustained overpressure of 25 psi was assumed in the wing center section. This number was selected because it is somewhat higher than the minimum breaking strength of center section spanwise beams which would make it reasonably representative of a fuel-air combustion minimum overpressure. The fuselage was pressurized to 4 psi cabin pressure differential.

The model confirms that the mass of the potable water tanks will impede the forward motion in the center region of the front spar under overpressure loading. Failure of the remaining upper chord and web at LBL 66 and RBL 66 would be the expected result from the model. The model was then run with the front spar and lower bulkhead webs fractured at LBL 66 and RBL 66. Figure E - 1 shows the predicted fuselage ring chord and skin stress in the hoop direction to be approximately 60 KSI. This would therefore exceed an allowable stress of approximately 55 KSI resulting in a predicted net tension failure of the fuselage at S-40 (BL 66).

E.3 Sequence of Wing Tip Failure and Wing Center Section Failure in Wing Bending

The objective of this phase was to determine that the wing tips could be expected to fail prior to failure of the already damaged wing center section for an airplane configuration and flight condition rational for Flight 800 just prior to major breakup. It was assumed that with the forward fuselage gone that the remaining airplane would eventually reach a high angle of attack attitude due to the pronounced bias in aft center of gravity. Since secondary radar returns do not appear to show a significant speed change 300 knots was assumed. Most important was the relative loading and strength at the tip failure location (approximately WS 1195) versus the center section rather than the absolute loading values. Two different levels of wing center section damage were assumed to envelope what was believed to be represented by the wreckage. Damage was primarily introduced by "deleting" effectiveness of varying amounts of forward upward skin panel to simulate loss of support (i.e. front spar, SWB #3, longitudinal floor beams, SWB #2?) and resultant load carrying capability of the skin panel..

The analysis concluded that at a high angle of attack and approximately 5.5 to 6.0 "g" load factor the wing tips would fail while the wing center section with the lesser level of damage would continue to carry the predicted loads. Figure E - 2 shows the margin of safety for the upper wing panel in compression (up bending) buckling versus wing percent span. As the figure shows, the margin of safety just outboard of the outboard engine is minus four percent.

With the aerodynamic loading assumptions modified to account for the wing tip removed the analysis was then rerun to determine if it is still rational to expect the center wing box to fail after the tip is gone. Figure E - 3 shows the results of this analysis illustrating that the wing upper panel would buckle if the damage was somewhat more severe than the minimum level of "Case 1". This loading case represented a further increase in load factor of approximately 1 "g" over and above the flight condition which resulted in the prior wing tip failure. The two wing bending analyses (tip on and tip off) do appear to support the premise that SWB #2 was still sufficiently intact to provide substantial support to the wing upper panel. This would be consistent with localized damage to only the mid-portion of the beam due to keel beam separation.

E.4 Discussion of Original 747-100 Static Test Airplane Wing Destruction Test Results

As another check on the relative wing bending strength of the wing tip region versus the center section the original 747-100 static test airframe wing destruction test was reviewed. In this test the primary failure was upper panel compression buckling just outboard the left side of body. However there was also a secondary failure a fraction of a second later at (also upper panel compression buckling) at WS 1196 just outboard the #1 nacelle. A photo of the side of body failure is provided as Figure E - 4 and a photo of the wing tip failure is provided as Figure E - 5. Both photos are looking at the top of the left wing. The failure at the wing tip area on the test airplane is almost identical in location and type to those documented for left and right wing on Flight 800.

The test confirmed the similarity of relative bending strengths of the wing tip versus side of body region. It would be expected that with some center section

overpressure damage the upper panel buckling initiation would move from just outboard the side of body to just inboard (as documented near the left side of body on Flight 800). The fact that the initial wing failure on Flight 800 was biased toward the wing tip versus the compromised center section can still be explained by the respective wing loadings of the test airplane versus Flight 800. The most significant difference relates to loss of lift on the inboard wing of the Flight 800 airplane due to the aerodynamic inefficiencies associated with the missing forward body and wing to body fairing.

E.5 Summary

The Boeing analysis effort directed at providing additional confirmation of various aspects of the documented breakup sequence is still ongoing. Because of the size of the computer models involved this is a time consuming process and represents a significant resource commitment for Boeing. To date analysis has been done to replicate sequence elements for wing center section overpressure driven failure up to and including failure initiation of the red area fuselage lower lobe adjacent to the front spar. Analysis has also addressed the sequence of wing tip failure and wing center section failure due to upbending overload. Examples of areas of ongoing analysis are the forward keel beam separation and fracture propagation in the fuselage lower lobe. As of the time of inclusion of this appendix (April 8, 1997) the analysis has uncovered nothing to refute the basic findings of the Sequence Group.

Breakup Sequence

Failure Initiation; Fuselage Lower Lobe

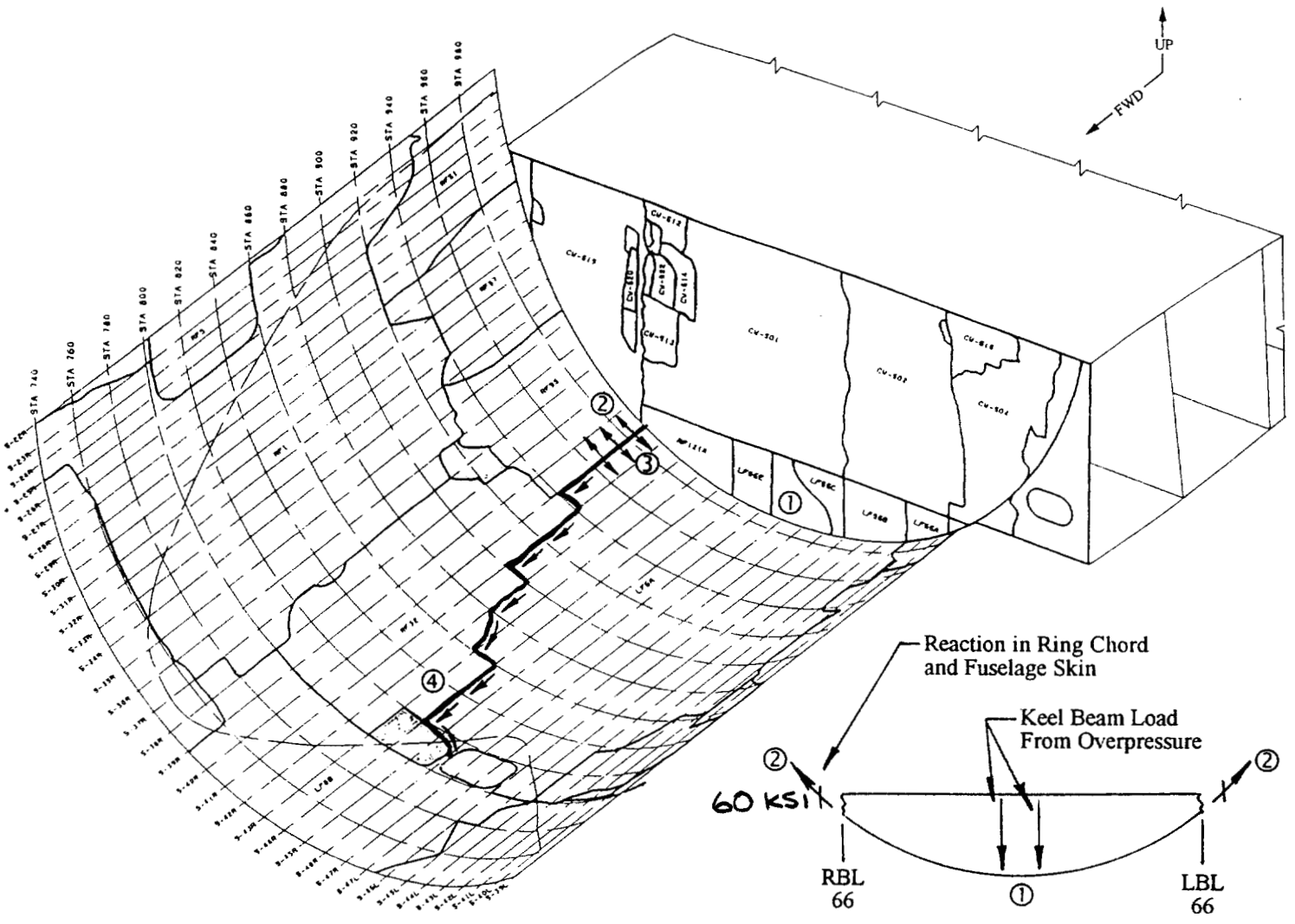

① Keel Beam overpressure related loading still present in lower pressure bulkhead (RELATED TO ASSUMED 25 PSI)

② Load reaction is concentrated in ring chord and adjacent fuselage skin at RBL 66 and LBL 66 where web has failed

③ Ring chord and adjacent fuselage fail in net tension at RBL 66 (S-40R) 60 KSI PREDICTED 55 KSI ALLOWABLE

④ Fuselage crack propagates forward to access door opening at STA 810

FIGURE E-1

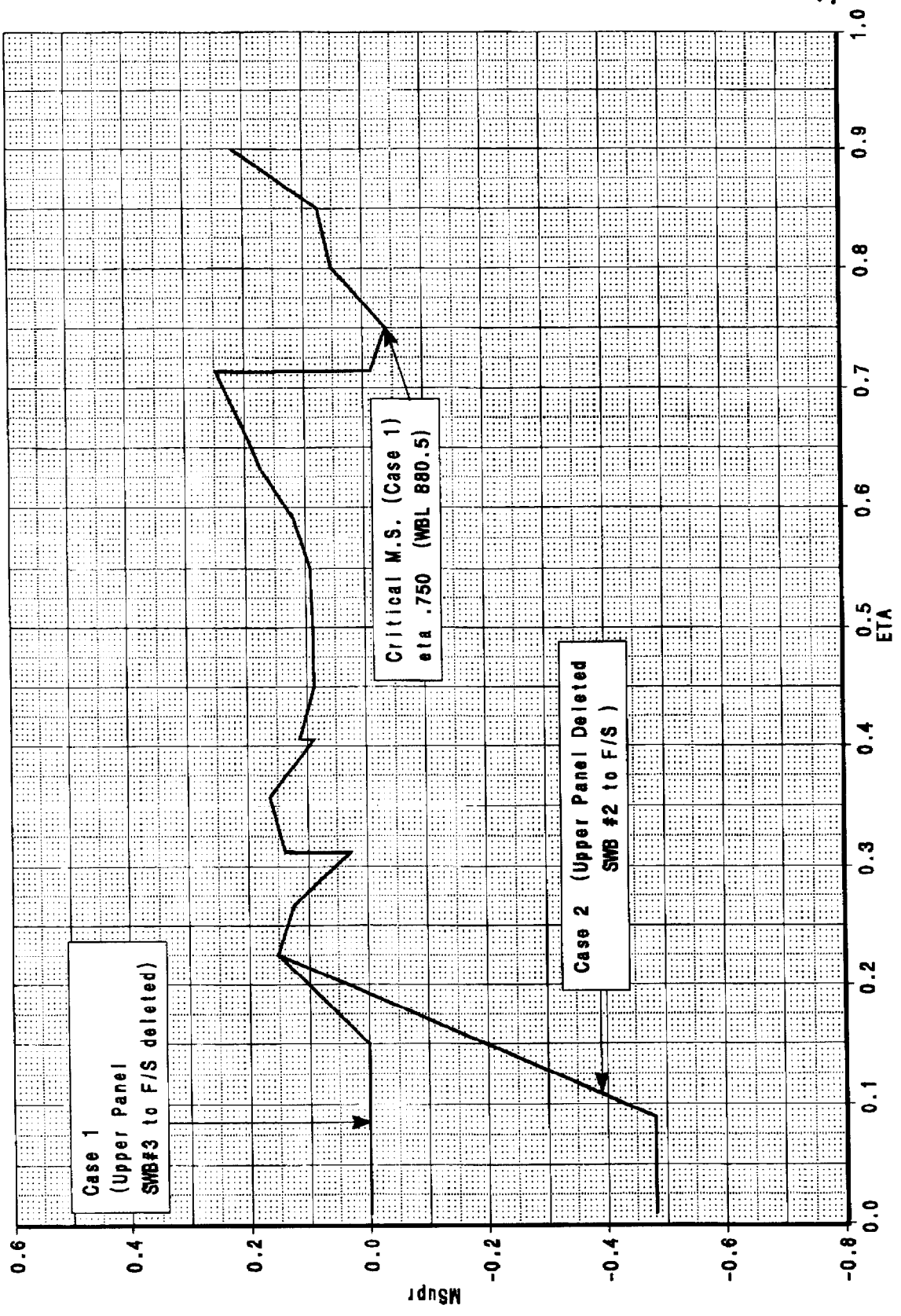

CALC		7Apr97	REVISED	DATE	747-100 Maximum Wing Load Tip On Margins of Safety - Upper Panel	
CHECK						
APPD.						
APPD.					BOEING	PAGE FIG. E-2

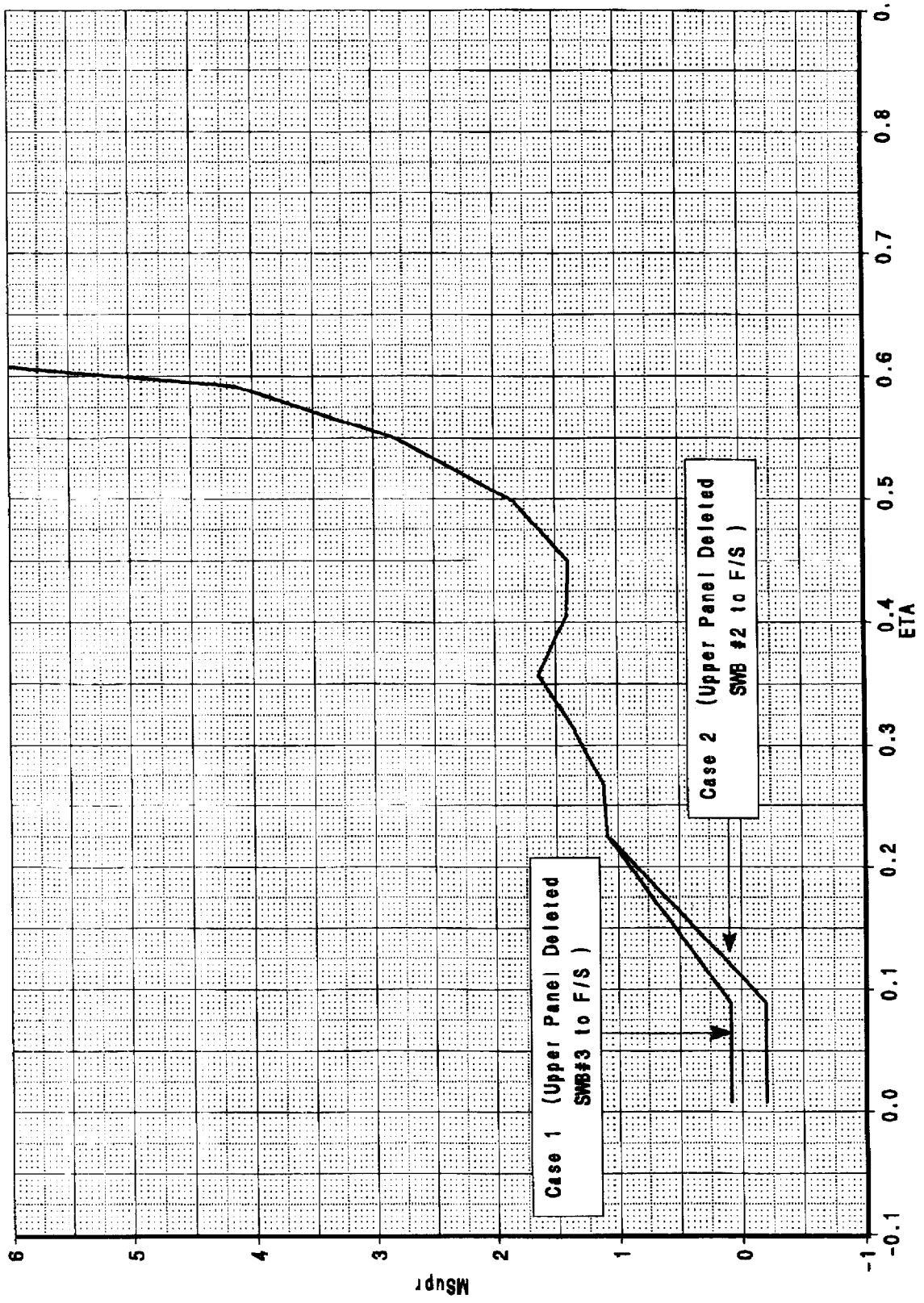

Mon Apr 7 1997 14:0(

CALC			REVISED	DATE	747-100	
CHECK					Maximum Wing Load Tip Off	
APPD.					Margins of Safety - Upper Panel	
APPD.					BOEING	PAGE FIG E-3

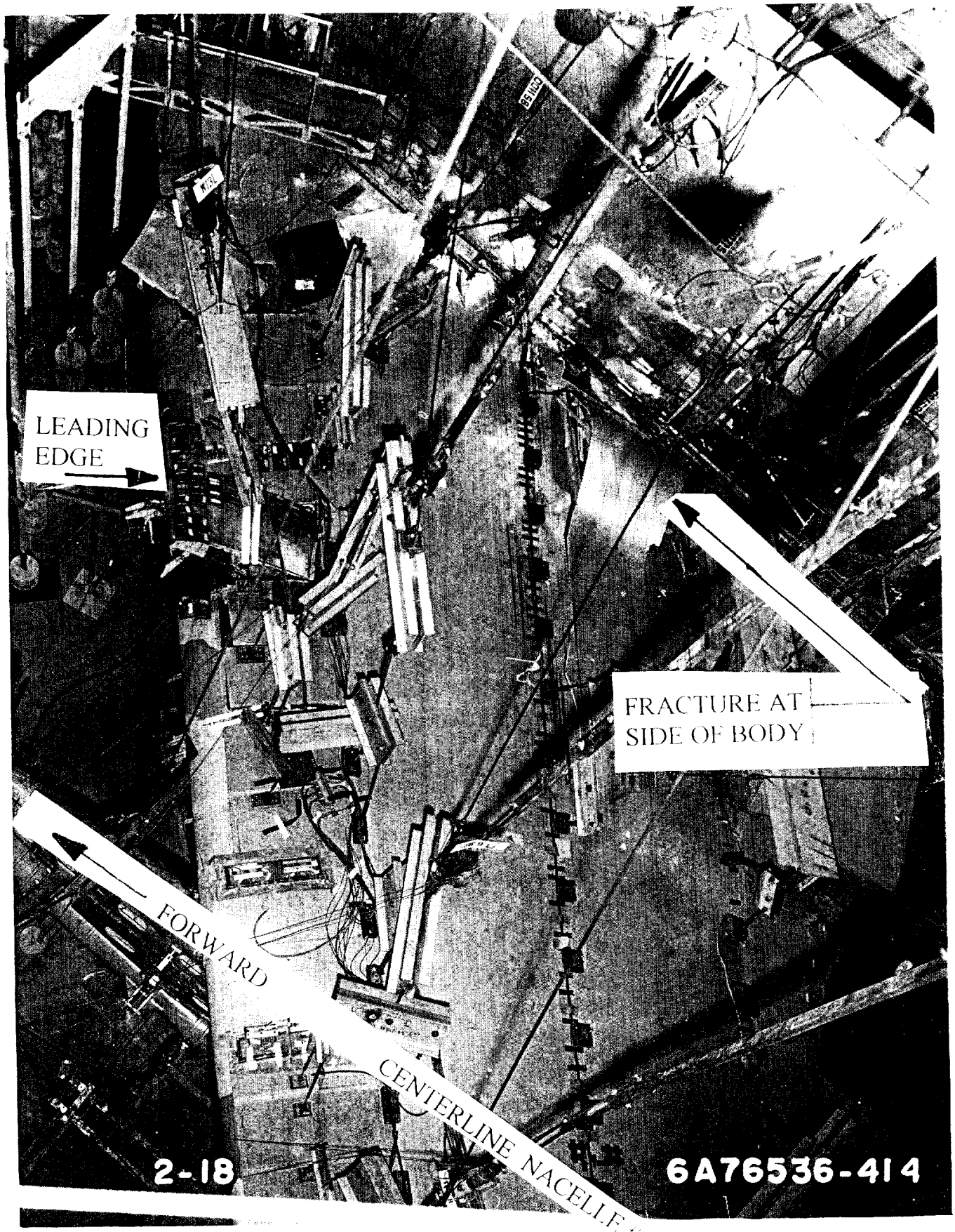

CALC		REVISED DATE	
CHECK			
APPD			
APPD			

BOEING COMPANY
RENTON WASHINGTON

PAGE

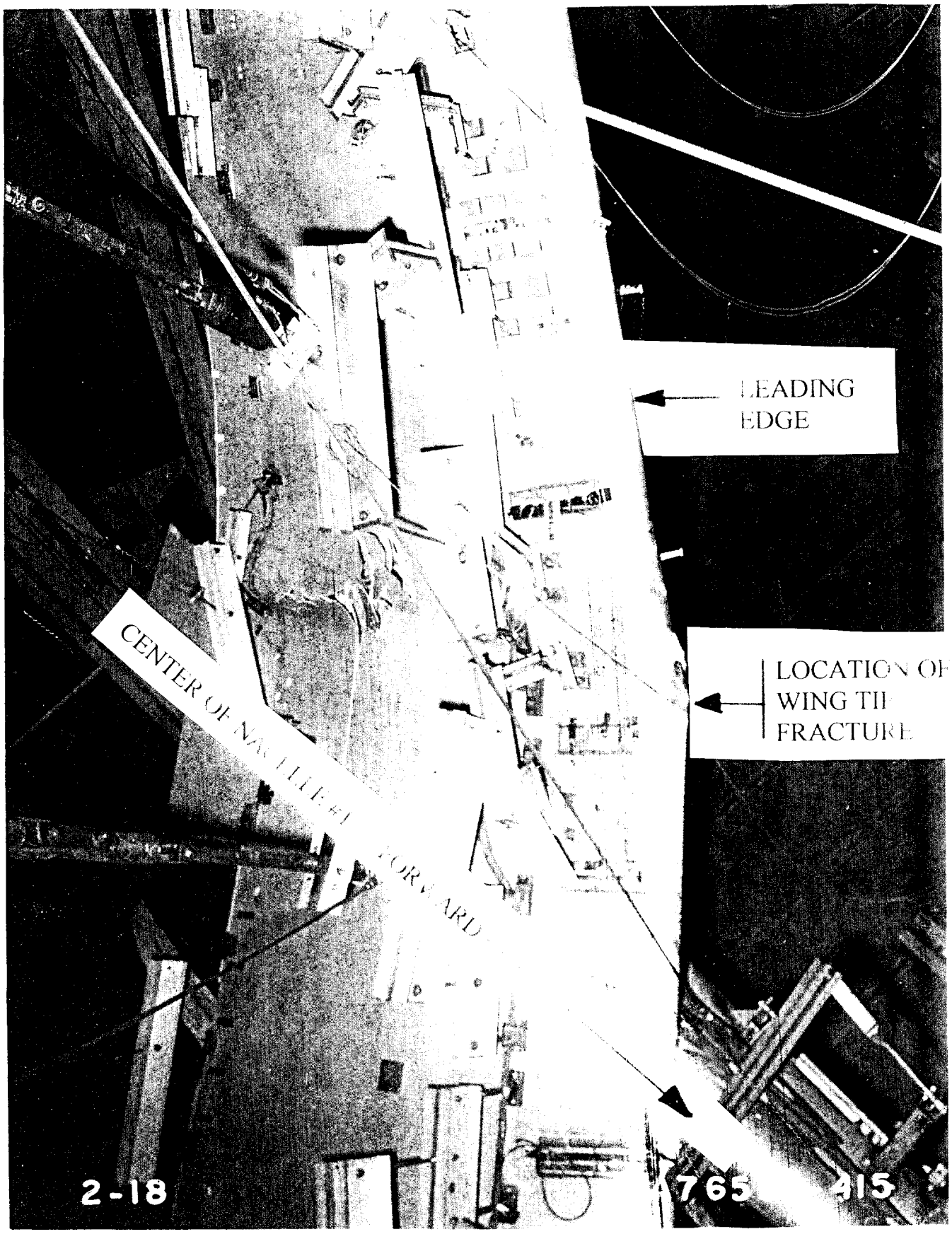

CALC			
CHECK			
APPD			
APPD		BOEING COMPANY RENTON WASHINGTON	PAGE